



NAVAL POSTGRADUATE SCHOOL

MONTEREY, CALIFORNIA

DISSERTATION

**ROBUST MODEL-BASED FAULT DIAGNOSIS FOR A DC
ZONAL ELECTRICAL DISTRIBUTION SYSTEM**

by

John D. Stevens

June 2007

Dissertation Supervisor:

R. Cristi

Approved for public release; distribution is unlimited

THIS PAGE INTENTIONALLY LEFT BLANK

REPORT DOCUMENTATION PAGE			<i>Form Approved OMB No. 0704-0188</i>	
Public reporting burden for this collection of information is estimated to average 1 hour per response, including the time for reviewing instruction, searching existing data sources, gathering and maintaining the data needed, and completing and reviewing the collection of information. Send comments regarding this burden estimate or any other aspect of this collection of information, including suggestions for reducing this burden, to Washington headquarters Services, Directorate for Information Operations and Reports, 1215 Jefferson Davis Highway, Suite 1204, Arlington, VA 22202-4302, and to the Office of Management and Budget, Paperwork Reduction Project (0704-0188) Washington DC 20503.				
1. AGENCY USE ONLY (Leave blank)		2. REPORT DATE June 2007	3. REPORT TYPE AND DATES COVERED Dissertation	
4. TITLE AND SUBTITLE: Robust Model-based Fault Diagnosis for a DC Zonal Electrical Distribution System			5. FUNDING NUMBERS	
6. AUTHOR(S) John D. Stevens				
7. PERFORMING ORGANIZATION NAME(S) AND ADDRESS(ES) Naval Postgraduate School Monterey, CA 93943-5000			8. PERFORMING ORGANIZATION REPORT NUMBER	
9. SPONSORING / MONITORING AGENCY NAME(S) AND ADDRESS(ES) N/A			10. SPONSORING / MONITORING AGENCY REPORT NUMBER	
11. SUPPLEMENTARY NOTES The views expressed in this thesis are those of the author and do not reflect the official policy or position of the Department of Defense or the U.S. Government.				
12a. DISTRIBUTION / AVAILABILITY STATEMENT Approved for public release; distribution is unlimited			12b. DISTRIBUTION CODE A	
13. ABSTRACT (maximum 200 words) <p>A key element of the U.S. Navy's transition to an electric naval force is an Integrated Power System (IPS) that provides continuity of service to vital systems despite combat damage. In order to meet subsequent survivability standards under a reduced manning constraint, the IPS system must include a fault tolerant control scheme, capable of achieving automated graceful degradation despite major disruptions involving cascading failures. Toward this objective, online model-based residual generation techniques are proposed, which identify explicitly defined faults within a stochastic DC Zonal Electrical Distribution System (DC ZEDS). Two novel polynomial approaches to the design of unknown input observers (UIO) are developed to estimate the partial state and, under certain conditions, the unknown input. These methods are shown to apply to a larger class of systems compared to standard projection based approaches where the UIO rank condition is not satisfied. It is shown that the partial-state estimate is sufficient to the computation of residuals for fault diagnosis, even in such cases where full-state estimation is not possible. In order to reduce the complexity of the system, a modular approach to Fault Detection and Isolation (FDI) is presented. Here, the innovations generated from a bank of Kalman filters (some of them UIOs) act as a structured residual set for the stochastic DC ZEDS subsystem modules and are shown to detect and isolate various classes of faults. Certain mathematical models are also shown to effectively identify input/output consistency of systems in explicitly defined fault conditions. Numerical simulation results are based on the well-documented Office of Naval Research Control Challenge benchmark system, which represents a prototypical U.S. Navy shipboard IPS power distribution system.</p>				
14. SUBJECT TERMS Unknown Input Observers, Fault Diagnosis, Residual Generation, Power Electronics, DC Zonal Electrical Distribution System			15. NUMBER OF PAGES 200	
			16. PRICE CODE	
17. SECURITY CLASSIFICATION OF REPORT Unclassified	18. SECURITY CLASSIFICATION OF THIS PAGE Unclassified	19. SECURITY CLASSIFICATION OF ABSTRACT Unclassified	20. LIMITATION OF ABSTRACT UL	

THIS PAGE INTENTIONALLY LEFT BLANK

Approved for public release; distribution is unlimited

**ROBUST MODEL-BASED FAULT DIGANOSIS FOR A DC ZONAL
ELECTRICAL DISTRIBUTION SYSTEM**

John D. Stevens
Lieutenant Commander, United States Navy
B.S., United States Naval Academy, 1993
M.S., Naval Postgraduate School, 2000

Submitted in partial fulfillment of the
requirements for the degree of

DOCTOR OF PHILOSOPHY IN ELECTRICAL ENGINEERING

from the

**NAVAL POSTGRADUATE SCHOOL
June 2007**

Author:

John D. Stevens

Approved by:

Roberto Cristi
Professor of Electrical Engineering
Dissertation Supervisor/
Committee Chair

Wei Kang
Professor of Mathematics
Applied Mathematics Minor
Committee Representative

Ed Zivi
Associate Professor of Weapons
and Systems Engineering
United States Naval Academy

John Ciezki
Associate Professor of
Electrical Engineering
United States Naval Academy

Roman Statnikov
Professor and NRC Fellow of
Information Systems

Fotis Papoulas
Associate Professor of
Mechanical Engineering

Approved by:

Jeffrey B. Knorr, Chair, Department of Electrical Engineering

Approved by:

Julie Filizetti, Associate Provost for Academic Affairs

THIS PAGE INTENTIONALLY LEFT BLANK

ABSTRACT

A key element of the U.S. Navy's transition to an electric naval force is an Integrated Power System (IPS) that provides continuity of service to vital systems despite combat damage. In order to meet subsequent survivability standards under a reduced manning constraint, the IPS system must include a fault tolerant control scheme, capable of achieving automated graceful degradation despite major disruptions involving cascading failures. Toward this objective, online model-based residual generation techniques are proposed, which identify explicitly defined faults within a stochastic DC Zonal Electrical Distribution System (DC ZEDS). Two novel polynomial approaches to the design of unknown input observers (UIO) are developed to estimate the partial state and, under certain conditions, the unknown input. These methods are shown to apply to a larger class of systems compared to standard projection based approaches where the UIO rank condition is not satisfied. It is shown that the partial-state estimate is sufficient to the computation of residuals for fault diagnosis, even in such cases where full-state estimation is not possible. In order to reduce the complexity of the system, a modular approach to Fault Detection and Isolation (FDI) is presented. Here, the innovations generated from a bank of Kalman filters (some of them UIOs) act as a structured residual set for the stochastic DC ZEDS subsystem modules and are shown to detect and isolate various classes of faults. Certain mathematical models are also shown to effectively identify input/output consistency of systems in explicitly defined fault conditions. Numerical simulation results are based on the well-documented Office of Naval Research Control Challenge benchmark system, which represents a prototypical U.S. Navy shipboard IPS power distribution system.

THIS PAGE INTENTIONALLY LEFT BLANK

TABLE OF CONTENTS

I.	INTRODUCTION.....	1
A.	ROADMAP TO AN ELECTRIC NAVAL FORCE	3
B.	FAULT TOLERANT CONTROL	4
C.	OVERVIEW AND CONTRIBUTIONS	6
II.	DC ZONAL ELECTRICAL DISTRIBUTION SYSTEM	9
A.	ONR INTEGRATED POWER SYSTEM TESTBED.....	9
B.	MODULES	12
	1. Power Supply	12
	<i>a. Detailed Model</i>	<i>12</i>
	<i>b. Average Value Model.....</i>	<i>13</i>
	<i>c. Power Supply Control.....</i>	<i>15</i>
	<i>d. Nonlinear State Space Model</i>	<i>16</i>
	2. Bus	18
	<i>a. Six-state Bus Model</i>	<i>20</i>
	<i>b. Three-state Bus Model.....</i>	<i>26</i>
	3. Ship's Service Converter Module.....	30
	<i>a. Detailed Model</i>	<i>30</i>
	<i>b. Average Value Model.....</i>	<i>32</i>
	<i>c. SSCM Control</i>	<i>32</i>
	<i>d. Nonlinear State Space Model</i>	<i>34</i>
	4. Oring Function	37
	5. Inverter Module and Constant Power Load	40
C.	METHOD FOR ANALYZING DC ZEDS SYSTEM.....	40
III.	A POLYNOMIAL APPROACH TO DYNAMIC MODELING AND FAULT DETECTION.....	43
A.	DYNAMIC SYSTEMS AND THE PARTIAL STATE.....	46
	1. Single Input Single Output (SISO) Systems	46
	2. Multiple Input Multiple Output (MIMO) Systems	48
B.	POLYNOMIAL-BASED UIO BY INPUT REPLACEMENT	52
	1. Theory	52
	2. Example	58
C.	POLYNOMIAL-BASED UIO BY PARAMETRIZATION	63
	1. Theory	63
	2. Example	67
D.	INPUT OBSERVABILITY AND ESTIMATION	75
	1. Input Observability Theory	76
	2. Examples.....	82
IV.	FAULT DIAGNOSIS APPLIED TO THE DC ZEDS SYSTEM	93
A.	MODULAR APPROACH TO INPUT-OUTPUT CONSISTENCY.....	94
B.	FDI BASED ON FAULT MODELING	103
V.	CONCLUSION	115

A.	SUMMARY OF FAULT DIAGNOSIS RESULTS TO THE DC ZEDS MODEL	115
B.	SUMMARY OF POLYNOMIAL UIO RESULTS	116
C.	FUTURE WORK	118
APPENDIX A: IFAC SAFEPROCESS FAULT DIAGNOSIS DEFINITIONS		121
APPENDIX B: POWER SUPPLY AVM TRANSFORMATION		125
APPENDIX C: SUBSPACE PROJECTION UNKNOWN INPUT OBSERVER		127
APPENDIX D: POLYNOMIAL MATRIX DEFINITIONS AND THEOREMS		135
LIST OF REFERENCES		147
INITIAL DISTRIBUTION LIST		181

LIST OF FIGURES

Figure I.1: Fault Management Architecture.....	4
Figure II.1: DC Zonal Electrical Distribution System Topology	10
Figure II.2: Power Supply (detailed)	12
Figure II.3: Power Supply Average Value Model	14
Figure II.4: Power Supply Control.....	15
Figure II.5: Comparison of Detailed and Average Value Models of the Power Supply	18
Figure II.6: Bus Model.....	19
Figure II.7: DC ZEDS Baseline Scenario Bus Current Distribution, Zone 1	24
Figure II.8: DC ZEDS Baseline Scenario Bus Current Distribution, Zone 2	25
Figure II.9: DC ZEDS Baseline Scenario Bus Current Distribution, Zone 3	26
Figure II.10: Ship's Service Converter Module Circuit	31
Figure II.11: SSCM Average Value Model Topology.....	32
Figure II.12: SSCM Control Architecture	33
Figure II.13: Zone 1 Starboard SSCM Simulation Regulates 400 V Output (bottom) from 500 V Input (top)	37
Figure II.14: Oring Function Simulation Results	38
Figure II.15: Oring Function Circuit Model	39
Figure III.1: SISO System in Transfer Function Form.....	46
Figure III.2: Partial-state Space Representation of SISO System.....	47
Figure III.3: Right Fraction Representation of MIMO System	50
Figure III.4: SIMO System Transfer Function	52
Figure III.5: SIMO Unknown Input System.....	53
Figure III.6: UIO Input Replacement Method Simulation.....	62
Figure III.7: State Estimate Comparison	74
Figure III.8: UIO Example, Signal Flow Diagram	83
Figure III.9: UIO Example, Structured Residual set for Input FDI.....	84
Figure III.10: UIO Example, Input Fault Trajectory	86
Figure III.11: Input Residuals (Fault on $u_i(t)$).....	87
Figure III.12: UIO Example, Output Residuals (Bus Current per Zone).....	88
Figure III.13: UIO Example, Output Residuals (Bus Voltage per Zone)	90
Figure III.14: Input Estimation of a Nonlinear System	91
Figure III.15: Results from Polynomial UIO with Input Reconstruction	92
Figure IV.1: DC ZEDS Module Topology	94
Figure IV.2: System Module Interconnection	95
Figure IV.3: Sensor FDI Structured Residual Set.....	97
Figure IV.4: Bus Voltage Showing Bus Current Sensor Fault.....	99
Figure IV.5: Bus Current Showing Bus Current Sensor Fault.....	100
Figure IV.6: Bus Sensor FDI Residuals for Bus Current Sensor Fault in Power Supply.....	101
Figure IV.7: Input Residuals for Bus Current Sensor Fault in Power Supply Controller	102
Figure IV.8: Output Residuals for Bus Current Sensor Fault in Power Supply Controller..	103
Figure IV.9: SSCM Switch Closed Failure: Port/Stbd Bus Voltage	105
Figure IV.10: SSCM Switch Closed Failure: Port/Stbd Bus Current.....	106
Figure IV.11: SSCM Switch Closed Failure: SSCM Inputs.....	107

Figure IV.12: SSCM Switch Closed Failure: SSCM Outputs	108
Figure IV.13: SSCM Switch Closed Failure: SSCM Control Signal d	109
Figure IV.14: SSCM Switch Closed Failure: Fault Model Residuals	111
Figure IV.15: SSCM Switch Closed Failure: Residual on Control Signal d	112
Figure IV.16: Bus Open Circuit in Zone 3: Bus Current.....	113
Figure IV.17: Bus Open Circuit: 3 Mode Residuals.....	114

LIST OF TABLES

Table II.1: Power Supply Parameters	13
Table II.2: Power Supply Control Parameters	16
Table II.3: Bus Model Parameters	19
Table II.4: Bus Zone Switch Configuration.....	20
Table II.5: DC ZEDS Baseline Scenario Parameters.....	23
Table II.6: SSCM Parameters	31
Table II.7: SSCM Control Parameters	33
Table II.8: Oring Function Parameters	40

THIS PAGE INTENTIONALLY LEFT BLANK

ACKNOWLEDGMENTS

On the occasion of completing this personal and professional milestone, I pause and give credit to a host of influential giants:

I thank my Ph.D. committee for their guidance and support from beginning to end. Thanks to Roberto Cristi for taking an active role as my PhD advisor and committee chairman. In particular, his thoughts on polynomial realizations of MIMO systems and collaboration on unknown input observer methods is greatly appreciated. Fotis Papoulias is greatly appreciated as a professor of mine in my Mechanical Engineering days and for providing me with research resources. As my mathematics minor representative on the committee, I thank Wei Kang for allowing me to sit under his tutelage for several nonlinear dynamics courses and educating me on various nonlinear estimation techniques. I thank Roman Statnikov for introducing me to his multicriteria optimization tools and it is my hope to conduct follow-on research in this area. I am grateful to my U.S. Naval Academy committee members for educating me on the DC Zonal Electrical Distribution System. Specifically, I wish to thank John Ciezki for his educating me on power electronics and Ed Zivi for his generosity in providing me with travel funds and research resources. Also, his keen insight into the naval application of this work and general advice is greatly appreciated. Finally, I thank Arthur Krener for being the “substitute” committee member at my defense.

There are others that greatly contribute to my continuing academic and professional pursuits. Among them are Purdue University professors Stan Zak for his friendly advice and work in unknown input observers and Scott Sudhoff for his work in power electronics and the Naval Combat Survivability Testbed. I also appreciate my good friend Yonggon Lee at the U.S. Naval Academy for his help in developing state space models on the DC Zonal Electrical Distribution System, operating the Beowulf cluster, and proofreading this work.

As an Engineering Duty Officer, I thank Tim McCoy, CDR, USN (ret.) for enabling this rare opportunity for me to pursue a Ph.D. while on active duty. I also want to thank CAPT Norbert Doerry, whose influence and sound advice extend beyond

academics. Specifically, I thank him for persuading me to pursue a relevant naval research topic in the area of Fault Tolerant Control and for his general advice as a Naval Officer.

On a personal note, I thank Pam Silva for her strategic decision to support me in transitioning from a Master's student in Mechanical Engineering to one in Electrical Engineering. Possessing great influence and tact, she convinced my military chain of command to allow me to switch to Electrical Engineering. Without this action, I would not have had this opportunity. It was a pleasure working with Roberto Cristi and Ed Zivi on this project. Their professional and personal qualities made this quite an enjoyable experience.

To conclude, I acknowledge that “every good gift and every perfect gift is from above, and cometh down from the Father of lights, with whom is no variableness, neither shadow of turning.”¹ Therefore, it is quite fitting to thank God for my family. I am grateful to be the father of Hannah, Eric, and Evelyn – for your love of learning inspires me. Finally, a very special “thank you” goes to the one and only love of my life – my wife Lori – for her unyielding support, encouragement and understanding. Indeed, “strength and honour *are* her clothing; and she shall rejoice in time to come.”²

Ad Maiorem Dei Gloriam

¹ *The Holy Bible : King James Version*. electronic ed. of the 1769 edition of the 1611 Authorized Version. Bellingham WA : Logos Research Systems, Inc., 1995, S. Jas 1:17

² *The Holy Bible : King James Version*. electronic ed. of the 1769 edition of the 1611 Authorized Version. Bellingham WA : Logos Research Systems, Inc., 1995, S. Pr 31:25

EXECUTIVE SUMMARY

The incorporation of an Integrated Power System (IPS) in the DDG 1000 Destroyer represents a first step in a transformation to an Electric Naval Force [72]. Moreover, the U.S. Navy is presently assessing alternative power and control system architectures for the Next Generation Integrated Power System (NGIPS) [395]. These systems must be survivable and increasingly capable of brokering propulsion and pulsed power demands while providing ships service power continuity to vital mission systems [91]. In an era of asymmetric warfare and reduced manning constraints, the NGIPS must provide automated continuity of service control to vital systems despite major disruptions involving cascading failures. Toward this objective, online physics-based fault detection and isolation (FDI) techniques are proposed and are expected to operate within a fault tolerant control (FTC) framework. The methods seek to identify explicitly defined faults within a DC Zonal Electrical Distribution System (DC ZEDS) portion of an IPS. Here, mathematical models, together with sensors providing real-time data, are used to validate the condition of the system. The results of this research demonstrate various methods of generating fault-indicating signatures for classes of sensor, actuator, and plant faults. In the case of system actuator FDI, several estimation techniques based on a polynomial realization are developed. Numerical simulation results are based on the well-documented Office of Naval Research Control Challenge benchmark system, which represents a prototypical U.S. Navy shipboard IPS power distribution system.

THIS PAGE INTENTIONALLY LEFT BLANK

I. INTRODUCTION

In keeping with the vision set forth by the Chief of Naval Operations, Naval warships in the Twenty-First Century must have the ability to “change, adapt and transform” to meet new threats. Indeed, Sea Power 21 defines a Navy capable of constantly improving its ability to “project offensive power, defensive assurance, and operational independence around the globe” [111]. To achieve the vision, the CNO outlines three fundamental pillars; among them is a continuing transformation of improved technology.

Achieving these goals require warships with a higher degree of survivability to enable decisiveness, sustainability, responsiveness and agility, which are the four fundamental qualities in Sea Power 21. From an operational point of view, survivability is the ability to avoid and withstand a hostile environment. From a system-level point of view, it can be thought of as a “fight hurt” or “fight-through” capability – that is, the warship’s ability to maintain continuity of service despite major disruptions and cascading failures in the presence of catastrophic events.

Within this framework, an automated fault-tolerant control scheme is essential to a warship’s fight-through capability. Of particular importance in achieving a graceful degradation of warship systems under these conditions is a design strategy that integrates combat systems with advanced hull, mechanical and electrical capabilities. According to the U.S. Navy Survivability Design Handbook for Surface Ships, developing affordable survivability measures under a distributed, dynamically interdependent system of systems framework will “constitute the hallmark of the Navy’s new approach to reliably automate damage control functions while operating with fewer crewmembers” [343].

Take for example an Integrated Fight Through Power (IFTP) system, which seeks to maintain power continuity resulting from a calamitous exogenous event. According to numerous Naval Research Advisory Committee (NRAC) reports and naval power systems and automation experts, there is a growing need to develop cost-effective ways to solve power automation issues by taking into account the following aspects: [390][391][91][264][72][76]

1. Automation will be essential to ensure survivable and effective surface combatants in the warfare environment [271].
2. Personnel costs comprise over 50% of operating and supporting costs, therefore it is necessary to reduce the number of shipboard war fighters. Smart Ship demonstrated that technology and procedural changes can improve ship operations [272].
3. Well-trained crew members are decision-makers that require real-time data to make informed decisions. No longer able to rely on a well-staffed crew for data and unable to react to rapid and complex nonlinear system interdependencies, an automation strategy must instead respond to cascading system faults and failures [392].
4. Life Cycle Costs (LCC), which include research and development, can be reduced by implementing simulation-based design environments – especially in cases where revolutionary technologies are being developed – where no historical cost data exists [273].
5. Advanced distributed simulations and simulation-based design/manufacturing to assess new technologies and ship design options is encouraged [273][392].

Given this trend, it is most desirable and advantageous to employ an on-line analytically redundant, robust Fault Tolerant Control (FTC) scheme designed to detect unpermitted deviations from a system's expected, acceptable or standard condition and perform actions as necessary to maintain continuity of service – in this case, power distribution. Herein, the first of a two-step FTC process is presented using robust model-based Fault Detection and Isolation (FDI) methods. Characteristics of faults such as time, location, size, and relative influence are determined through residual generation and analysis methods developed herein. The methods are applied to a DC Zonal Electrical Distribution System (DC ZEDS) testbed designed to resemble dc power distribution systems currently being researched for installation on future all-electric warships for reasons to be discussed.

A. ROADMAP TO AN ELECTRIC NAVAL FORCE

The NRAC report Roadmap to an Electric Naval Force identified several major motivations for the navy to shift away from a separated power and propulsion platform and towards an all-electric warship [271][390][391][392]:

- Electric weapons and advanced sensors for superior firepower range and resolution require far greater pulse power than currently available.
- Electric propulsion and auxiliaries possess superior mobility, stealth and endurance.
- Integrated Power System (IPS) allows provision for common electric power system for real-time power allocation, reconfigurability, and superior survivability.
- Electric ship platform provides support for off board weapons and sensors for superior reach and warfighter sustainment.

These reasons among many others make transitioning to an all-electric drive warship as significant a change as shifting from steam to gas turbine and possibly even from sail to steam. With this change comes the challenge of managing far greater power requirements – on the order of tens of megawatts, which is only the beginning [11][72][90]. Already committed to fielding an electric warship, the U.S. Navy is currently building DDG 1000 as the baseline for future DC zonal electric power systems [271]. Again, survivability requirements and current trends in power electronics technology obviate the need for a power automation scheme capable of providing continuity of service under temporal and spatial bursts of natural or hostile disruption [390]. A Fault Tolerant Control scheme, then, provides a framework upon which to build a desirable, realizable, and tractable solution.

B. FAULT TOLERANT CONTROL

A fault can be described as any deviation from nominal system behavior that can negatively impact overall desired system performance. A mathematical model-based approach to the detection of a fault, therefore, is sought. From a system automation point of view, a representative Fault Tolerant Control architecture can be depicted as in Figure I.1 [44].

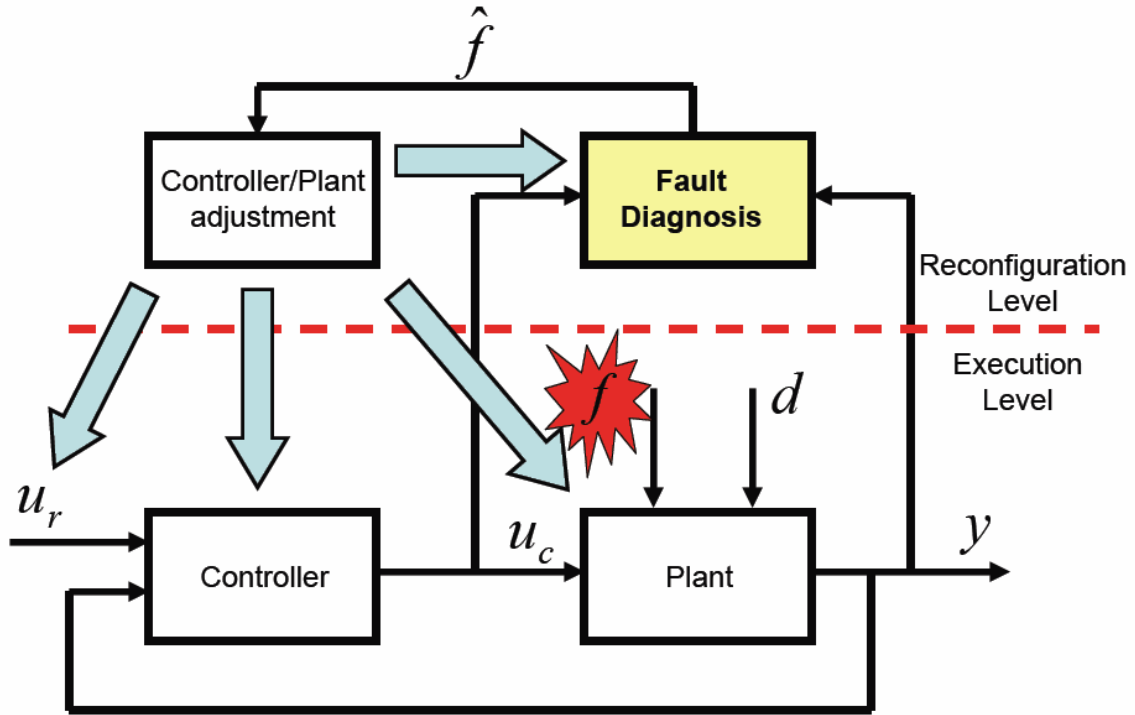


Figure I.1: Fault Management Architecture

Notice the fault management architecture contains an execution level, which resembles common model-based state feedback control system architecture and a supervisory level, which depicts two major processes – diagnosis and controller re-design. The plant includes modeling uncertainties defined as a vector of unknown inputs d . A vector of faults f , cause the plant to deviate from a nominal condition.

Assuming linearity, a plant model (depicted in Figure I.1) can be expressed in continuous time as

$$\begin{aligned}\dot{x} &= Ax + Bu + Ed + Gf \\ y &= Cx + Fd + Hf\end{aligned}\tag{0.1}$$

where state vector $x \in \mathbb{R}^n$, input $u \in \mathbb{R}^m$, and output $y \in \mathbb{R}^r$ and matrices A , B , C , E , F , G and H are of appropriate dimensions. The terms Ed and Gf model uncertain (unknown) inputs and faults, respectively, in the actuator(s) and plant model. In the output equation, Fd and Hf represent uncertain (unknown) inputs and faults in the sensors. Note that matrices A , B , and C represent the nominal system where all faults and uncertainties are assumed to be contained within f and d . It is further assumed that matrices E , F , G and H are constant and known, while f and d are typically unknown.

Looking at the reconfiguration level in Figure I.1, the main objective of the on-line Fault Diagnosis process block is to determine if the system is subjected to a fault and its time of occurrence. Then, all subsequent actions should focus on characterizing the fault(s) to the greatest extent possible. These actions should include estimating the fault's location, identification, and severity. If a history of fault activity is needed for conditioned-based maintenance or scenario reconstruction, then developing fault statistics would be advantageous. This step is represented as the output to the Fault Diagnosis process block and is annotated by \hat{f} .

The Controller/Plant adjustment process block then receives the fault information and performs appropriate controlling action as depicted in the figure. This action might be to adjust the parameters of the controller or reconfigure the controller altogether. If a fault becomes a failure in the nominal plant, then it might be necessary to operate in a reduced capability, damage control reconfiguration mode in order to maintain continuity of service. If this is the case, then it might be advantageous to have the Controller/Plant

adjustment process block initiate a reconfiguring of the nominal plant and associated mathematical models in the Fault Diagnosis block.

Some work has been done at the execution level within a Fault Tolerant Control framework. To a limited degree, fault tolerance can be achieved under a robust or adaptive control design. In Robust Control, *passive* fault tolerance is achieved by a fixed controller that is designed to satisfy pre-defined performance specifications. Adaptive control methods, on the other hand, are considered *active* fault tolerance measures since controller parameters are adjusted to changing plant parameters (possibly caused by faults) as a function of time. In both cases, however, the classes of faults are restricted in the sense that they must be “well-behaved” according to their fault definitions and mathematical formulations. Adaptive control, for example, performs well only for linear systems with slowly changing parameters [44]. Neither method attempts to diagnose a broader range of faults nor do they attempt to change the controller or plant structure to mask, compensate, correct, re-configure, re-design or otherwise “tolerate” faults. This work looks beyond the restricted class of faults to generate residuals at the supervisory level.

C. OVERVIEW AND CONTRIBUTIONS

As described in Figure I.1, the flow in the reconfiguration level of a representative FTC architecture begins with Fault Diagnosis. It is the intent of this work to provide the output of the Fault Diagnosis process block – that is, the necessary fault information for further processing to obtain the Navy’s goal: achieve automated fight-through capability despite major disruptions and cascading failures. Common error masking and error recovery methods are poorly suited for a system description under this framework [390][392].

The goal of this work is to develop Fault Diagnosis strategies applied to the DC Zonal Electrical Distribution System (DC ZEDS) by generating model-based residuals from estimates of the partial state. The following chapters will establish a methodology for establishing the DC ZEDS models, estimation methods, and Fault Detection and Isolation (FDI) methods.

Chapter II details the modules of the DC ZEDS system to include how some of the nonlinear dynamics are averaged. Since a deductive approach will be taken to identify the effects of a system fault, a close observation of fault effects will be monitored. It will be shown that output sensor measurements are selected to guarantee observability and are consistent with algebraic relationships and conservation of energy laws. Chapter III then explains the methodology for choosing estimation methods, including several novel polynomial unknown input observer methods. An explanation for using linear methods on nonlinear models will also be addressed. Chapter IV identifies common mode failures and identifies classes of faults through simulation, then provides a methodology for choosing the Fault Diagnosis schemes to developing fault indications in the residuals. Finally, Chapter V provides a summary of results.

Overall, the contributions of this work can be categorized into 2 main areas. The first is in a novel polynomial approach to the design of unknown input observers (UIO) with particular attention paid to partial-state and input estimation. The second area is in the FDI techniques applied to the DC ZEDS application.

A structural residual set – predicated upon physics-based mathematical model estimation – is developed to decouple the effects from a defined set of faults in order to determine fault indications. The unknown input observer (UIO) developed in this research will be part of this task.

Even though UIOs are used for Fault Detection and Isolation (FDI), little application research has been done to take advantage of input estimation, which is shown to enhance analytical redundancy. In addition, it will be shown that the proposed polynomial based approach can be applied to a more general class of systems, compared to the standard projection based approach of [175].

A polynomial approach to a general UIO for state and input estimation for both discrete and continuous time systems is presented for the purpose of fault detection and isolation. Unlike UIO methods that are based on a subspace projection of the whole state onto a subspace of known state components (such as [73], [80] and [175]), this robust

estimation method is based on an estimate of the *partial-state* representation of the system. This is sufficient to the computation of a residual, even in cases when full-state estimation is not possible.

II. DC ZONAL ELECTRICAL DISTRIBUTION SYSTEM

Among all shipboard distributed systems, it can be argued that the power distribution system is the most vital. If not for its tightly coupled interdependence with every shipboard distributed system (including propulsion), it would be in terms of potential vulnerability. Indeed, an all-electric drive warship depends absolutely upon its power system to provide quality and continuity of service while operating in a hostile environment. And with future warships potentially requiring eight to ten times the power generated on today's warships, it will only increase its stock.

The prototypical power electronics based dc zonal electrical distribution system is uniquely designed as an efficient high power density, fast transient response, tightly coupled finite inertia system. The sophisticated and robust power converter control elements provide nearly-ideal load regulation and transient performance (tens of milliseconds) with a high degree of fault tolerance. The system is also characterized as having a high degree of automation and nearly instantaneous reconfiguration capabilities. For example, a dc/dc buck converter – which is the Ship's Service Converter Module (SSCM) in the representative DC ZEDS system herein – is capable of maintaining a constant output voltage regardless of input disturbances. From the output side, this attribute is highly desirable for power quality-sensitive loads.

A. ONR INTEGRATED POWER SYSTEM TESTBED

The nonproprietary, well-characterized, reduced-scale ONR IPS Testbed DC ZEDS model serves as an ideal resource for initial validation of electric warship power distribution analysis methods and control schemes. Through sponsorships from the National Science Foundation (NSF) and the Office of Naval Research (ONR), the MATLAB Simulink based model was developed by a collaboration of academic communities from Purdue University and the U.S. Naval Academy. The distribution system topology is also representative of the Naval Combat Survivability Testbed, a reduced-scale hardware testbed designed to achieve the same purpose.

For the purpose of this research, the DC ZEDS model – in both average value and detailed model forms – is used to apply novel estimation and residual generation techniques for robust model-based fault diagnosis. When considering the topology, the DC ZEDS system is spatially designed to improve survivability and redundancy by splitting the DC power distribution into a two-bus system – one on the port side, the other on the starboard – each being fed by a dedicated power supply. The power distribution system is subdivided into 3 zones (numbered forward to aft) that are separated by water-tight compartments as shown in Figure II.1.

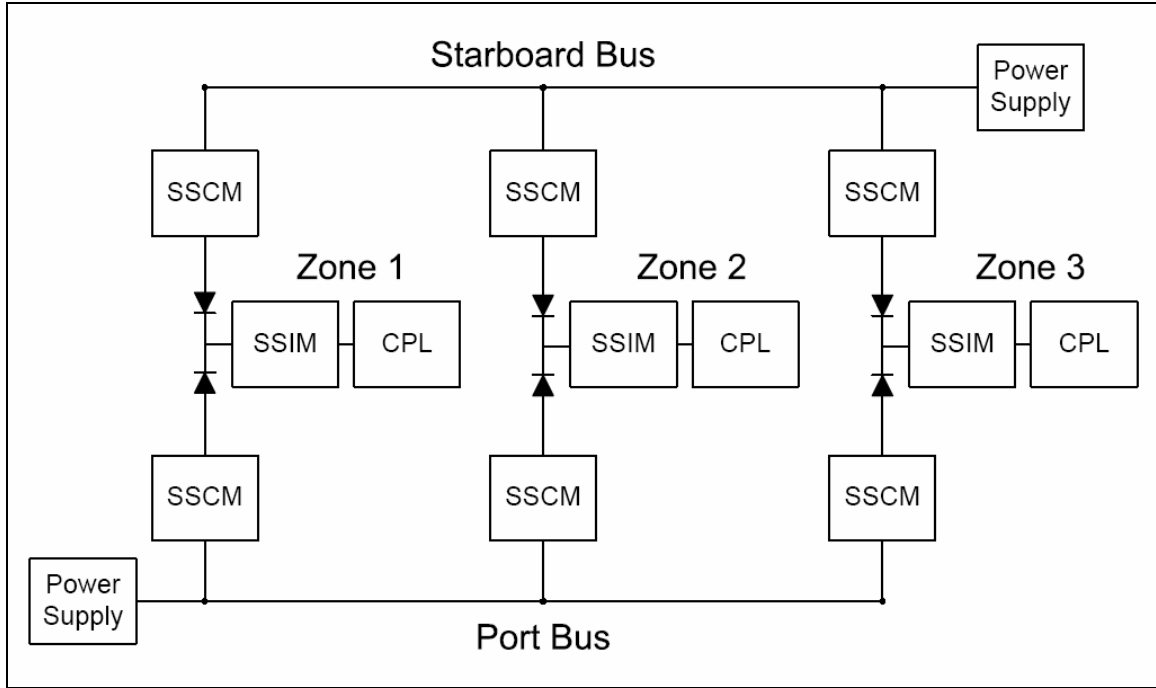


Figure II.1: DC Zonal Electrical Distribution System Topology

Within each zone, two Ship's Service Converter Modules (SSCM) are fed from the port bus and starboard bus, respectively. Both of their regulated voltage outputs are compared and all the zonal load current demand is supplied from the bus with the higher voltage. The converter modules have the capability to share power requirements in droop mode, but is not considered in this study. Opposing diodes on the lines leading to the

load prevent one bus from providing power to the other. The load in each zone is identical, consisting of a Ship's Service Inverter Module (SSIM) feeding an ac load bank.

If either power supply fails, the remaining bus will supply the entire load without interruption. Current limits on the SSCMs alleviate faults at the oring (diode) function while some faults within the modules are mitigated through robust controls. It should be noted here that the control scheme improves the robustness of the system, but this can have a masking effect on detecting and isolating faults. Further discussion on this will be addressed in a later chapter.

As stated before, there are two time-domain simulation models considered in this work: the Average Value Model (AVM) and the more accurate Detailed Model. Power electronics modeling experts have noted that a so-called 'detailed' model is unfortunate because the term is rather arbitrary, but have also documented its sufficient accuracy as a truth model for initial system analysis and control architecture simulations. For the purpose of this dissertation, which is consistent with the literature, 'detailed' refers to a simulation in which semiconductor switching action is included, even if only on an on or off basis. By comparison, the nonlinear average value model refers to simulations where the switching is represented on an average value basis resulting in state variables constant in the steady state. Although the average value model removes the switching dynamics present in the detailed model, both models are comparable in every other respect, which includes parameter values, control architecture, dc steady state, and transient response.

By comparison, the detailed model is the more representative simulation of the DC ZEDS system, but the average value model provides the basis for the state space models used for Fault Diagnosis. The remaining part of the chapter describes these modules in more detail starting with the detailed model, followed by the nonlinear state space models of the average value model. It should be noted here that the red markings on each circuit diagram represent sensor measurements. By convention, a red sensor marking with a negative slope indicates a current sensor, while a positive slope indicates a voltage sensor (always measured with respect to ground). Finally, a frequency analysis of the two models is presented and a method is proposed to generate residuals based on the AVM state space models and measurement data from the Detailed Model.

B. MODULES

1. Power Supply

a. Detailed Model

Each 15 kW power supply is fed from a dedicated 3-phase ac source that may vary from 480 – 560 V line-to-line rms at 60 Hz and provides 500 V dc output to the bus. The power supply consists of an isolating transformer (modeled as part of the leakage inductance), a controlled 3-phase bridge rectifier, and dc link capacitance, inductance and resistance as shown in Figure II.2.

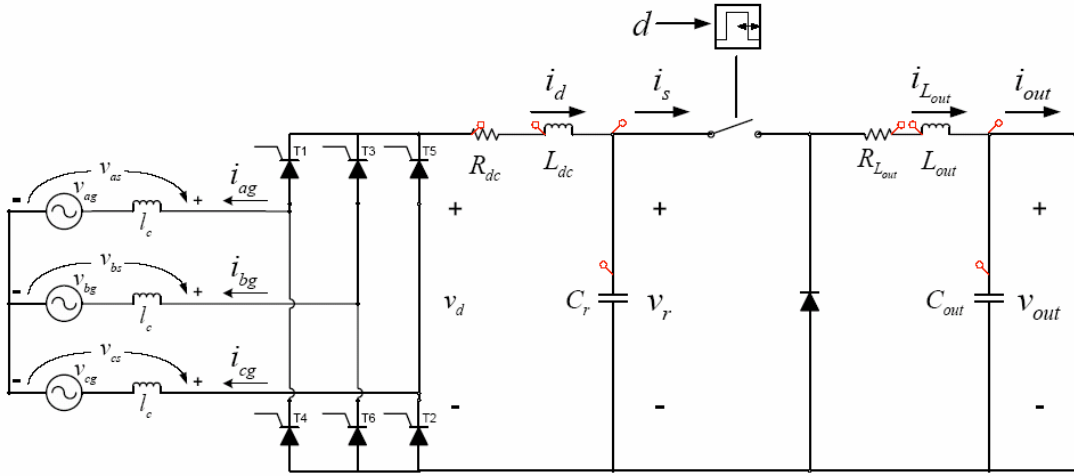


Figure II.2: Power Supply (detailed)

For the simulations herein, the uncontrolled rectifier mode is considered with a zero firing angle ($\alpha = 0$). The output voltage v_{out} is regulated by a buck converter/controller scheme connected to the output of the rectifier. Parameters for the system are shown in Table II.1.

Parameter	Description	Value	Units
l_c	Source Commutating Inductance	1.0	mH
R_{dc}	Rectifier Line resistance (dc link resistance)	0.03	Ω
L_{dc}	Rectifier line inductance (dc link inductance)	0	H
C_r	Rectifier output (dc capacitor)	500.0	μF
ω_g	Input ac voltage frequency	377	rad / sec
$R_{L_{out}}$	Buck controller line resistance	0.03	Ω
L_{out}	Buck controller line inductance	3.0	mH
C_{out}	Buck controller output capacitance	500.0	μF

Table II.1: Power Supply Parameters

b. Average Value Model

The average value model for the power supply is developed in [220] and makes the assumptions that the rms amplitude of the ac source voltages E is constant, only one commutation occurs at a time, and the dc load current i_{dc} is constant (or at least near-constant). The average value model makes several reference frame transformations of the input voltage to obtain the time-dependent peak voltage of the input, $\sqrt{2}E$. A more detailed derivation of the transformation is shown in Appendix B. Since the output waveform of the bridge rectifier circuit is periodic over a $\pi/3$ interval of the angular position of the source voltage θ_g , the average dc voltage can be expressed as

$$v_d = \frac{3}{\pi} \int_{\pi/3+\alpha}^{2\pi/3+\alpha} (v_{bs} - v_{cs}) d\theta_g. \quad (0.2)$$

With further substitution and simplification, the average dc voltage from the rectifier can be expressed as

$$v_d = \frac{3\sqrt{3}}{\pi} \sqrt{2} E \cos \alpha \quad (0.3)$$

and the average dc current i_d is a state in the average value model as shown in Figure II.3.

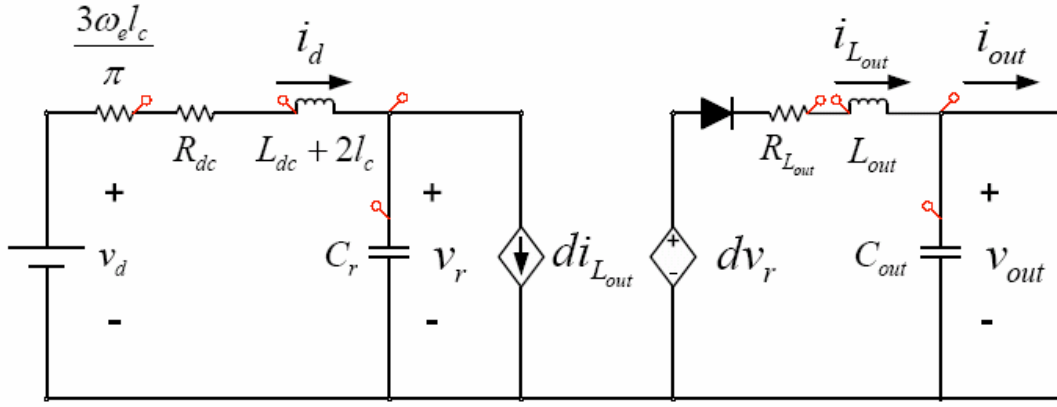


Figure II.3: Power Supply Average Value Model

From the model in Figure II.3, the power supply rectifier and buck converter are dynamically coupled through a current and voltage source dependent on the duty cycle d , which is the control input used to regulate the output voltage v_{out} .

c. Power Supply Control

The power supply controller design is shown in Figure II.4 with its associated parameters listed in Table II.2.

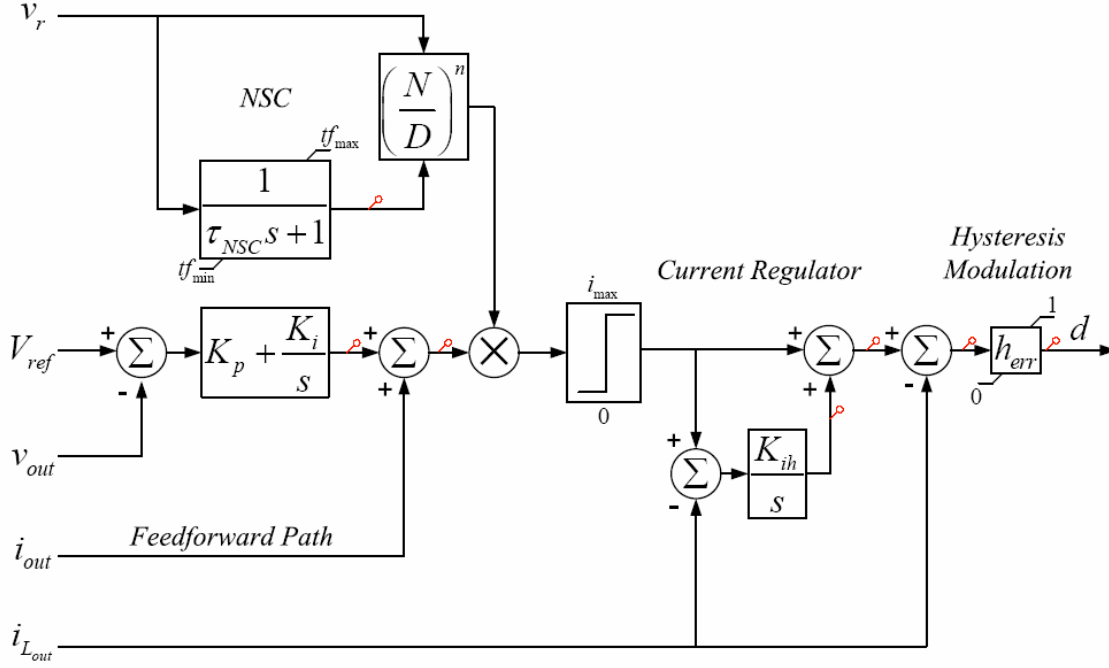


Figure II.4: Power Supply Control

The nonlinear controller allows for voltage and current regulation as it calculates the control signal d that determines the on/off state of the switch. For the average value model, d is the duty cycle of the input state. The measured output voltage v_{out} is compared with the reference voltage V_{ref} and the error signal is fed through a proportional plus integral (PI) controller. To provide a fast response to changes in load, the load current i_{out} is added to the output of the PI controller and is multiplied by the output of nonlinear stabilizing control (NSC), which has a scaling effect on the influence of the output voltage and current. The resulting reference current signal is bounded and compared with the measured current $i_{L_{out}}$ in the current regulator. The output of the current regulator is used for the hysteresis modulator so that the actual current closely tracks the measured current.

Parameter	Description	Value	Units
V_{ref}	Reference voltage (command output voltage)	500.0	V
i_{max}	Maximum command current	40.0	A
K_p	PI controller, proportional gain	1.0	
K_i	PI controller, integral gain	100.0	
K_{ih}	Current regulator, integral gain	100.0	
n	NSC exponent	1.0	
h_{err}	Hysteresis error bandwidth	1.0	A
$K_{i,max}$	PI controller, integral gain output max	100.0	
$K_{i,min}$	PI controller, integral gain output min	-100.0	
tf_{max}	NSC Transfer Function output max	1000.0	
tf_{min}	NSC Transfer Function output min	400.0	

Table II.2: Power Supply Control Parameters

d. Nonlinear State Space Model

Looking at the power supply average value model circuit in Figure II.3, the inputs to the system can be defined as

$$\underline{u} = \begin{bmatrix} u_1 \\ u_2 \\ u_3 \\ u_4 \end{bmatrix} = \begin{bmatrix} \sqrt{2}E \\ di_{L_{out}} \\ dv_r \\ i_{L_{out}} \end{bmatrix}.$$

If the controller is considered external to the model, the control signal d can be viewed as an external input dynamically coupled to states of the system. In this manner, nonlinear terms are defined as external inputs u_2 and u_3 . The model is then expressed as a linear state space model driven by inputs u_1 and u_4 with a decoupled nonlinear term as shown

$$\dot{x} = A_{ps}x + B_{1,ps} \begin{bmatrix} u_1 \\ u_4 \end{bmatrix} + B_{2,ps} \begin{bmatrix} u_2 \\ u_3 \end{bmatrix}, \quad (0.4)$$

where

$$A_{ps} = \begin{bmatrix} \frac{-(R_{dc} + 3\omega_g l_c / \pi)}{L_{dc} + 2L_c} & \frac{-1}{L_{dc} + 2L_c} & 0 & 0 \\ \frac{1}{C_r} & 0 & 0 & 0 \\ 0 & 0 & \frac{-R_{L_{out}}}{L_{out}} & \frac{-1}{L_{out}} \\ 0 & 0 & \frac{1}{C_{out}} & 0 \end{bmatrix}, \quad B_{1,ps} = \begin{bmatrix} \frac{3\sqrt{3}}{\pi(L_{dc} + 2l_c)} & 0 \\ 0 & 0 \\ 0 & 0 \\ 0 & \frac{-1}{C_{out}} \end{bmatrix}, \quad B_{2,ps} = \begin{bmatrix} 0 & 0 \\ \frac{-1}{C_r} & 0 \\ 0 & \frac{1}{L_{out}} \\ 0 & 0 \end{bmatrix},$$

and the output equations are chosen as

$$y = \begin{bmatrix} 1 & 0 & 0 & 0 \\ 0 & 1 & 0 & 0 \\ \frac{-3\omega_g l_c}{\pi} & 0 & 0 & 0 \\ 1 & 0 & 0 & 0 \\ 0 & 0 & 1 & 0 \\ 0 & 0 & 0 & 1 \\ 0 & 0 & -R_{L_{out}} & 0 \\ 0 & 0 & 1 & 0 \end{bmatrix} x + \begin{bmatrix} 0 & 0 \\ 0 & 0 \\ 1 & 0 \\ 0 & 0 \\ 0 & 0 \\ 0 & 0 \\ 0 & 0 \\ 0 & -1 \end{bmatrix} \begin{bmatrix} u_1 \\ u_4 \end{bmatrix} + \begin{bmatrix} 0 & 0 \\ 0 & 0 \\ 0 & 0 \\ -1 & 0 \\ 0 & 0 \\ 0 & 0 \\ 0 & 1 \\ 0 & 0 \end{bmatrix} \begin{bmatrix} u_2 \\ u_3 \end{bmatrix}. \quad (0.5)$$

Although the dynamic model has only four states, we included a larger number of observations for the purpose of redundancy and fault detection. Figure II.5 shows a simulation of the power supply, plotting the input and output voltage for both the detailed and average value models. Therein, the input voltage is shown to have the same dc value between the two models, but the detailed model shows a small amount of ac content and switching dynamics. The output, however, is nearly identical.

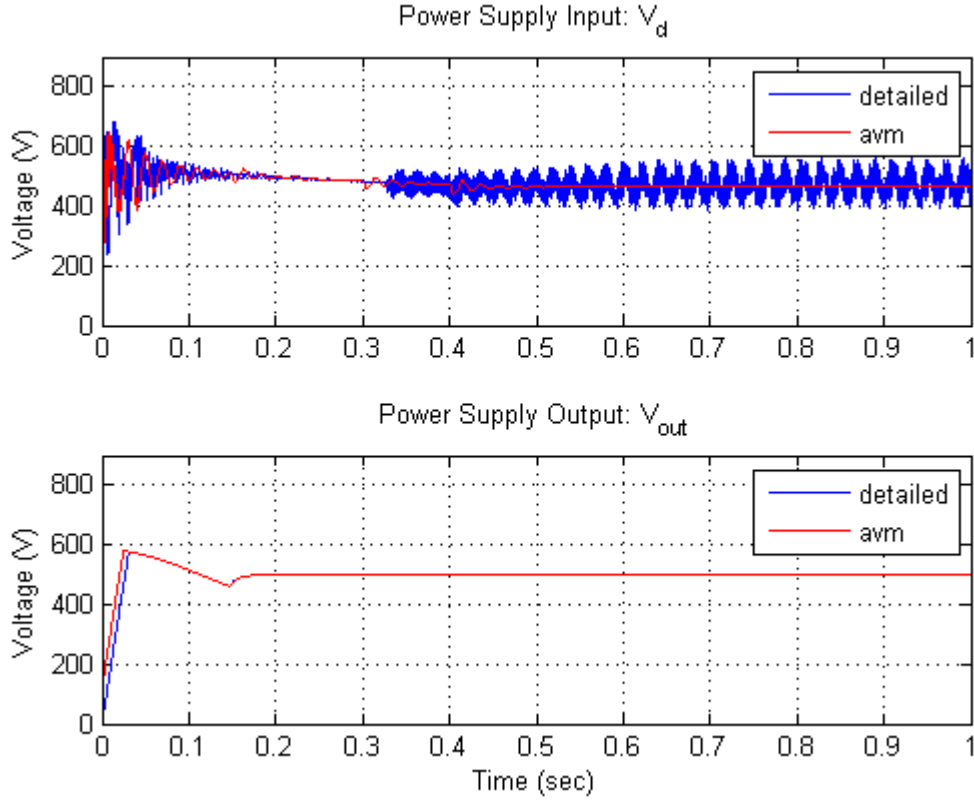


Figure II.5: Comparison of Detailed and Average Value Models of the Power Supply

2. Bus

The bus model connects the power supply to the SSCM in each zone. It is a medium length Nominal-T circuit transmission model with switches separating the three zones as shown in Figure II.6. The series impedance and shunt admittance parameters are equivalent in each zone and are shown in Table II.3.

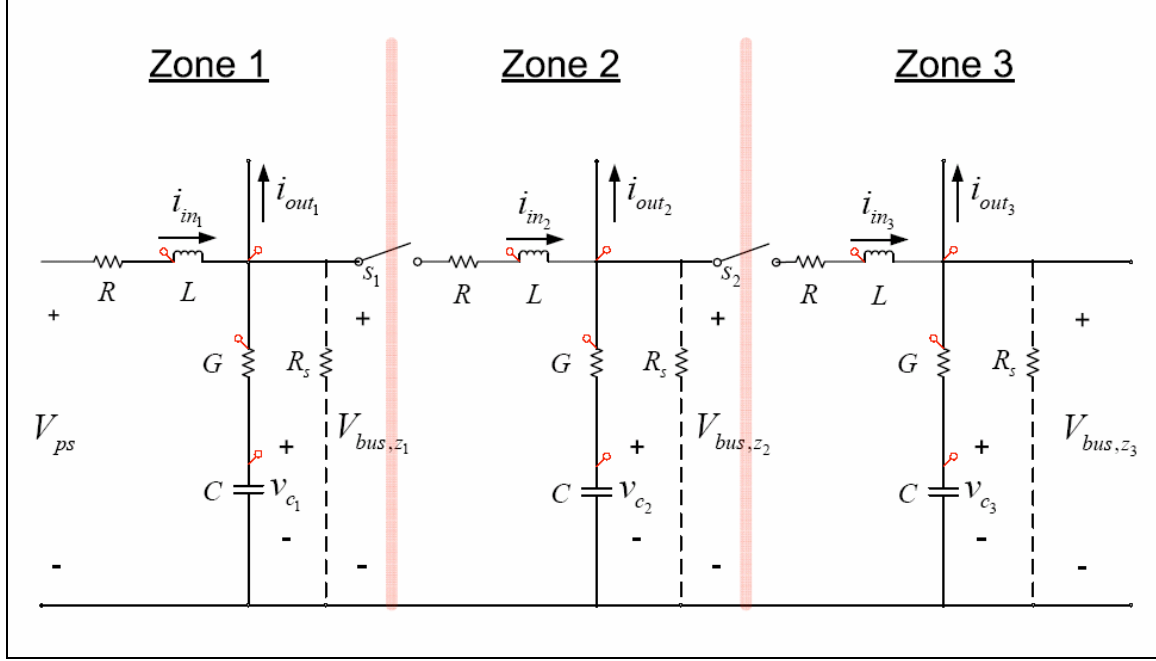


Figure II.6: Bus Model

Parameter	Description	Value	Units
R	Bus line resistance	34.0	$m\Omega$
L	Bus line inductance	2.26	μH
C	Bus shunt line capacitance	0.5	μF
G	Bus shunt line admittance	10.0	Ω^{-1}
R_s	Bus zone short line resistance	1.0	Ω

Table II.3: Bus Model Parameters

Included in the bus model is a shunt resistance R_s used to model bus shorts. During no-fault operations, the shunt resistance is infinite to model an open line. While not part of the power electronics modules, the bus model has proven to be quite an

important link between modules. Generalized forms of the bus model are developed such that n zones can be considered on larger scale systems.

a. Six-state Bus Model

Consider three operating modes of the bus system where Mode 1 represents the power supply providing power to Zone 1 only, Mode 2 is where Zone 1 and Zone 2 are energized, and Mode 3 is where all 3 zones are energized. The mode switch configurations for each zone are described in Table II.4.

	Switch s_1	Switch s_2
Mode 1	Open	Closed
Mode2	Closed	Open
Mode 3	Closed	Closed

Table II.4: Bus Zone Switch Configuration

It is desired to express the bus model in matrix equation form. From Kirchhoff's conservation laws, the following equations are derived from the circuit in Figure II.6:

$$\dot{\underline{x}} = -\frac{R}{L}\underline{x} + \frac{1}{L}\tilde{Q}_m v_z + \frac{1}{L}S\underline{u} \quad (0.6)$$

$$\underline{i}_z = -\tilde{Q}_m^T \underline{x} - \frac{1}{R_s} v_z - M\underline{u} \quad (0.7)$$

$$v_z = \frac{1}{G}\underline{i}_z + \underline{z} \quad (0.8)$$

$$\dot{\underline{z}} = \frac{1}{C}\underline{i}_z, \quad (0.9)$$

where

$$\underline{u} = \begin{bmatrix} u_1 \\ u_2 \\ u_3 \\ u_4 \end{bmatrix} = \begin{bmatrix} i_{bz_1} \\ i_{bz_2} \\ i_{bz_3} \\ v_{ps} \end{bmatrix}$$

$$\underline{x} = \begin{bmatrix} x_1 & x_2 & x_3 \end{bmatrix}^T \equiv \text{bus current through zones ,}$$

$$\underline{z} = \begin{bmatrix} z_1 & z_2 & z_3 \end{bmatrix}^T \equiv \text{voltage across zone shunt capacitance ,}$$

$$v_z = \begin{bmatrix} v_{z_1} & v_{z_2} & v_{z_3} \end{bmatrix} \equiv \text{zone bus voltage , and}$$

$$i_z = \begin{bmatrix} i_{z_1} & i_{z_2} & i_{z_3} \end{bmatrix} \equiv \text{zone shunt admittance line current .}$$

From equations (0.6) through (0.9), it can be shown that the six-state model can be expressed as

$$\begin{bmatrix} \dot{\underline{x}} \\ \dot{\underline{z}} \end{bmatrix} = \begin{bmatrix} -\frac{R}{L} \left(I + \frac{1}{R\tilde{G}} \tilde{Q}_m \tilde{Q}_m^T \right) & \frac{G}{L\tilde{G}} \tilde{Q} T_x \\ -\frac{G}{C\tilde{G}} T_x \tilde{Q}_m^T & -\frac{G}{R_s C\tilde{G}} I \end{bmatrix} \begin{bmatrix} \underline{x} \\ \underline{z} \end{bmatrix} + \begin{bmatrix} -\frac{1}{L} \left(s - \frac{1}{\tilde{G}} \tilde{Q}_m M \right) \\ -\frac{G}{C\tilde{G}} M \end{bmatrix} \underline{u} \quad (0.10)$$

with output equations

$$\begin{bmatrix} \underline{x} \\ \underline{z} \\ v_z \\ i_z \end{bmatrix} = \begin{bmatrix} I_6 & \\ & \frac{1}{\tilde{G}} T_x \tilde{Q}^T & \frac{G}{\tilde{G}} I_3 \\ & -\frac{G}{\tilde{G}} T_x \tilde{Q}^T & -\frac{G}{R_s \tilde{G}} I_3 \end{bmatrix} \begin{bmatrix} \underline{x} \\ \underline{z} \end{bmatrix} + \begin{bmatrix} 0_{6 \times 4} \\ -\frac{1}{\tilde{G}} M \\ -\frac{G}{\tilde{G}} M \end{bmatrix} \underline{u} \quad (0.11)$$

where

$$\tilde{G} = G + \frac{1}{R_s}, \quad (0.12)$$

$$M = \begin{bmatrix} 1 & 0 & 0 & 0 \\ 0 & 1 & 0 & 0 \\ 0 & 0 & 1 & 0 \end{bmatrix}, \quad (0.13)$$

and

$$S = \begin{bmatrix} 0 & 0 & 0 & 0 \\ 0 & 0 & 0 & 0 \\ 0 & 0 & 0 & 1 \end{bmatrix}. \quad (0.14)$$

The effective conductance \tilde{G} shown in (0.12) includes the shunt resistance term used in modeling a bus short. Under no-fault conditions, the shunt resistance line in Figure II.6 is modeled as an open circuit ($R_s = \infty$). The model also includes the three mode configurations with the matrix \tilde{Q}_m defined as

$$\tilde{Q}_m = \begin{cases} \begin{bmatrix} 0 & 0 & -1 \\ 1 & -1 & 0 \\ -1 & 0 & 0 \end{bmatrix}, m=1 \text{ (mode 1)} \\ \begin{bmatrix} 0 & 1 & -1 \\ 0 & -1 & 0 \\ -1 & 0 & 0 \end{bmatrix}, m=2 \text{ (mode 2)} \\ \begin{bmatrix} 0 & 1 & -1 \\ 1 & -1 & 0 \\ -1 & 0 & 0 \end{bmatrix}, m=3 \text{ (mode 3)} \end{cases}$$

Note: $\tilde{Q}_2 = \tilde{Q}_1^T$ and $\tilde{Q}_3 = \tilde{Q}_3^T$.

State ordering assignments for the port and starboard busses are also considered in the model using the transformations

$$T_{port} = \begin{bmatrix} 1 & 0 & 0 \\ 0 & 1 & 0 \\ 0 & 0 & 1 \end{bmatrix} \quad \text{and} \quad T_{stbd} = \begin{bmatrix} 0 & 0 & 1 \\ 0 & 1 & 0 \\ 1 & 0 & 0 \end{bmatrix}$$

to account for opposite-side state numbering. To demonstrate the bus model, a baseline scenario is identified for all fault diagnosis experiments. In further chapters, any induced system faults will reference the baseline system dynamics for analysis. Table II.5 defines the nominal plant configuration.

	Zone 1	Zone 2	Zone 3
Load on (sec)	0.4	0.3	0.4
Stbd SSCM v_{ref} (V)	400	400	390
Port SSCM v_{ref} (V)	380	410	410

Table II.5: DC ZEDS Baseline Scenario Parameters

Herein, both busses are in Mode 3 with all six SSCMs on at the start of the simulation. Each zone supplies an identical constant power load of 5.65 kW. From the Oring Function dynamics, current is supplied from the starboard bus in zone 1 and from the port bus in zones 2 and 3. Figures II.7 – II.9 show an example of the bus current distribution of the DC ZEDS baseline scenario for both the detailed and average value models.

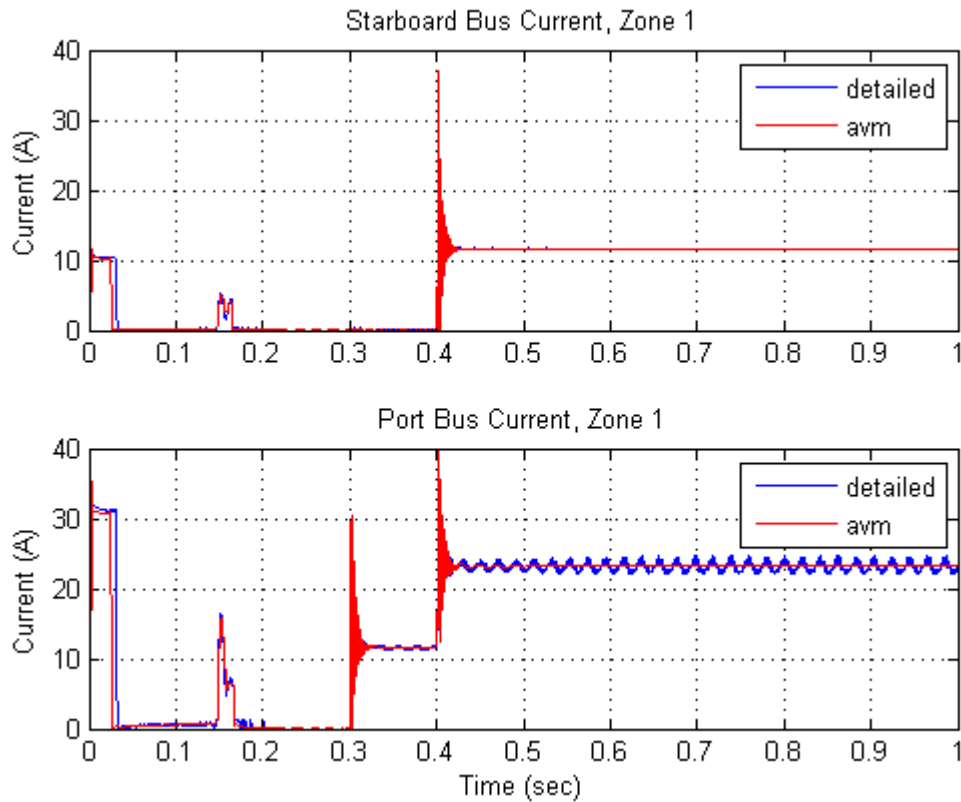


Figure II.7: DC ZEDS Baseline Scenario Bus Current Distribution, Zone 1

From the results in Figure II.7, it can be seen that the load in each zone requires about 12 Amps. For Zone 1, the port bus (bottom) is directly connected to the port power supply, which shows current flowing through to Zone 2 at $t=0.3$ seconds. An additional 12 Amps is added to the port bus, which is being sent to Zone 3 at $t=0.4$ sec.

The starboard bus (top) is at the end of the line since it is directly connected to Zone 3 at the opposite end. Here, Figures II.7 – II.9 show that the starboard bus only feeds Zone 1.

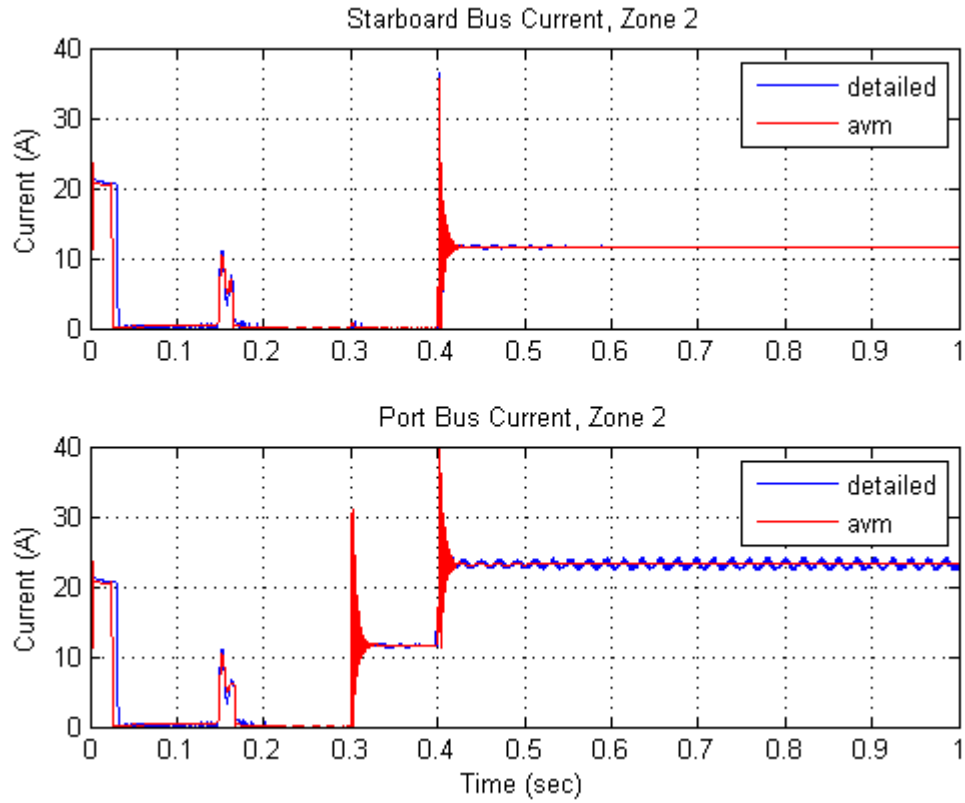


Figure II.8: DC ZEDS Baseline Scenario Bus Current Distribution, Zone 2

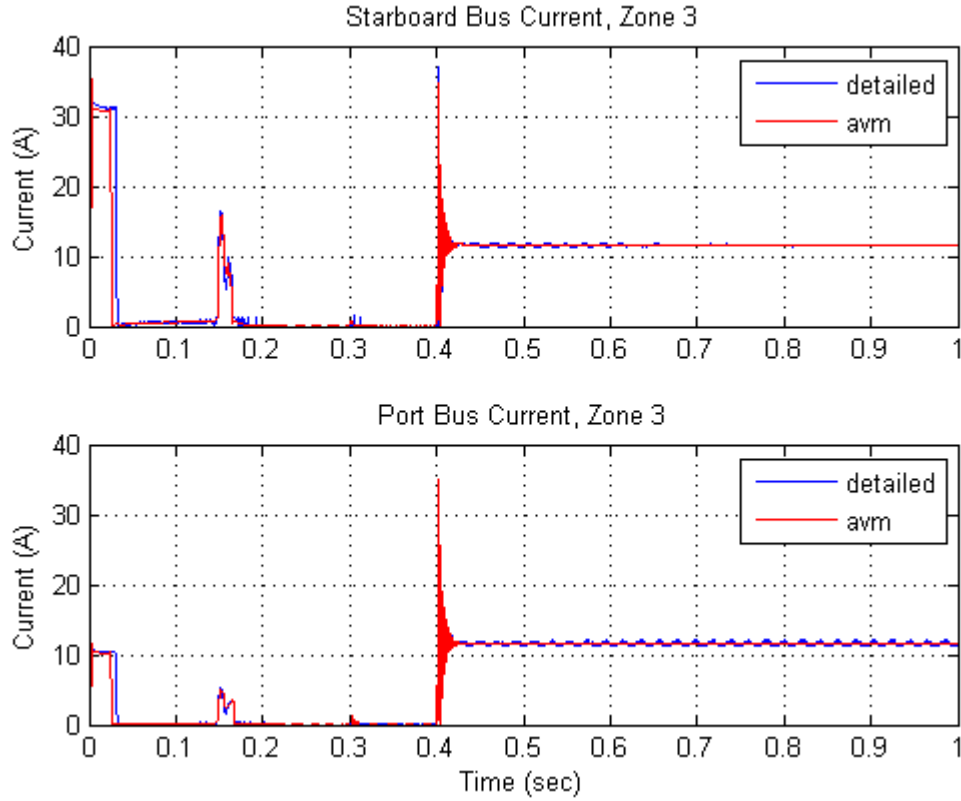


Figure II.9: DC ZEDS Baseline Scenario Bus Current Distribution, Zone 3

b. Three-state Bus Model

The three-state bus model uses the same parameter values as the six-state model as shown in Table II.3 with the exception of completely passive line impedance in each zone. This is equivalent to setting the line inductance L to zero. From a modeling and simulation point of view, the states to describe the dynamics of the bus current can no longer be found by integration, but by algebraic relationship. The six-state model is essentially a double-cascaded, medium length Normal-T circuit transmission line model described in [323]. The energy storage elements are very small and equate to transient dynamics three orders of magnitude faster than that of the power electronics. It also implies that most of the power is transferred from the power supply to the SSCMs with very little energy storage in the bus, which is desired. Reducing the number of states may improve the realism of the model, but might incur unresolved algebraic loops in the

model. It will be shown that a three-state model can be derived and is demonstrated to be useful for input estimation on the unknown input observers.

To begin the model derivation, the same matrix definitions are used except this time the three modes are expressed as subspace projections of the full mode. Consider the bus model in Figure II.6 and the switching configurations in Table II.4. If the bus is operating in the full mode (Mode 3), it can be represented as an orthogonal basis in three dimensions as

$$q_3 = I_3,$$

with each column (x, y, z from left to right) representing the bus current through Zone 3, Zone 2, and Zone 1 (from left to right) respectively. The numbering convention in reverse order is an unfortunate result of having 2 power supplies entering the DC ZEDS system from opposite zones. Each lesser mode can be expressed as a subspace basis of q_3 . For example, the Mode 2 basis spans the $y-z$ plane as

$$q_2 = \begin{bmatrix} 0 & 0 \\ 1 & 0 \\ 0 & 1 \end{bmatrix},$$

while the Mode 1 basis spans the $x-z$ plane as

$$q_1 = \begin{bmatrix} 1 & 0 \\ 0 & 0 \\ 0 & 1 \end{bmatrix}.$$

In a physical sense, the Mode 2 basis describes opening the switch between Zone 2 and Zone 3, which sets the current in Zone 3 to zero and the dynamics follow. Likewise the Mode 1 basis is like opening the switch between Zone 1 and Zone 2, which sets the current in Zone 2 to zero. Now define the mode projection matrix as

$$P_m = q_m \left(q_m^T q_m \right)^{-1} q_m^T$$

where $m = 1, 2, 3$ denotes the mode. Removing the inductance in the bus line changes the dynamics of the bus and shunt line current Kirchhoff law equations to

$$\underline{x} = \frac{1}{R} Q v_z + \frac{1}{R} S \underline{u} \quad (0.15)$$

and

$$i_z = -Q \underline{x} - M \underline{u} . \quad (0.16)$$

With some substitution and algebra on equations (0.8), (0.9), (0.15) and (0.16), the three-state model is expressed as

$$\dot{\underline{z}} = -\frac{G}{C\tilde{G}} \left(T_x Q C_1 + \frac{1}{R_s} I \right) \underline{z} - \frac{G}{C\tilde{G}} (T_x Q D_1 + M) \underline{u} \quad (0.17)$$

Where G , \tilde{G} , T_x , C , R , R_s , and M are the same as in the six-state model and

$$Q = \begin{bmatrix} 0 & 1 & -1 \\ 1 & -1 & 0 \\ -1 & 0 & 0 \end{bmatrix}.$$

The corresponding output equations (defined similarly to the six-state model) are

$$\begin{bmatrix} \underline{x} \\ \underline{z} \\ v_z \\ i_z \end{bmatrix} = \begin{bmatrix} C_1 \\ C_2 \\ C_3 \\ C_4 \end{bmatrix} \underline{z} + \begin{bmatrix} D_1 \\ D_2 \\ D_3 \\ D_4 \end{bmatrix} \underline{u} \quad (0.18)$$

where

$$C_1 = \frac{G}{R\tilde{G}} \left(I + \frac{1}{R\tilde{G}} P_m Q^2 \right)^{-1} P_m Q T_x$$

$$C_2 = I$$

$$C_3 = -\frac{1}{\tilde{G}} (TQ C_1 - GI)$$

$$C_4 = -\frac{G}{\tilde{G}} \left(TQ C_1 + \frac{1}{R_s} I \right)$$

and

$$\begin{aligned}
D_1 &= \frac{1}{R} \left(I + \frac{1}{R\tilde{G}} P_m Q^2 \right)^{-1} P_m \left(S - \frac{1}{\tilde{G}} Q T_x M \right) \\
D_2 &= 0 \\
D_3 &= -\frac{1}{\tilde{G}} (T_x Q D_1 + M) \\
D_4 &= -\frac{G}{\tilde{G}} (T_x Q D_1 + M).
\end{aligned}$$

The properties of the 3-state model show that the D matrix is full rank, which turns out to be important for full input estimates from unknown input observers as will be explained in the following chapter.

3. Ship's Service Converter Module

The purpose of the Ship's Service Converter Module (SSCM) is to step the bus voltage down to an acceptable power quality and rating for zonal loads. As shown in Figure II.1, the DC ZEDS system has 2 SSCMs in each zone – one receiving input power from the port bus, and the other from the starboard. All six SSCMs are identical in topology and parameters. Rated at 8 kW, the SSCM accepts a 500 V input (that may vary) and provides a clean, 400 V output and a maximum of 20 Amps.

a. Detailed Model

The SSCM topology is a standard Buck Converter as shown in Figure II.10 with parameters listed in Table II.6. The signal d for the detailed model controls the semiconductor switch position to achieve the desired command voltage.

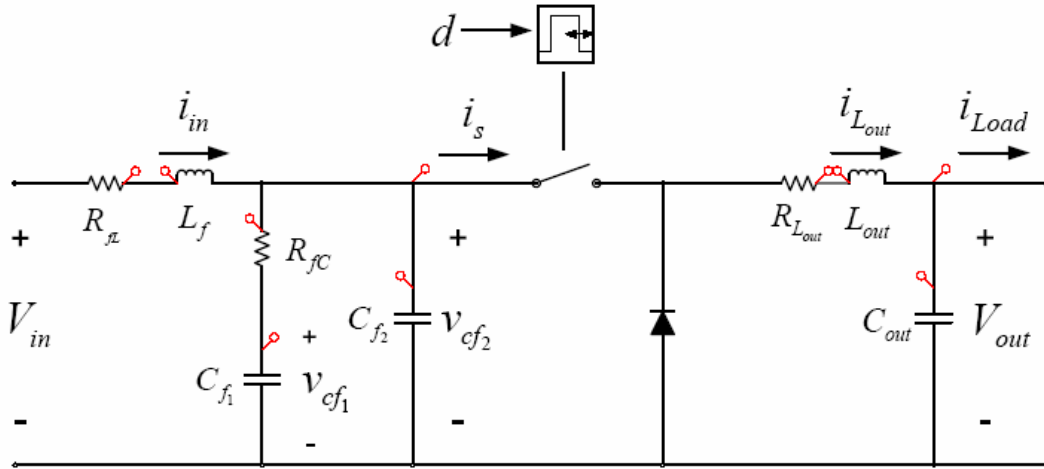


Figure II.10: Ship's Service Converter Module Circuit

Parameter	Description	Value	Units
L_f	Input filter inductor	357.0	μH
R_{fL}	Input inductor resistance	0.2	Ω
C_{f1}	Input filter capacitor 1	500.0	μF
R_{fC}	Input filter series resistor	1.0	Ω
C_{f2}	Input filter capacitor 2	45.0	μF
C_{out}	Buck Converter output capacitor	500.0	μF
L_{out}	Buck Converter dc inductor	3.0	mH
$R_{L_{out}}$	Resistance of the dc inductor	0.5	Ω
P_{out}	Rated power output	8.0	kW

Table II.6: SSCM Parameters

b. Average Value Model

Similar to the power supply model, the SSCM average value model simulates a fast-average of the semiconductor switching dynamics of the detailed model such that state variables are constant in steady state. Again, the average value model maintains transient response accuracy and implements the same model and control parameters. The model topology depicted in Figure II.11 shows the averaged command signal (duty cycle) d being multiplied by states of the system, which acts as a dependent voltage and current source.

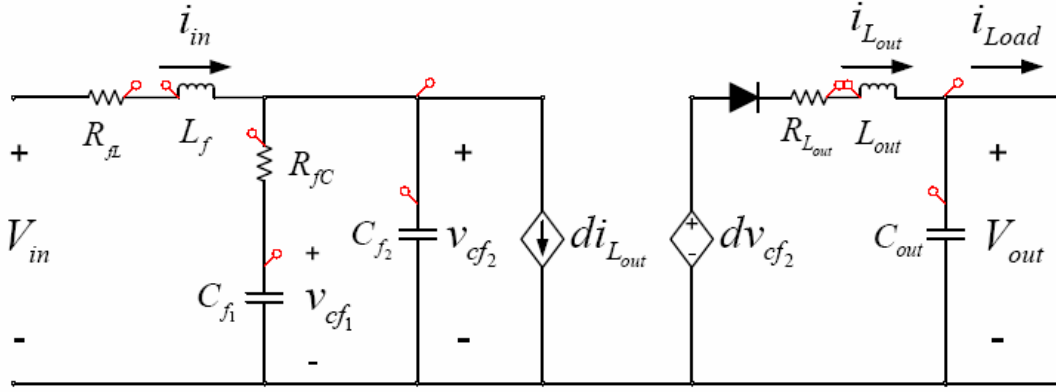


Figure II.11: SSCM Average Value Model Topology

c. SSCM Control

Because of the fast semiconductor switching action of the SSCM and near-ideal nature of the control scheme, the desired output voltage can be met even in the presence of input disturbances. For this DC ZEDS model, the controller design is depicted in Figure II.12 with associated parameters listed in Table II.7.

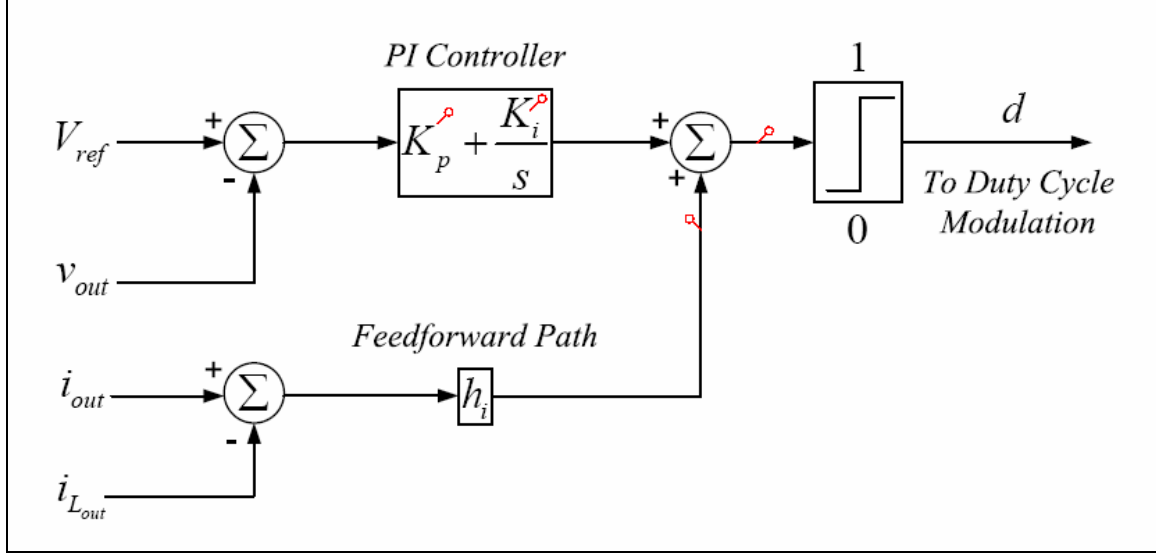


Figure II.12: SSCM Control Architecture

Parameter	Description	Value	Units
V_{ref}	Output reference voltage	400.0	V
K_p	PI controller, proportional gain	0.1	
K_i	PI controller, integral gain	23.0	
h_i	Current feedforward proportional gain	0.015	
f_{sw}	switching frequency	20.0	kHz

Table II.7: SSCM Control Parameters

Here, the output voltage is regulated through a PI controller design (with gains K_p and K_i). For simultaneous current regulation the error signal, based on the difference between i_{out} and i_{Lout} and scaled by h_i , is placed on the feedforward path and added to the PI control output.

d. Nonlinear State Space Model

Similar to the power supply model, the control signal d is viewed as external to the model and dynamically coupled to states of the system such that the inputs can be defined as

$$\underline{u} = \begin{bmatrix} u_1 \\ u_2 \\ u_3 \\ u_4 \end{bmatrix} = \begin{bmatrix} V_{in} \\ di_{L_{out}} \\ dv_{cf_2} \\ i_{L_{out}} \end{bmatrix}.$$

In the same manner as the power supply model, nonlinear terms are expressed as unknown inputs while the remaining linear dynamics can be viewed as 2 subsystems (pre-filter and buck portions) coupled together as shown:

$$\dot{x} = A_{sscm}x + B_{1,sscm} \begin{bmatrix} u_1 \\ u_4 \end{bmatrix} + B_{2,sscm} \begin{bmatrix} u_2 \\ u_3 \end{bmatrix} \quad (0.19)$$

with plant dynamics

$$A_{sscm} = \begin{bmatrix} -\frac{R_{fL}}{L_f} & 0 & -\frac{1}{L_f} & 0 & 0 \\ 0 & -\frac{1}{R_{fC}C_{f_1}} & \frac{1}{R_{fC}C_{f_1}} & 0 & 0 \\ \frac{1}{C_{f_2}} & \frac{1}{R_{fC}C_{f_2}} & -\frac{1}{R_{fC}C_{f_2}} & 0 & 0 \\ 0 & 0 & 0 & -R_{L_{out}} & -1 \\ 0 & 0 & 0 & \frac{1}{C_{out}} & 0 \end{bmatrix},$$

and known and unknown input matrices associated with linear and nonlinear inputs

$$B_{1,sscm} = \begin{bmatrix} \frac{1}{L_f} & 0 \\ 0 & 0 \\ 0 & 0 \\ 0 & -\frac{1}{C_{out}} \\ 0 & 0 \end{bmatrix}, \quad B_{2,sscm} = \begin{bmatrix} 0 & 0 \\ 0 & 0 \\ -\frac{1}{C_{f_2}} & 0 \\ 0 & 0 \\ 0 & \frac{1}{L_{out}} \end{bmatrix}.$$

The states of the SSCM depicted in Figures II.10 and II.11 are the energy storage elements from left to right in the model as

$$x = \begin{bmatrix} i_{in} \\ v_{cf_1} \\ v_{cf_2} \\ i_{L_{out}} \\ v_{C_{out}} \end{bmatrix}.$$

It should be noted here that there is a limit to the direction of the current through the inductor path such that $i_{L_{out}}$ is always in the positive direction defined in Figure II.10 and Figure II.11. The model handles this state restriction by setting a lower bound on the integrator to zero. The output equations are defined as

$$y = \begin{bmatrix} 1 & 0 & 0 & 0 & 0 \\ 0 & 1 & 0 & 0 & 0 \\ 0 & 0 & 1 & 0 & 0 \\ 1 & \frac{1}{R_{fC}} & -\frac{1}{R_{fC}} & 0 & 0 \\ 1 & 0 & 0 & 0 & 0 \\ -R_{fL} & 0 & 0 & 0 & 0 \\ 0 & 0 & 0 & 1 & 0 \\ 0 & 0 & 0 & 0 & 1 \\ 0 & 0 & 0 & 0 & 1 \\ 0 & 0 & 0 & 0 & -R_{L_{out}} \end{bmatrix} x + \begin{bmatrix} 0 & 0 & 0 & 0 \\ 0 & 0 & 0 & 0 \\ 0 & 0 & 0 & 0 \\ 0 & 0 & 0 & 0 \\ 0 & -1 & 0 & 0 \\ 1 & 0 & 0 & 0 \\ 0 & 0 & 0 & 0 \\ 0 & 0 & 0 & 0 \\ 0 & 0 & 0 & -1 \\ 0 & 0 & 1 & 0 \end{bmatrix} \underline{u}. \quad (0.20)$$

Notice that the feed-through term in (0.20), defined as the D matrix, is full rank, which implies that full input estimation can be achieved from an unknown input observer. The SSCM model will be used as an example in the following chapter to demonstrate the unknown input observer methods with input reconstruction. Simulation results from the Zone 1, Starboard SSCM are shown in Figure II.13 where the DC ZEDS baseline scenario depicted in Table II.5 is used.

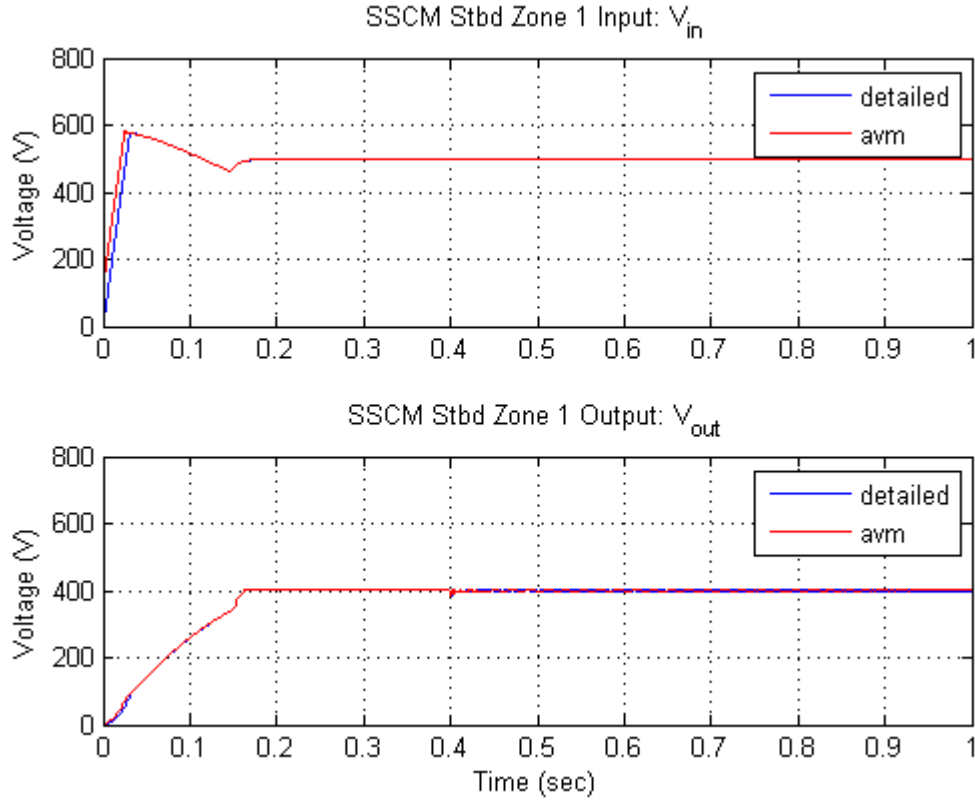


Figure II.13: Zone 1 Starboard SSCM Simulation Regulates 400 V Output (bottom) from 500 V Input (top)

4. Oring Function

The Oring function is the model in Figure II.1 that determines which bus supplies the power to the load in each zone. The port and starboard SSCMs have slightly different voltage regulation set points so that the SSCM output voltage with the higher set point picks up all of the required power to the load in the zone. The set points are close so that if the primary SSCM is lost, then the alternate SSCM picks up the load requirement at nearly the correct voltage. As an example, for the nominal simulation configuration shown in Table II.5, Zone 1 load current is supplied from the starboard bus as shown in Figure II.14.

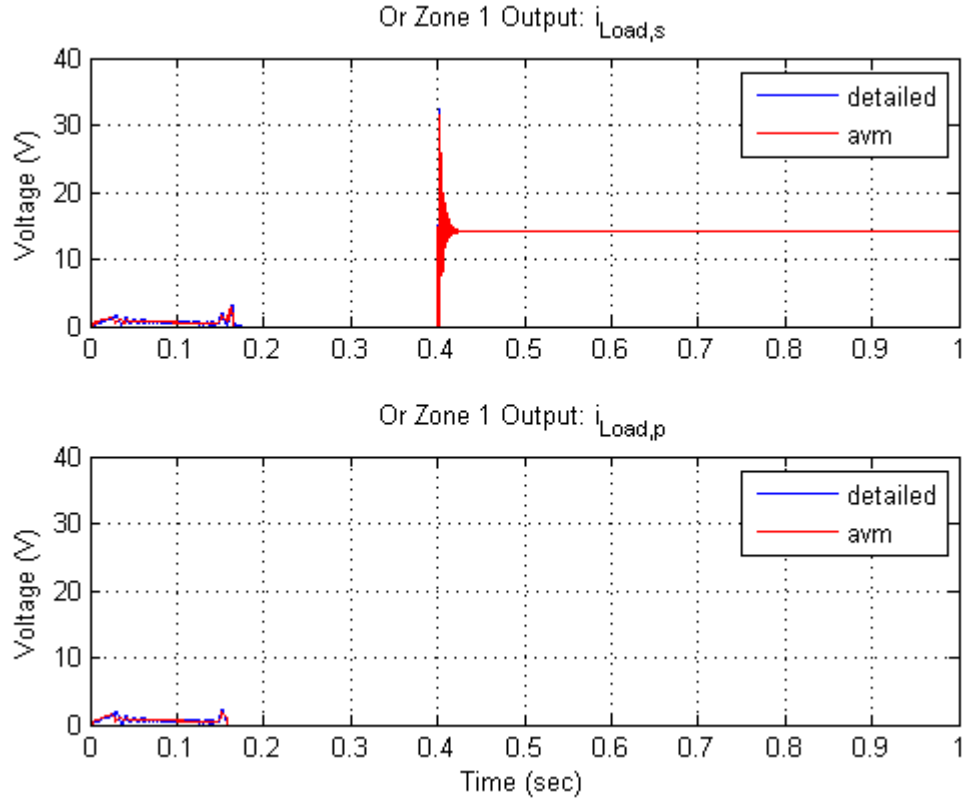


Figure II.14: Oring Function Simulation Results

The function is modeled as two voltage sources on opposite ends of a circuit providing current to a common constant power load through opposing diodes as shown in Figure II.15 and parameters detailed in Table II.8. If the inputs and states of the state space model are defined as (respectively)

$$\underline{u} = \begin{bmatrix} V_p \\ V_s \\ V_{load} \end{bmatrix} \quad \text{and} \quad \begin{bmatrix} x_p \\ x_s \end{bmatrix} = \begin{bmatrix} i_{Load,p} \\ i_{Load,s} \end{bmatrix},$$

then the state space model is defined as

$$\begin{bmatrix} \dot{x}_p \\ \dot{x}_s \end{bmatrix} = \begin{bmatrix} -\frac{R_{or}}{L_{or}} & 0 \\ 0 & -\frac{R_{or}}{L_{or}} \end{bmatrix} \begin{bmatrix} x_p \\ x_s \end{bmatrix} + \begin{bmatrix} \frac{1}{L_{or}} & 0 & -\frac{1}{L_{or}} \\ 0 & \frac{1}{L_{or}} & -\frac{1}{L_{or}} \end{bmatrix} \underline{u} \quad (0.21)$$

with output equations

$$y = \begin{bmatrix} 1 & 0 \\ 0 & 1 \\ 1 & 1 \\ -R_{or} & 0 \\ 0 & -R_{or} \end{bmatrix} \begin{bmatrix} x_p \\ x_s \end{bmatrix} + \begin{bmatrix} 0 & 0 & 0 \\ 0 & 0 & 0 \\ 0 & 0 & 0 \\ 1 & 0 & 0 \\ 0 & 1 & 0 \end{bmatrix} \underline{u}. \quad (0.22)$$

The opposing diodes in the model are simulated as lower bounds on the state integrators.

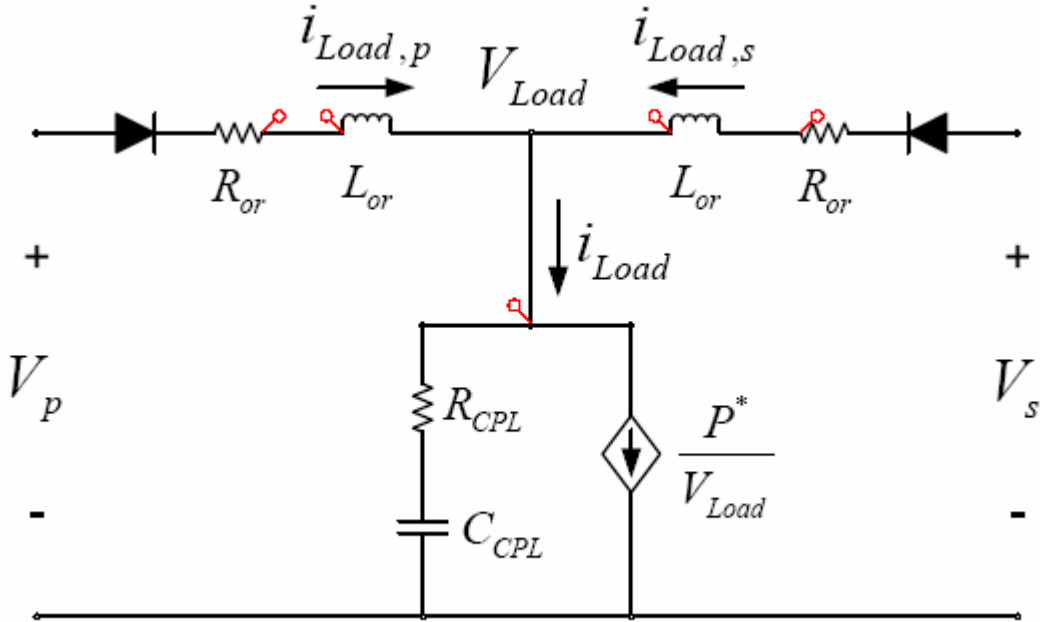


Figure II.15: Oring Function Circuit Model

Parameter	Description	Value	Units
R_{or}	Port/stbd line resistance	1.0	$m\Omega$
L_{or}	Port/stbd line inductance	100.0	μH

Table II.8: Oring Function Parameters

5. Inverter Module and Constant Power Load

According to the DC ZEDS model, the load in each zone is a Ship's Service Inverter Module – converting dc voltage back to ac – followed by a constant power load bank. Although the simulation model is more detailed, the relevant dynamics may be represented by a capacitor and effective series resistance in parallel with an ideal constant power load of 5.65 kW. Herein, the FDI analysis is conducted on the DC side of the power distribution system, which encompasses the rectifier dc input voltage of the Power Supply to the dc voltage and current leading to the SSIM in each zone.

C. METHOD FOR ANALYZING DC ZEDS SYSTEM

With respect to the complete set of state space models, including power supply and SSCM control, the DC ZEDS model is comprised of 21 distinct state space models with a total of 83 inputs, 159 outputs and 68 states. Among the inputs, 2 are external plus 8 reference voltage set points. The remaining 88% of inputs are either output measurements from connecting modules or nonlinear components that are a function of control signals and internal states. This fact demonstrates the high degree of dynamic interdependence between the modules and also the model's propensity to propagate faults from one module to another. Among all the output measurements, only about 30% of them are directly used as inputs to controllers or other DC ZEDS modules. The positioning of the remaining 70% of output measurements is based solely on enabling

observer sufficiency conditions for full-state and input estimation. In other words, almost 70% of the sensors throughout the DC ZEDS system are used exclusively for detecting faults and analytical redundancy.

It is shown that the average value model accurately represents the signature of the detailed model – even in the transient response. In steady state, a frequency analysis between the two models reveals additional frequency content in the detailed model due to the switching action and it can be made to closely resemble the AVM dynamics with a simple lowpass filter (cutoff frequency of 100 Hz).

THIS PAGE INTENTIONALLY LEFT BLANK

III. A POLYNOMIAL APPROACH TO DYNAMIC MODELING AND FAULT DETECTION

The fundamental framework to detecting fault characteristics in this work is based on analytical redundancy. Indeed, the large-scale dynamically interdependent DC ZEDS system must rely on mathematical models to provide fault indications for two main reasons: first, as outlined in Chapter I, it is efficient in terms of hardware invested compared to current methods [390][271][272][273][289][343][90]. The second reason is that the DC ZEDS model is well-defined as shown in Chapter II, which lends itself well to model-based estimation techniques[220][335]. By combining the physics-based dynamical models and sensor information, we compute estimates of the states of the DC ZEDS modules. Then, a comparison of the sensor measurements and their estimates is made, yielding residuals that are used as a measure of input-output consistency.

Perhaps the most widely used approach to generate residuals is to measure the consistency between observations and their prediction based on a mathematical model [60]. Standard approaches are the observer for deterministic linear and nonlinear models and the Kalman Filter for stochastic models. In both cases, the model-based estimation technique require knowledge of all inputs $u(t)$ and outputs $y(t)$. There are cases however (especially in residual generation), where it is desirable to estimate the system when one or more (perhaps even all) inputs are unknown. For example, it could be that the dynamical model of a system can be separated into linear and nonlinear parts and the nonlinear part could be modeled as an unknown input. Also, it might be desirable to remove the dynamical influence of a particular input from an observer estimate for the purpose of detecting and isolating actuator faults. In either case, it has been shown that unknown input observers are well-suited to solve the problem [110][175][297].

One such method to obtain an unknown input observer is the subspace method where the full state is estimated based on dynamics residing in a subspace of known inputs and outputs as stated in [170] and [175]. The conditions for UIO existence are proved in [60] and [230] in which a full-state unknown input observer is assumed.

To this goal, consider a dynamic system

$$\begin{cases} \dot{x}(t) = \Phi x + \Gamma_1 u_1(t) + \Gamma_2 u_2(t) \\ y(t) = Cx(t) \end{cases}$$

and we want to find conditions to estimate the state x without the input $u_2(t)$. This problem can be solved by decomposing the state in two components [175]

$$\begin{aligned} x &= (I - MC)x + MCx \\ &= q + My. \end{aligned}$$

The matrix M is chosen so that $(I - MC)$ is a projection matrix and $q = (I - MC)x$ is independent on the input $u_2(t)$. The component $q(t)$ satisfies the differential equation

$$\dot{q}(t) = (I - MC)\Phi x(t) + (I - MC)\Gamma_1 u_1(t) + (I - MC)\Gamma_2 u_2(t) \quad (0.23)$$

where $u_1(t)$ and $u_2(t)$ represents all the known and unknown inputs, respectively.

If M is such that

$$(I - MC)\Gamma_2 = 0 \quad (0.24)$$

$q(t)$ is clearly independent of $u_2(t)$. For a more detailed explanation of the subspace method, refer to Appendix C.

Lemma 4.1 *Equation (0.24) is solvable iff:*

$$\text{rank}(C\Gamma_2) = \text{rank}(\Gamma_2) \quad (0.25)$$

Proof: Necessity: When (0.24) has a solution M , it becomes $MC\Gamma_2 = \Gamma_2$ or

$$(C\Gamma_2)^T H^T = \Gamma_2^T$$

which means Γ_2 belongs to the range space of the matrix $(C\Gamma_2)^T$ resulting in:

$$\text{rank}(\Gamma_2^T) \leq \text{rank}((C\Gamma_2)^T)$$

and

$$\text{rank}(\Gamma_2) \leq \text{rank}(C\Gamma_2).$$

However,

$$\text{rank}(C\Gamma_2) \leq \min\{\text{rank}(C), \text{rank}(\Gamma_2)\} \leq \text{rank}(\Gamma)$$

Hence, $\text{rank}(\Gamma_2) = \text{rank}(C\Gamma_2)$ and the necessary condition is proved.

Sufficiency: When $\text{rank}(C\Gamma_2) = \text{rank}(\Gamma_2)$ holds true, $C\Gamma_2$ is a full column rank matrix (because Γ_2 is assumed to be full column rank), and a left inverse of $C\Gamma_2$ exists:

$$(C\Gamma_2)^\dagger = ((C\Gamma_2)^T C\Gamma_2)^{-1} (C\Gamma_2)^T$$

Clearly, $M = \Gamma_2 (C\Gamma_2)^\dagger$ is a solution to (0.24) [60]. The rank condition also implies that the number of independent output measurements must be greater than the number of unknown inputs [175].

A full-state UIO estimate is achievable if the rank condition (0.25) is satisfied. This condition can be rather restrictive. A simple example of a system in controllable canonical form would show that a necessary condition would be that at least one of the transfer functions to have a relative degree at most equal to one.

For the purpose of fault diagnosis, what is actually needed is a residual generator, not necessarily the full-state estimate. In the case where the full-state estimate is not achievable, it is still possible to compute the residual based on the partial state. The purpose of the polynomial method is to take advantage of this property by generating residuals based on the partial state.

The remainder of the chapter develops two unknown input observer (UIO) methods generalized to the multivariable case on a polynomial approach. The first process, called the input replacement method, is limited to a more restrictive class of systems, but has a simpler combined input and state Kalman estimation implementation algorithm suitable for fault diagnosis. By comparison, the second method (called the parametrization method), takes a more general class of systems and is based on the nonuniqueness property of the Diophantine equation to establish an unknown input Kalman estimation implementation. In both cases, a partial-state representation of the system is sought, which is directly related to the controllable canonical form.

A. DYNAMIC SYSTEMS AND THE PARTIAL STATE

1. Single Input Single Output (SISO) Systems

Consider a single input single output (SISO) system represented as a proper rational fraction of scalar polynomials $B(p)$ and $A(p)$ as shown in Figure III.1 and expressed as a transfer function along with its relationship to the state space realization in (0.26).

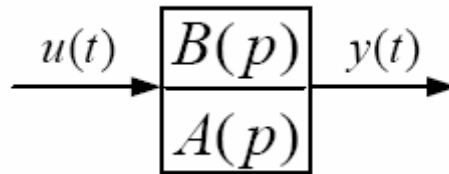


Figure III.1: SISO System in Transfer Function Form

$$H(p) = \frac{B(p)}{A(p)} = C(pI - \Phi)^{-1} \Gamma + D \quad (0.26)$$

The numerator $B(p)$ is of order n_s or at least of order $n_s - 1$ ($b_0 = 0$) for a proper or strictly proper transfer function $H(p)$, respectively, and is of the form

$$B(p) = b_0 p^{n_s} + b_1 p^{n_s-1} + b_2 p^{n_s-2} + \dots + b_{n_s}. \quad (0.27)$$

Likewise, let the denominator characteristic equation be a monic polynomial of order n_s as

$$A(p) = p^{n_s} + a_1 p^{n_s-1} + \dots + a_{n_s} \quad (0.28)$$

where p is the differential operator s in continuous time and the time-shift operator z in discrete time. If there are no common factors (i.e. no pole-zero cancellations) between $B(p)$ and $A(p)$, then the transfer function is said to be *coprime* and the system is a minimal realization. Now referring to Figure III.2, define $z(t)$ as the *partial state* [200] (or sometimes called the *pseudo state* [61]).

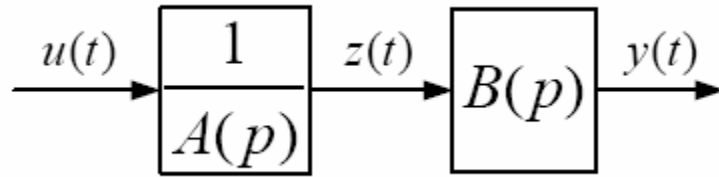


Figure III.2: Partial-state Space Representation of SISO System

It is easy to see that it can be related to the input and output signal, $u(t)$ and $y(t)$ as

$$A(p)z(t) = u(t) \quad (0.29)$$

$$y(t) = B(p)z(t) \quad (0.30)$$

The meaning of the partial state is that (0.26) can be related directly to the state of a controllable canonical form realization. Again, in the SISO case this is straightforward, since the state of the system is

$$\underline{z}(t) = \left[z(t), pz(t), \dots, p^{n_s-1}z(t) \right]^T \quad (0.31)$$

where $z(t)$ is a scalar and $\underline{z}(t) \in \mathbb{R}^{n_s}$.

2. Multiple Input Multiple Output (MIMO) Systems

Expanding the discussion of partial state to the more general multivariable case, consider the class of systems represented in state space as

$$px(t) = \Phi x(t) + \Gamma u(t) \quad (0.32)$$

$$y(t) = Cx(t) + Du(t) \quad (0.33)$$

where $x \in \mathbb{R}^{n_s}$, $u \in \mathbb{R}^{n_u}$, $y \in \mathbb{R}^{n_y}$ and Φ, Γ, C , and D are of appropriate dimensions. Again p in the state dynamics equation (0.32) denotes the differential operator in continuous time or the time-shift operator in discrete time and its notation is consistent throughout. Equations (0.32)-(0.33) can also be represented in transfer function form,

only the “numerator” $B(p)$ and “denominator” $A(p)$ are matrices whose elements are polynomials. Together, $H(p)$ is called the *transfer function matrix* or simply the *transfer matrix* and can be written as

$$H(p) = B(p)A^{-1}(p) \quad (0.34)$$

$$H(p) = \bar{A}^{-1}(p)\bar{B}(p) \quad (0.35)$$

The right fraction pair $B(p)$ and $A(p)$ has dimensions $n_y \times n_u$ and $n_u \times n_u$, respectively while the left fraction pair $\bar{A}(p)$ and $\bar{B}(p)$ has dimensions $n_y \times n_y$ and $n_y \times n_u$. The “denominator” polynomial matrices $A(p)$ and $\bar{A}(p)$ are always square. If the pair (Φ, Γ) is controllable and (Φ, C) observable then the system is a minimal realization, and the polynomial pairs $(B(p), A(p))$ and $(\bar{B}(p), \bar{A}(p))$ are mutually coprime. In the SISO case, this implies that the numerator and denominator polynomials have no common roots (no pole-zero cancellations). The more general MIMO case requires an appropriate extension of this concept, as shown in Appendix D. Under these conditions, the three representations

$$(\Phi, \Gamma, C, D)$$

in state space form,

$$(A(p), B(p))$$

in right polynomial matrix fraction form, and

$$(\bar{A}(p), \bar{B}(p))$$

in left polynomial matrix fraction form are equivalent and one can be computed from the other [61]. Of particular interest is the right coprime factorization in (0.34) which leads to the MIMO *partial-state* representation of the system shown in Figure III.3.

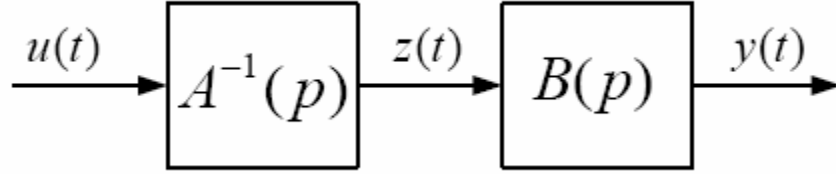


Figure III.3: Right Fraction Representation of MIMO System

By extension to the SISO systems, the partial state in the multivariable case is related to the input and output signals $u(t)$ and $y(t)$ of (0.29) and (0.30) and the system can be realized as

$$\begin{bmatrix} p^{\mu_1} z_1(t) \\ \vdots \\ p^{\mu_{n_u}} z_{n_u}(t) \end{bmatrix} = -A_h^{-1} A_l \underline{z}(t) + A_h^{-1} u(t) \quad (0.36)$$

$$y(t) = (B_l - B_h A_h^{-1} A_l) \underline{z}(t) + B_h A_h^{-1} u(t) \quad (0.37)$$

where the state space equations (0.36)-(0.37) are related to the original system (0.32)-(0.33) by a nonsingular matrix T such that

$$x(t) = T \underline{z}(t). \quad (0.38)$$

The matrices A_h , B_h are matrices of high degree coefficients whose dimensions are $n_u \times n_u$ and $n_y \times n_u$, respectively, and A_l , B_l are the matrices of all lower order coefficients with dimension $n_u \times n_s$ and $n_y \times n_s$, respectively. It should also be noted here that a method for determining T in (0.38) to transform the original system in (0.32)-(0.33) directly to control canonical form in (0.36)-(0.37) is found in [386]. A more detailed explanation of the system partial-state realization for the MIMO case is found in [61] and in Appendix D.

Similar to the vector of partial states (with derivatives) in (0.31) for the SISO case, we see that the partial state is a vector related to the system as

$$\underline{z}(t) = \left[z_1(t), \dots, p^{\mu_1-1} z_1(t) : z_2(t), \dots, p^{\mu_2-1} z_2(t) : \dots : z_{n_u}(t), \dots, p^{\mu_{n_u}-1} z_{n_u}(t) \right]^T \quad (0.39)$$

where $\underline{z}(t) \in \mathbb{R}^{n_s = \mu_1 + \mu_2 + \dots + \mu_{n_u}}$ and $\mu_1, \mu_2, \dots, \mu_{n_u}$ are called the *column degrees* (i.e. the maximum degree of the polynomials in each column) of the denominator matrix $A(p)$ and is related to the *controllability index* in [200] and [386]. From (0.39), it can be seen that the maximum degree of the polynomials in each column of the denominator polynomial matrix $A(p)$ is directly related to the full-state estimate of the observer. It is an important distinction, then, to define the partial state alone (without derivatives) as

$$z(t) = \left[z_1(t), z_2(t), \dots, z_{n_u}(t) \right]^T \quad (0.40)$$

where $z(t) \in \mathbb{R}^{n_u}$ has exactly the same elements in $\underline{z}(t)$, only without the associated derivatives. This reduced partial-state vector is important as it relates to developing unknown input observers when the UIO rank condition is not satisfied.

It should be noted here that in Fault Diagnosis, the goal is to generate residuals, not necessarily to estimate the full state. We will see that in many situations, it is possible to estimate the partial state $z(t)$ but not the entire state $x(t) = T\underline{z}(t)$, especially when $u(t)$ is unknown or assumed unknown. In this case, however, if a full-state estimate must be made, it *still* can by including the appropriate number of derivatives to the partial-state vector through a variety of filtering methods to obtain $\underline{z}(t)$ in (0.39).

B. POLYNOMIAL-BASED UIO BY INPUT REPLACEMENT

1. Theory

In order to illustrate the UIO concept, let us consider a simple case of a SIMO system with equations (0.32)-(0.33) with one input and two outputs as shown in Figure III.4. The goal is to estimate the partial state $z(t)$ based on outputs $y_1(t)$ and $y_2(t)$ only.

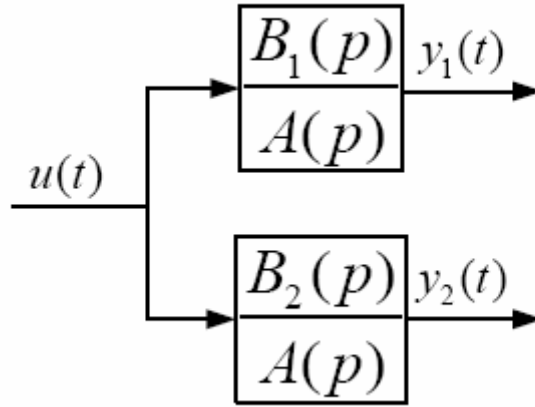


Figure III.4: SIMO System Transfer Function

As previously discussed, $z(t)$ satisfies the equations

$$\begin{aligned} A(p)z(t) &= u(t) \\ y_1(t) &= B_1(p)z(t) \\ y_2(t) &= B_2(p)z(t). \end{aligned}$$

If the input $u(t)$ is not available, we can use the last two equations as

$$\begin{aligned} B_1(p)z(t) &= y_1(t) \\ y_2(t) &= B_2(p)z(t) \end{aligned}$$

with the same partial state $z(t)$.

From the definition of the partial-state vector in (0.31), a set of equations can be derived from the input/output relationships as if $y_1(t)$ and $y_2(t)$ are the input and output of the system as shown in Figure III.5.

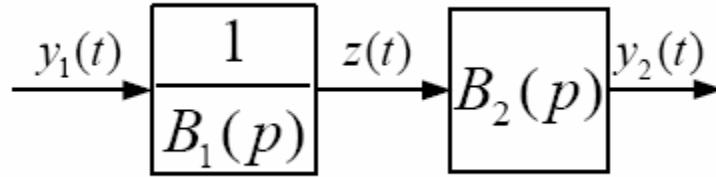


Figure III.5: SIMO Unknown Input System

Figure III.5 shows that $z(t)$ is the partial state associated to the transfer function $B_2(p)/B_1(p)$ and therefore it can be estimated by a standard observer or Kalman Filter.

In order for the UIO to exist, $B_1(p)$ and $B_2(p)$ must be mutually coprime (no pole-zero cancellations), which is the same as saying the system in Figure III.5 must be observable. Note that there are more linearly independent outputs (2) than there are unknown inputs (1), consistent with the rank condition (0.25) [230]. To add robustness to the state estimation, a standard Kalman Filter can be used to minimize the mean square error of the estimates.

In general, consider a MIMO system of the form (0.32)-(0.33) where at least one of n_u inputs is unknown and the input matrix Γ with corresponding input vector function u are partitioned into known and unknown inputs as

$$\Gamma u(t) = \begin{bmatrix} \Gamma_1 & \Gamma_2 \end{bmatrix} \begin{bmatrix} u_1(t) \\ u_2(t) \end{bmatrix} \quad (0.41)$$

where input is partitioned into n_{u_1} known inputs and $n_{u_2} = n_u - n_{u_1}$ unknown inputs. In this manner, using equation (0.41) we can write

$$\dot{x}(t) = \Phi x(t) + \Gamma_1 u_1(t) + \Gamma_2 u_2(t) \quad (0.42)$$

$$y(t) = Cx(t) + Du(t) \quad (0.43)$$

where $\Gamma_1 \in \mathbb{R}^{n_{u_1}}$ and $\Gamma_2 \in \mathbb{R}^{n_{u_2}}$. For the unknown input observer to exist for full-state estimation, $\text{rank}(C\Gamma_2) = \text{rank}(\Gamma_2)$, which implies that there must be at least as many independent outputs as there are unknown inputs. From the right polynomial matrix fraction of the transfer function matrix $H(p)$, combine the partial-state input/output equations (0.29) and (0.30) as

$$\begin{bmatrix} A(p) \\ \cdots \\ B(p) \end{bmatrix} z(t) = \begin{bmatrix} u(t) \\ \cdots \\ y(t) \end{bmatrix} \quad (0.44)$$

where $A(p) \in \mathbb{R}^{n_u \times n_u}$, $B(p) \in \mathbb{R}^{n_y \times n_u}$, $z(t) \in \mathbb{R}^{n_u}$, $u(t) \in \mathbb{R}^{n_u}$, and $y(t) \in \mathbb{R}^{n_y}$. It can be seen in equation (0.44) that there are a total of $n_u + n_y$ equations relating the input and output measurements to the partial state $z(t)$. The main idea is to replace all the

unknown input row equations in $A(p)$ with the same number of output row equations in $B(p)$ to obtain a new transfer matrix

$$\tilde{H}(p) = \tilde{B}(p)\tilde{A}^{-1}(p) \quad (0.45)$$

where $\tilde{B}(p) \in \mathbb{R}^{n_y - n_{u_2} \times n_u}$ and $\tilde{A}(p) \in \mathbb{R}^{n_u \times n_u}$. Right coprimeness of $\tilde{H}(p)$ and column reducedness of $\tilde{A}(p)$ must be verified since there is no guarantee that the system will have satisfied those conditions.

To illustrate this argument, suppose a system described in (0.42)-(0.43) where $n_s = 5$, $n_u = 2$, and $n_y = 4$ and suppose the second input $u_2(t)$ is unknown. Then equation (0.44) is represented as

$$\begin{bmatrix} {}_1a_{10}p^3 + {}_1a_{11}p^2 + {}_1a_{12}p^1 + {}_1a_{13} & \vdots & {}_1a_{20}p^2 + {}_1a_{21}p^1 + {}_1a_{22} \\ {}_2a_{10}p^3 + {}_2a_{11}p^2 + {}_2a_{12}p^1 + {}_2a_{13} & \vdots & {}_2a_{20}p^2 + {}_2a_{21}p^1 + {}_2a_{22} \\ \dots & \dots & \dots \\ {}_1b_{10}p^3 + {}_1b_{11}p^2 + {}_1b_{12}p^1 + {}_1b_{13} & \vdots & {}_1b_{20}p^2 + {}_1b_{21}p^1 + {}_1b_{22} \\ {}_2b_{10}p^3 + {}_2b_{11}p^2 + {}_2b_{12}p^1 + {}_2b_{13} & \vdots & {}_2b_{20}p^2 + {}_2b_{21}p^1 + {}_2b_{22} \\ {}_3b_{10}p^3 + {}_3b_{11}p^2 + {}_3b_{12}p^1 + {}_3b_{13} & \vdots & {}_3b_{20}p^2 + {}_3b_{21}p^1 + {}_3b_{22} \\ {}_4b_{10}p^3 + {}_4b_{11}p^2 + {}_4b_{12}p^1 + {}_4b_{13} & \vdots & {}_4b_{20}p^2 + {}_4b_{21}p^1 + {}_4b_{22} \end{bmatrix} \cdot \begin{bmatrix} z_1(t) \\ \dots \\ z_2(t) \end{bmatrix} = \begin{bmatrix} u_1(t) \\ u_2(t) \\ \dots \\ y_1(t) \\ y_2(t) \\ y_3(t) \\ y_4(t) \end{bmatrix}.$$

It is desired to have the third output $y_3(t)$ replace the unknown input $u_2(t)$ in the input polynomial matrix $A(p)$. The rank condition has been satisfied and assuming the leading coefficients on the polynomials for the third output, ${}_3b_{10}$ and ${}_3b_{20}$ are nonzero (which implies that A_h in (0.36)-(0.37) is nonsingular), the replacement can be made as shown

$$\begin{bmatrix}
{}_1a_{10}p^3 + {}_1a_{11}p^2 + {}_1a_{12}p^1 + {}_1a_{13} & \vdots & {}_1a_{20}p^2 + {}_1a_{21}p^1 + {}_1a_{22} \\
{}_3b_{10}p^3 + {}_3b_{11}p^2 + {}_3b_{12}p^1 + {}_3b_{13} & \vdots & {}_3b_{20}p^2 + {}_3b_{21}p^1 + {}_3b_{22} \\
\cdots & \cdots & \cdots \\
{}_1b_{10}p^3 + {}_1b_{11}p^2 + {}_1b_{12}p^1 + {}_1b_{13} & \vdots & {}_1b_{20}p^2 + {}_1b_{21}p^1 + {}_1b_{22} \\
{}_2b_{10}p^3 + {}_2b_{11}p^2 + {}_2b_{12}p^1 + {}_2b_{13} & \vdots & {}_2b_{20}p^2 + {}_2b_{21}p^1 + {}_2b_{22} \\
\vdots & \vdots & \vdots \\
{}_4b_{10}p^3 + {}_4b_{11}p^2 + {}_4b_{12}p^1 + {}_4b_{13} & \vdots & {}_4b_{20}p^2 + {}_4b_{21}p^1 + {}_4b_{22}
\end{bmatrix} \cdot \begin{bmatrix} z_1(t) \\ \cdots \\ z_2(t) \end{bmatrix} = \begin{bmatrix} u_1(t) \\ y_3(t) \\ \cdots \\ y_1(t) \\ y_2(t) \\ \cdots \\ y_4(t) \end{bmatrix}$$

The top $n_u = 2$ rows are now the new input polynomial matrix $\tilde{A}(p)$ and the bottom $n_y - 1 = 3$ rows comprise the new $\tilde{B}(p)$. The transfer matrix $\tilde{H}(p) = \tilde{B}(p)\tilde{A}^{-1}(p)$ is checked for right coprimeness and $\tilde{A}(p)$ is verified to be column reduced. Finally, the new system of equations is represented in state space form for Kalman Filtering implementation. Note that the estimate for the new system will be on the partial state, so it must be transformed through the linear transformation in (0.38) if the original full-state estimation is desired.

The relationship of the UIO rank condition in (0.25) to the polynomial representation for full-state estimation implies that $B(p)$ must have higher degree coefficients. Consider the input and output matrices Γ, C for the controllable canonical form realization both partitioned as

$$\begin{aligned}
\Gamma^T &= \begin{bmatrix} \Gamma_1^T & \cdots & \Gamma_{n_u}^T \end{bmatrix} \\
C &= \begin{bmatrix} C_1 & \cdots & C_{n_u} \end{bmatrix}
\end{aligned} \tag{0.46}$$

with

$$\begin{aligned}
\Gamma_i^T &= [0 \cdots 0 \ \gamma_i] \in R^{n_u \times \mu_i} \\
C_i &= [\times \cdots \times c_i] \in R^{n_y \times \mu_i}
\end{aligned} \tag{0.47}$$

for $i = 1, \dots, n_u$. It turns out that the terms C_i are the coefficients of the polynomial $B(p)$. In particular we can write

$$\begin{aligned} A(p) &= \begin{bmatrix} \gamma_1^T \\ \vdots \\ \gamma_{n_i}^T \end{bmatrix}^{-1} \Sigma_\mu(p) + \text{terms of lower degree} \\ B(p) &= \begin{bmatrix} c_1 p^{\mu_1-1} & \dots & c_{n_u} p^{\mu_{n_u}-1} \end{bmatrix} + \text{terms of lower degree} \end{aligned} \quad (0.48)$$

where

$$\Sigma_\mu(p) = \text{diag} \left\{ p^{\mu_1}, p^{\mu_2}, \dots, p^{\mu_{n_u}} \right\} \in \mathbb{R}^{n_u \times n_u}.$$

In the case of a UIO we can see some of the conditions of existence. Let Γ be partitioned as $\Gamma = \begin{bmatrix} \bar{\Gamma}_1 & \bar{\Gamma}_2 \end{bmatrix}$ where $\bar{\Gamma}_2$ is associated with the unknown inputs. In Kudva *et al* [230], the condition for existence of the UIO for full-state estimation is $\text{rank}(C\bar{\Gamma}_2) = \text{rank}(\bar{\Gamma}_2)$. From (0.46)-(0.48) it can be seen that

$$C\bar{\Gamma}_2 = \sum_{i=1}^{n_u} c_i \bar{\gamma}_i^T \quad (0.49)$$

with $\bar{\gamma}_i$ the part of the vector γ_i associated to the unknown input. From (0.48) we see that a necessary condition is that not all c_i can be zero, which means that the polynomial $B(p)$ must have higher degree terms.

While the unknown input observer rank condition (0.25) must be satisfied for full-state estimation, it does not need to be satisfied for estimating the partial state. This is the advantage of using the polynomial UIO technique and is illustrated in the following example.

2. Example

Consider a third-order, single-input, two-output system shown in Figure III.4 where the continuous time system is represented in right matrix fraction form as in (0.34) with $B(s) = [s+1 \quad s+2]^T$ and $A(s) = s^3 + 6s^2 + 11s + 6$. It can be seen that the greatest common right divisor between $B(s)$ and $A(s)$ is 1, which is unimodular. In [61] this implies that the system transfer matrix $H(p)$ is controllable and observable and an equivalent minimal realization representation of the system in state space form is

$$\dot{x}(t) = \begin{bmatrix} 0 & 1 & 0 \\ 0 & 0 & 1 \\ -6 & -11 & -6 \end{bmatrix} x(t) + \begin{bmatrix} 0 \\ 0 \\ 1 \end{bmatrix} u(t) \quad (0.50)$$

$$y(t) = \begin{bmatrix} 1 & 1 & 0 \\ 2 & 1 & 0 \end{bmatrix} x(t) + \begin{bmatrix} 0 \\ 0 \end{bmatrix} u(t). \quad (0.51)$$

Notice all the terms in (0.50)-(0.51) are directly related to the coefficients of the polynomials $A(s)$, $B_1(s)$, and $B_2(s)$. By observation, the system of equations is indeed controllable because it is realized in controllable canonical form where the state vector $x(t)$ happens to be the partial-state vector $\underline{z}(t)$ with derivatives up to order 2 as shown in (0.31). Since there is only one input, there is only one partial state $z(t)$. It can be verified that the system of equations is also observable. To design a full-state unknown input observer, the rank condition (0.25) must be satisfied. For this example, it means that

$$\text{rank} \left(\begin{bmatrix} 1 & 1 & 0 \\ 2 & 1 & 0 \end{bmatrix} \begin{bmatrix} 0 \\ 0 \\ 1 \end{bmatrix} \right) \neq \text{rank} \left(\begin{bmatrix} 0 \\ 0 \\ 1 \end{bmatrix} \right)$$

and a full-state UIO does not exist for this system. However, an unknown input observer still exists from a polynomial approach.

With the polynomial input replacement UIO method described in this chapter, an estimate of the partial state can still be achieved as outlined in the following steps to the algorithm. We start with the example state space representation in (0.50)-(0.51).

- 1) *Represent the system of equations in right matrix fraction form as in (0.34) and ensure that $H(p)$ is right coprime, which implies a minimum realization.*

$$H(s) = B(s)A^{-1}(s) = \begin{bmatrix} s+1 \\ s+2 \end{bmatrix} \frac{1}{s^3 + 6s^2 + 11s + 6}$$

The polynomial transfer matrix is right coprime.

- 2) *Represent the system of input/output equations in partial-state form as in (0.44).*

$$\begin{bmatrix} s^3 + 6s^2 + 11s + 6 \\ \dots & \dots & \dots & \dots \\ & \textcolor{red}{s+1} & & \\ & s+2 & & \end{bmatrix} z(t) = \begin{bmatrix} u(t) \\ \dots \\ \textcolor{red}{y_1(t)} \\ y_2(t) \end{bmatrix}$$

- 3) *Determine the right matrix fraction form of the UIO where $\tilde{H}(p) = \tilde{B}(p)\tilde{A}^{-1}(p)$ by replacing the rows in the input polynomial matrix $A(p)$ that correspond to $u_2(t)$ with the rows in the output polynomial matrix $B(p)$ that correspond to the desired input replacement equations.*

For this example, there is only one input and two options for replacement. Let us choose the output $y_1(t)$ to replace $u(t)$.

$$\begin{bmatrix} \dots & \dots & \dots & \dots \\ & s+1 & & \\ & & s+2 & \end{bmatrix} z(t) = \begin{bmatrix} y_1(t) \\ \dots \\ y_2(t) \end{bmatrix}$$

This leads to the system shown in Figure III.5 with the new scalar transfer function $\tilde{H}(p)$ written as

$$\tilde{H}(p) = \frac{\tilde{B}(s)}{\tilde{A}(s)} = \frac{B_2(s)}{B_1(s)} = \frac{s+2}{s+1}.$$

Since $\tilde{H}(p)$ is a first order system – while the original $H(p)$ was third order – we can estimate $z(t)$, but not $\dot{z}(t)$ and $\ddot{z}(t)$. This means that we can still create a residual, but not a full-state estimate. The principle can be generalized to say that for any column degree reduction of the original $A(s)$ to the new $\tilde{A}(s)$, it will result in an unknown input observer that cannot obtain a full-state estimate.

4) Check $\tilde{H}(p) = \tilde{B}(p)\tilde{A}^{-1}(p)$ for right coprimeness and column reducedness.

The new transfer function is

$$\tilde{H}(s) = \tilde{B}(s) / \tilde{A}(s) = \frac{s+2}{s+1}$$

since $\tilde{B}(s)$ and $\tilde{A}(s)$ are scalar polynomials. By inspection, there are no pole-zero cancellations of $\tilde{H}(s)$ and a scalar polynomial is always column (and row) reduced [61]. Note that an equivalent observer (in the steady state) can be determined from $\tilde{H}^{-1}(s)$.

- 5) *Represent $\tilde{H}(p)$ in state space form and implement any standard observer method. If the UIO can estimate the partial state (i.e. the UIO rank condition is satisfied), determine the nonsingular matrix T such that $x(t) = T\underline{z}(t)$ to determine the original state estimate.*

For this example, the UIO rank condition is not satisfied and a full-state estimate cannot be achieved. The state space representation for $\tilde{H}(s)$ is

$$\begin{aligned}\dot{z}(t) &= -z + y_1(t) + v_1 \\ y_2(t) &= z + y_1(t) + v_2\end{aligned}$$

where the “input” is $y_1(t)$ and the “output” is $y_2(t)$. The additional terms v_1, v_2 account for possible measurement noise. For this problem, let the input $u(t) = \sin(t)$ and the measurement noise variances $\sigma_{v_1}^2$ and $\sigma_{v_2}^2$ be 1% of the amplitude of the input signal. Also, all measurement noise are assumed to be uncorrelated. Under these conditions, the Kalman Gain is $L = 0.5811$ and the observer implementation equation is

$$\dot{\hat{z}}(t) = -1.5811\hat{z}(t) + [0.4189 \quad 0.5811] \begin{bmatrix} y_1(t) \\ y_2(t) \end{bmatrix}$$

and the output is the partial-state estimate $\hat{z}(t)$ itself. From the form of the observer equation, it can be easily seen that the estimate is independent of $u(t)$.

A simulation of the polynomial UIO input replacement method is shown in Figure III.6 and the noise terms were removed in the simulation to see the convergence.

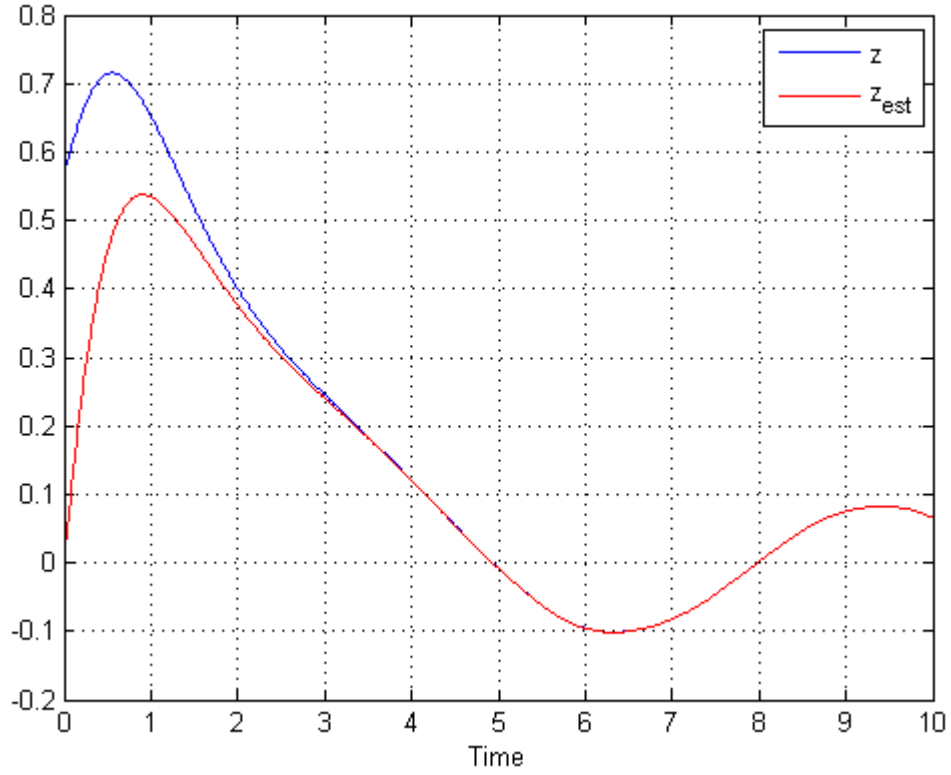


Figure III.6: UIO Input Replacement Method Simulation

In this example the replacement of the unknown input $u(t)$ with one of the outputs $y_1(t)$ is straightforward, since the resulting transfer function $B_2(s)/B_1(s)$ is scalar. In the more general MIMO case, the system resulting from input substitution has to be realizable, which might not always be the case. In the next section we present a general observer parametrization which has the unknown input observer as a particular representation.

C. POLYNOMIAL-BASED UIO BY PARAMETRIZATION

1. Theory

In the previous section, the UIO input replacement method took advantage of the partial-state realization in right polynomial transfer matrix form (0.34). This polynomial method, on the other hand, is based on the left polynomial transfer matrix in (0.35).

In this section a polynomial transfer matrix formulation of the observer or Kalman Filter yields a class of stable solutions easily parametrized. Consider the LTI system in (0.42)-(0.43) rewritten here as

$$\dot{x}(t) = \Phi x(t) + \Gamma_1 u_1(t) + \Gamma_2 u_2(t) \quad (0.52)$$

$$y(t) = Cx(t) + D_1 u_1(t) + D_2 u_2(t) \quad (0.53)$$

where $x \in \mathbb{R}^{n_x}$, $u \in \mathbb{R}^{n_u}$, $y \in \mathbb{R}^{n_y}$ and Φ, Γ , and C are of appropriate dimensions. Furthermore, $\Gamma_1 \in \mathbb{R}^{n_{u_1}}$ and $\Gamma_2 \in \mathbb{R}^{n_{u_2}}$ are the subdivided constant input matrices such that $u_1(t)$ and $u_2(t)$ are vectors containing all the known and unknown inputs, respectively. If the system (0.52)-(0.53) is a minimal realization, it can be equally realized in partial-state form from (0.44) with the additional known and unknown input partitioned as

$$u(t) = \begin{bmatrix} u_1(t) \\ u_2(t) \end{bmatrix} = \begin{bmatrix} A_1(p) \\ A_2(p) \end{bmatrix} z(t) \quad (0.54)$$

$$y(t) = B(p)z(t) \quad (0.55)$$

Now from the general form for the Kalman estimator, a polynomial representation of the observer that estimates the partial state $z(t)$ is expressed as

$$C(p)\hat{z}(t) = E(p)u(t) + F(p)y(t) \quad (0.56)$$

with $C(p) \in \mathbb{R}^{n_u \times n_u}$, $E(p) \in \mathbb{R}^{n_u \times n_u}$, and $F(p) \in \mathbb{R}^{n_u \times n_y}$. These polynomial matrices can be computed either from the Diophantine Equation (Appendix D)

$$C(p) = E(p)A(p) + F(p)B(p) \quad (0.57)$$

or directly from (0.32)-(0.33) as an observer of the form

$$\begin{aligned} p\hat{\underline{z}}(t) &= T^{-1}(\Phi - LC)T\hat{\underline{z}}(t) + T^{-1}\Gamma u(t) + T^{-1}Ly(t) \\ y^*(t) &= \bar{C}\hat{\underline{z}}(t) \end{aligned} \quad (0.58)$$

where $y^*(t)$ is the partial-state vector estimate (with derivatives) $\hat{\underline{z}}(t) \in \mathbb{R}^{n_s}$ in (0.39) when the UIO rank condition is satisfied ($\bar{C} = I_{n_s}$), and the partial state $\hat{z}(t) \in \mathbb{R}^{n_u}$ in (0.40) when it is not. In the latter case, \bar{C} is an $n_u \times n_s$ matrix that contains the rows of I_{n_s} that extracts the partial-state estimate $\hat{z}(t) \in \mathbb{R}^{n_u}$ from the partial-state vector (with derivatives) $\hat{\underline{z}}(t) \in \mathbb{R}^{n_s}$. Also, T is the nonsingular matrix transformation to the partial-state space shown as $x(t) = Tz(t)$.

For convergence of the observer in polynomial form, it is shown that the substitution of $u(t)$ and $y(t)$ in (0.54)-(0.55) into the polynomial representation of the partial-state observer in (0.56), along with the Diophantine equation identity in (0.57), yields the state error equation

$$C(p)(\hat{z}(t) - z(t)) = 0. \quad (0.59)$$

Equation (0.59) implies that $\lim_{t \rightarrow \infty} \hat{z}(t) - z(t) = 0$ provided $\det(C(p))$ has all roots in the stable region.

The useful feature of the Diophantine equation approach is that the solution is not unique. In fact, if $E_0(p) \in \mathbb{R}^{n_u \times n_u}$ and $F_0(p) \in \mathbb{R}^{n_u \times n_y}$ together are a solution of the Diophantine Equation (0.57) it can be shown in [61], [200], and [229] that, for any arbitrary polynomial matrix $W(p)$ of appropriate dimensions

$$E(p) = E_0(p) - W(p)\bar{B}(p) \quad (0.60)$$

$$F(p) = F_0(p) + W(p)\bar{A}(p) \quad (0.61)$$

are solutions to the differential equations. As a consequence, from (0.56) and (0.60)-(0.61) we obtain a family of observers, parametrized by $W(p) \in \mathbb{R}^{n_u \times n_y}$ as

$$C(p)\hat{z}(t) = (E_0(p) - W(p)\bar{B}(p))u(t) + (F_0(p) + W(p)\bar{A}(p))y(t) \quad (0.62)$$

where $\bar{A}(p) \in \mathbb{R}^{n_y \times n_y}$ and $\bar{B}(p) \in \mathbb{R}^{n_y \times n_u}$ are the left coprime representation of the original system transfer matrix $H(p) = \bar{A}^{-1}(p)\bar{B}(p)$.

Now partitioning $u(t)$ into known and unknown inputs we obtain

$$E(p)u(t) = \left(\begin{bmatrix} E_{01}(p) & E_{02}(p) \end{bmatrix} - \begin{bmatrix} W_1(p) & W_2(p) \end{bmatrix} \begin{bmatrix} \bar{B}_{11}(p) & \bar{B}_{12}(p) \\ \bar{B}_{21}(p) & \bar{B}_{22}(p) \end{bmatrix} \right) \begin{bmatrix} u_1(t) \\ u_2(t) \end{bmatrix} \quad (0.63)$$

where $E_{01}(p) \in \mathbb{R}^{n_u \times n_{u_1}}$, $E_{02}(p) \in \mathbb{R}^{n_u \times n_{u_2}}$, $W_1(p) \in \mathbb{R}^{n_u \times n_y - n_{u_2}}$, $W_2(p) \in \mathbb{R}^{n_u \times n_{u_2}}$, $\bar{B}_{11}(p) \in \mathbb{R}^{n_y - n_{u_2} \times n_{u_1}}$, $\bar{B}_{12}(p) \in \mathbb{R}^{n_y - n_{u_2} \times n_{u_2}}$, $\bar{B}_{21}(p) \in \mathbb{R}^{n_{u_2} \times n_{u_1}}$, and $\bar{B}_{22}(p) \in \mathbb{R}^{n_{u_2} \times n_{u_2}}$. In order to make the observer insensitive to $u_2(t)$, we choose the polynomial matrix $W(p)$ so that

$$E_{02}(p) - W_1(p)\bar{B}_{12}(p) + W_2(p)\bar{B}_{22}(p) = 0.$$

It can be seen that the row dimension of $\bar{B}_{12}(p)$ requires that $n_y > n_{u_2}$, which means that in order to have a solution, the number of independent outputs must be greater than the number of unknown inputs. This is the same result in Lemma 4.1 where $\text{rank}(C\Gamma_2) = \text{rank}(\Gamma_2)$.

If we choose two polynomial matrices $W_1(p)$, and $W_2(p)$ that satisfy the Diophantine equation

$$E_{02}(p) = W_1(p)\bar{B}_{12}(p) + W_2(p)\bar{B}_{22}(p) \quad (0.64)$$

then a viable solution can be obtained, provided that $\bar{B}_{12}(p)$, and $\bar{B}_{22}(p)$ are right coprime. Finally, combine (0.62)-(0.64) to obtain

$$C(p)\hat{z}(t) = \left(E_{01}(p) - W^*(p) \begin{bmatrix} \bar{B}_{11}(p) \\ \bar{B}_{22}(p) \end{bmatrix} \right) u_1(t) + (F_o(p) + W^*(p)\bar{A}(p))y(t) \quad (0.65)$$

with $W^*(p) = [W_1(p) \ W_2(p)]$ being the combined solution to (0.64). From (0.65), it can be seen that the parametrized observer is now independent of $u_2(t)$.

2. Example

In summary, the steps to obtain a UIO using parametrization is shown in the following example. The goal is to demonstrate how the observer is obtained and compare the simulation results to the subspace projection method in [175] and to a standard Kalman Filter estimation.

We start with the state space representation in (0.52)-(0.53) where the system, introduced in [175], is a fifth-order, two-input, four-output model where

$$\Phi = \begin{bmatrix} 0.0000 & 0.0000 & 1.0000 & 0.0000 & 0.0000 \\ 0.0000 & -0.1540 & -0.0042 & 1.5400 & 0.0000 \\ 0.0000 & 0.2490 & -1.0000 & -5.2000 & 0.0000 \\ 0.0386 & -0.9960 & -0.0003 & -0.1170 & 0.0000 \\ 0.0000 & 0.5000 & 0.0000 & 0.0000 & -0.5000 \end{bmatrix},$$

$$\Gamma_2 = \begin{bmatrix} 0.0000 & 0.0000 \\ -0.7440 & -0.0320 \\ 0.3370 & -1.1200 \\ 0.0200 & 0.0000 \\ 0.0000 & 0.0000 \end{bmatrix}, \text{ and } C = \begin{bmatrix} 0 & 1 & 0 & 0 & -1 \\ 0 & 0 & 1 & 0 & 0 \\ 0 & 0 & 0 & 1 & 0 \\ 1 & 0 & 0 & 0 & 0 \end{bmatrix}.$$

For this problem, both inputs are considered unknown where $u_2(t) = [\cos(t) \quad \sin(t)]^T$. Added white Gaussian noise is also imposed on the inputs and output measurements where the variance for each is 1.0% of the amplitude of the input. All measurements are assumed to be uncorrelated. Given that the initial conditions in [175] are arbitrarily chosen to be

$$x(0) = [0.3420 \quad 0.3200 \quad 0.0718 \quad -0.2870 \quad -0.9497]^T$$

and the initial conditions of the observers are set to zero, we set out to determine the polynomial-based UIO from the following steps:

- 1) *Verify the system is a minimal realization and transform the state space system to controllable canonical form.*

The system is controllable and observable (and therefore a minimal realization [61]). From the system of equations

$$\begin{aligned}\dot{\underline{z}}(t) &= T^{-1}\Phi T\underline{z}(t) + T^{-1}\Gamma_2 u_2(t) \\ y &= CT\underline{z}(t),\end{aligned}$$

and the system matrices Φ , Γ_2 , and C previously defined, the nonsingular matrix T is determined to be

$$T = \begin{bmatrix} -0.0001 & 0.0119 & -0.0003 & 0.4478 & 0.8941 \\ 0.0173 & -0.0009 & 0.0000 & -0.0323 & -0.4470 \\ -0.0012 & -0.1912 & 0.0173 & 0.0023 & 0.2235 \\ -0.9950 & 0.0024 & -0.0001 & 0.0894 & -0.0449 \\ 0.0034 & -0.1119 & -0.9950 & -0.0065 & 0.0225 \end{bmatrix}$$

which transforms the original system into controllable canonical form where the partial-state vector (with derivatives) is $\underline{z}(t) = T^{-1}x(t)$.

- 2) *Design a standard observer or Kalman Filter based on the partial-state realization.*

From the model, the plant and measurement noise covariance matrices are set to be $Q_w = 0.1I_{n_u}$ and $R_v = 0.01I_{n_y}$, respectively. The steady-state Kalman Gain is determined to be

$$L_z = \begin{bmatrix} 0.0225 & -0.0471 & 0.0174 & -0.0135 \\ -0.0115 & -0.0377 & 0.0277 & 0.0098 \\ -0.0513 & 0.0563 & -0.0015 & 0.0267 \\ 0.0937 & -0.5402 & 0.0793 & -0.8628 \\ 0.1225 & -1.3764 & 0.3712 & -0.4888 \end{bmatrix}$$

and the full-state Kalman Filter can be implemented as in equation (0.58).

- 3) *Check UIO rank condition. Determine \bar{C} such that*
 - a. *If the rank condition is satisfied, then a full-state estimate can be achieved and $\bar{C} = I_{n_s}$.*
 - b. *If the rank condition is not satisfied, then determine \bar{C} such that n_u partial states are extracted (no derivatives) from $\underline{z}(t)$ resulting in the partial state $z(t)$ in (0.40).*

The rank condition is satisfied and therefore for this example $\bar{C} = I_5$.

- 4) *Determine the polynomial matrices $C(p)$, $E_0(p)$, and $F_0(p)$ from (0.57), which is the equivalent polynomial representation of the partial-state observer designed Step 3.*

In the example,

$$C(s) = \begin{bmatrix} -s-0.0420 & 0.9300 & 0.0720 & -0.0150 & -0.0460 \\ -0.0740 & -s-0.1500 & 0.9600 & 0.0073 & -0.0390 \\ -1.0000 & -2.2000 & -s-1.1000 & -0.0097 & 0.0560 \\ -0.0020 & -0.2500 & -0.7900 & s+0.8700 & -0.4700 \\ 12.0000 & 26.0000 & 3.8000 & -0.0560 & -s-2.3000 \end{bmatrix},$$

and $E_0(s)$ and $F_0(s)$ are constant polynomial matrices

$$E_0(s) = \begin{bmatrix} 0.0000 & 0.0000 \\ 0.0000 & 0.0000 \\ -0.1500 & 0.0130 \\ 0.0000 & 0.0000 \\ 0.2500 & -1.1000 \end{bmatrix}, F_0(s) = \begin{bmatrix} -0.0091 & 0.0470 & -0.0170 & 0.0130 \\ 0.0120 & 0.0380 & -0.0280 & -0.0098 \\ 0.0510 & -0.0560 & 0.0015 & -0.0270 \\ 0.0940 & -0.5400 & 0.0790 & -0.8600 \\ -0.1200 & 1.4000 & -0.3700 & 0.4900 \end{bmatrix}.$$

5) In (0.62), determine $\bar{A}(p)$ and $\bar{B}(p)$ from the left coprime realization of the original system, $H(p) = \bar{A}^{-1}(p)\bar{B}(p)$.

Because the example is a minimal realization, the original system of equations defined by the matrices Φ , Γ_2 , and C can be realized in left matrix fraction form where

$$\bar{A}(s) = \begin{bmatrix} s^2 + 0.845s + 0.470 & -2.400s^2 - 2.500s - 0.610 & 0.450s^2 - 12.000s - 5.100 & -0.95s^2 - 0.41s + 0.010 \\ -0.200s - 0.098 & -0.053s + 0.035 & 0.017s + 0.029 & -0.089s - 0.001 \\ 0.08s + 0.040 & 0.570s + 1.300 & 0.130s + 2.900 & -0.680s - 0.005 \\ -0.025s - 0.012 & -0.210s + 0.440 & -0.049s - 1.100 & -0.65s + 0.002 \end{bmatrix}$$

and

$$\bar{B}(s) = \begin{bmatrix} -0.670s - 0.280 & 2.700s + 1.100 \\ 0.130 & 0.066 \\ 0.140 & -0.640 \\ -0.054 & 0.240 \end{bmatrix}$$

Notice that the sum of the *row degrees* (maximum polynomial degree of each row) of $\bar{A}(s)$ is equal to the total number of states ($n_s = 5$), which implies that $\bar{A}(s)$ is row reduced. Since the degree of the i^{th} row in $\bar{B}(s)$ is less than the degree of the i^{th} row in $\bar{A}(s)$, the polynomial transfer matrix is proper [61].

- 6) *From the structure of the input vector in (0.52), determine $u_1(t)$ and $u_2(t)$. Partition polynomial matrices $E_0(p)$ and $\bar{B}(p)$ accordingly from equation (0.63)*

Since both inputs are unknown, $n_{u_1} = 0$ and $n_{u_2} = 2$ and so $E_{01}(s)$ is an empty matrix and $E_{02}(s) = E_0(s)$. From the dimensions of the polynomials in equation (0.63), it can be seen that from the previous step, $\bar{B}(s)$ is partitioned as

$$\bar{B}_{12}(s) = \begin{bmatrix} -0.670s - 0.280 & 2.700s + 1.100 \\ 0.130 & 0.066 \end{bmatrix}, \text{ and } \bar{B}_{22}(s) = \begin{bmatrix} 0.140 & -0.640 \\ -0.054 & 0.240 \end{bmatrix}.$$

- 7) *Verify $\bar{B}_{12}(p)$ and $\bar{B}_{22}(p)$ are right coprime and solve Diophantine equation to obtain $W_1(p)$ and $W_2(p)$ in (0.64).*

In the example, $\bar{B}_{12}(s)$ and $\bar{B}_{22}(s)$ are right coprime. The solution to the Diophantine equation

$$E_{02}(p) = W_1(p)\bar{B}_{12}(p) + W_2(p)\bar{B}_{22}(p)$$

are the constant polynomial matrices

$$W_1(s) = \begin{bmatrix} 0.000 & 0.000 \\ 0.000 & 0.000 \\ 0.000 & -1.000 \\ 0.000 & 0.000 \\ 0.000 & 0.099 \end{bmatrix} \quad \text{and} \quad W_2(s) = \begin{bmatrix} 0.000 & 0.000 \\ 0.000 & 0.000 \\ -0.100 & 0.064 \\ 0.000 & 0.000 \\ 1.500 & -0.580 \end{bmatrix}.$$

8) Form $W^*(p) = [W_1(p) \ W_2(p)]$ and from (0.62) go back to the state space realization of the partial-state representation for simulation.

The observer from the original system has now been successfully designed such that, in choosing the polynomial matrix $W^*(p)$ in (0.62), the parametrized Kalman Filter in polynomial form is now independent of unknown inputs $u_2(t)$. Changing back to state space form from the left matrix fraction realization yields the following system of equations:

$$\Phi^* = \begin{bmatrix} -0.0419 & 0.9311 & 0.0719 & 0.0150 & -0.4610 \\ -0.0743 & -0.1462 & 0.9586 & -0.0073 & -0.0386 \\ -1.0051 & -2.1930 & -1.1025 & 0.0097 & 0.0556 \\ -0.0020 & -0.2488 & -0.7881 & -0.8657 & -0.4708 \\ 12.1667 & 25.8504 & 3.7543 & 0.0563 & -2.3256 \end{bmatrix},$$

$$\Gamma^* = \begin{bmatrix} -0.0008 & 0.0000 & -0.0304 & 0.0532 \\ 0.1894 & -0.0172 & -0.0609 & 0.1289 \\ -0.0568 & -0.1159 & -0.3352 & -0.1925 \\ -0.1118 & -0.9950 & -0.0027 & -0.6358 \\ 0.3771 & 0.6721 & 3.9845 & 2.4990 \end{bmatrix},$$

$$C^* = \begin{bmatrix} -0.2405 & -0.5811 & -0.0000 & -0.9950 & 0.0000 \\ 0.1779 & 2.9439 & 5.1764 & -0.0449 & 0.0899 \\ 0.0000 & -0.2405 & -0.5811 & 0.0000 & 0.9950 \\ -2.5932 & -5.2463 & -0.1378 & 0.0906 & -0.0016 \\ 0.1779 & 2.5882 & 0.0000 & -0.0449 & -0.0000 \end{bmatrix},$$

and $D^* = 0_{n_s \times n_y}.$

For implementation, the resulting unknown input observer is independent of $u(t)$ and the output is the full partial state (with derivatives) as

$$\dot{q}(t) = \Phi^* q(t) + \Gamma^* y(t)$$

$$\hat{\underline{z}}(t) = C^* q(t) + D^* y(t)$$

where $q(t)$ denotes the state of the new system.

A simulation was conducted using the above example and the estimation results on the original state x_4 are shown in Figure III.7. The red line shows the actual state trajectory, while the other trajectories are from the three different observer designs. It can be seen that the polynomial UIO method (blue) outlined in this section performed just as good as the subspace projection UIO method (green). Both UIO methods, which only used output measurements to estimate the state, performed as well as the standard Kalman Filter, which depends on both inputs and outputs to estimate the state.

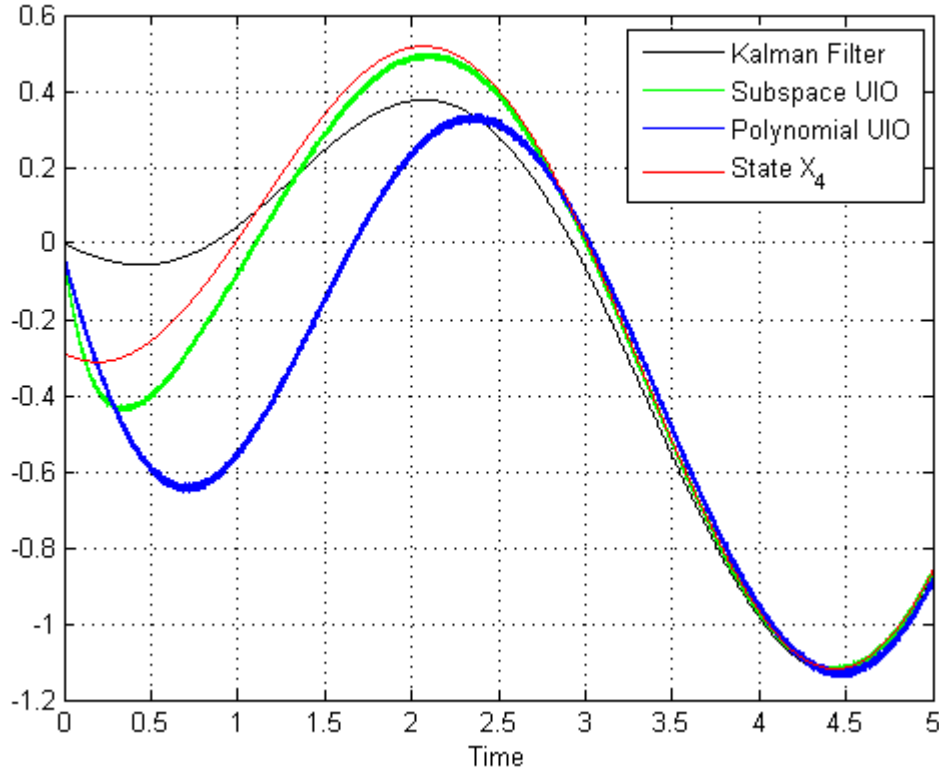


Figure III.7: State Estimate Comparison

When deciding on a method for estimation, it is desirable to design an observer so that one or more inputs have no effect on the state estimation. Perhaps a system model has an unknown disturbance or other model uncertainties. In the case of residual generation, perhaps an input is assumed unknown to develop a structured residual set for Fault Diagnosis. When considering the subspace UIO methods and the polynomial ones described herein, each is designed to effectively obtain an estimate of the full state when the UIO rank condition is satisfied. The advantage of the polynomial methods is that they can still generate a residual through an estimate of the partial state.

As mentioned before, the input replacement UIO method is limited if the replacement polynomials do not have higher degrees. As a consequence, this method works best when the degree of the numerator polynomial matrix $B(p)$ is the same as the denominator polynomial matrix $A(p)$, which is the same as saying that $D \neq 0$ in the equivalent state space realization.

The parametrization UIO method is the more general polynomial method and is comparable to the subspace projection UIO in complexity and performance. The main idea is to develop a standard Kalman Filter in polynomial form and parametrize the solution such that it is made independent of the unknown inputs. This method works well in the presence of plant and sensor disturbances with known first and second order statistics. One drawback common to both polynomial methods is that they require a linear transformation to the controllable canonical form to accommodate estimating the partial state. In cases where system eigenvalues are very large (i.e. greater than 10^6), the inverse of the transformation matrix T can be near singular.

Besides being able to generate residuals based on the partial state, another advantage to the parametrization method is that since the solution to the Diophantine equation is nonunique, it can be represented by a family of observers. If one of the inputs is suddenly made unavailable for the estimation, the observer can be adjusted adaptively. This idea is being explored as a developing possibility.

D. INPUT OBSERVABILITY AND ESTIMATION

Throughout the discussion so far in this chapter is the idea that if the UIO rank condition (0.25) is not satisfied, a partial-state estimate is still possible and can be obtained through polynomial UIO techniques. Specifically, it has also been shown that the column degrees of the denominator polynomial matrix $A(p)$ (in the right matrix fraction realization $H(p) = B(p)A^{-1}(p)$) are directly related to the ability to estimate the full state in (0.39). For any column degree reduction of the original $A(p)$ to the new observer denominator polynomial $\tilde{A}(p)$, it will result in an unknown input observer that cannot obtain a full-state estimate. This also implies that $B(p)$ must have higher order terms.

We have discussed residual generation based on the state and partial state. Now we consider it based on input and output measurements. It will be shown that in some cases, it is desirable to compute residuals not only on the outputs, but on the inputs as well. Depending on system structure, this would give added information on the class of

faults. It will be shown that while output estimation is straightforward when the full-state estimate is determined, the input estimation problem is non-trivial and it requires certain conditions for existence that relate to the system inversion problem.

Compared to state estimation techniques for unknown input observers, little research has been conducted on input estimation [73]. Some input reconstruction methods base their estimation on derivatives of the output measurements [168][169]. Here again, it is shown that input estimates can be determined on a larger class of systems from taking derivatives on the partial state. The remainder of this section addresses the necessary condition for input estimation and how the output equations can be chosen so that it can be satisfied. Similarities between the unknown input observer with input reconstruction and system inversion will also be addressed. Moylan [268] showed a method for determining the inverted system in state space. It will be shown here how this result relates to a system in right polynomial transfer matrix form through the partial state. Finally, two DC ZEDS examples will be shown to demonstrate the concepts.

1. Input Observability Theory

The goal of the input reconstruction problem is to formulate a system filter whose inputs are the measurements and known inputs of the original system and whose outputs converge to the inputs of the original system. We begin with a short example. Suppose we have a third order, single input, 2-output system as shown in Figure III.4 and is represented by the polynomial matrix fraction $H(p) = B(p)A^{-1}(p)$. If a UIO is developed (not necessarily polynomial-based) such that a partial-state vector estimate $\hat{\underline{z}}(t)$ is determined, then by the polynomial matrices $B(p) = [B_1(p) \ B_2(p)]^T$ and $A(p)$ defined as in (0.27) and (0.28), an estimate of the input $\hat{u}(t)$ and output $\hat{y}(t)$ can be determined from (0.29)-(0.30) as

$$\begin{cases} \hat{y}_1(t) = {}_1b_0\ddot{\hat{z}}(t) + {}_1b_1\dot{\hat{z}}(t) + {}_1b_2\dot{\hat{z}}(t) + {}_1b_3\hat{z}(t) \\ \hat{y}_2(t) = {}_2b_0\ddot{\hat{z}}(t) + {}_2b_1\dot{\hat{z}}(t) + {}_2b_2\dot{\hat{z}}(t) + {}_2b_3\hat{z}(t) \end{cases} \quad (0.66)$$

$$\hat{u}(t) = \ddot{\hat{z}}(t) + a_1 \dot{\hat{z}}(t) + a_2 \dot{\hat{z}}(t) + a_3 \hat{z}(t). \quad (0.67)$$

Let $\hat{y}_1(t)$ be arbitrarily chosen to be the “input” to the estimation $\hat{u}(t)$, meaning that we solve for the highest degree term in (0.66) and substitute in (0.67) to obtain

$$\hat{u}(t) = \frac{1}{{}_1b_0} \left((a_1 - {}_1b_1) \ddot{\hat{z}}(t) + (a_2 - {}_1b_2) \dot{\hat{z}}(t) + (a_3 - {}_1b_3) \hat{z}(t) \right) + \frac{1}{{}_1b_0} y_1(t), \quad (0.68)$$

provided that ${}_1b_0$ is nonzero. This constraint implies that the polynomial $B_1(p)$ must be the same order as $A(p)$. In the state space realization, this means that the matrix D in the state space model must be nonzero. If ${}_1b_0$ is zero, then the input can be estimated directly from (0.67) by taking the derivative on the highest order in $\hat{z}(t)$ to obtain $\ddot{\hat{z}}(t)$. Notice that the equation (0.68) is similar to the system inversion process, since the “output” is the system input estimate $\hat{u}(t)$ and the “input” is the measurement $y_1(t)$ [268][169].

Now consider the more general MIMO case, again represented in state space as

$$\dot{x}(t) = \Phi x(t) + \Gamma u(t) \quad (0.69)$$

$$y(t) = Cx(t) + Du(t) \quad (0.70)$$

where $x(t) \in \mathbb{R}^{n_x}$, $u(t) \in \mathbb{R}^{n_u}$, $y(t) \in \mathbb{R}^{n_y}$ and the constant matrices Φ , Γ , C , and D are of appropriate dimensions. If the system is a minimal realization and a UIO is designed to estimate the partial-state vector, then similar to solving for the high order derivative in (0.66) for the SIMO case, we use the result in (0.36)-(0.37) to relate the input estimate $\hat{u}(t)$ in terms of the coefficients of the right matrix fraction polynomials $B(p)$, $A(p)$ and the output $y(t)$ as

$$\hat{u}(t) = -\left(B_h A_h^{-1}\right)^\dagger \left(B_l - B_h A_h^{-1} A_l\right) \hat{z}(t) + \left(B_h A_h^{-1}\right)^\dagger y(t) \quad (0.71)$$

where $A_h \in \mathbb{R}^{n_u \times n_u}$ and $B_h \in \mathbb{R}^{n_y \times n_u}$ are constant matrices of high degree coefficients of $A(p)$ and $B(p)$, respectively. Likewise, $A_l \in \mathbb{R}^{n_u \times n_s}$ and $B_l \in \mathbb{R}^{n_y \times n_s}$ are the matrices of all lower order coefficients of $A(p)$ and $B(p)$, respectively. The superscript † represents the Moore-Penrose pseudoinverse. For more details on this representation, see Appendix D. Clearly, in order to have an inverse, A_h must be nonsingular and the product $B_h A_h^{-1}$ (which is the D matrix in state space) cannot be zero for a nontrivial solution. Again, a nonzero B_h implies that $B(p)$ must have the same column degree as $A(p)$. If it does not, then the input estimate can be found from (0.36) as

$$\hat{u}(t) = A_h \dot{\hat{z}}_\mu(t) + A_l \hat{z}(t) \quad (0.72)$$

where $\dot{\hat{z}}_\mu(t) = \begin{bmatrix} p^{\mu_1} \hat{z}_1(t) & \cdots & p^{\mu_{n_u}} \hat{z}_{n_u}(t) \end{bmatrix}^T$ is the vector of μ_{1,\dots,n_u}^{th} derivatives on the partial state $z(t)$, determined by any standard derivative filter. We have shown in Section IV.B.1 that in cases where the UIO rank condition is not satisfied, the partial state can still be estimated. This result can be extended to determining an input estimate by adding all derivatives of all partial states up to the column degree μ_i , $i = 1, \dots, n_u$.

Input estimation is very closely related to system left inversion where a system's inputs are determined from knowledge of its output. Necessary and sufficient conditions for the stable inversion problem are provided in [268]. Hou and Patton show the similarities between input estimation and system inversion and provide a necessary and sufficient condition for input observability [169].

For both polynomial methods herein, special attention is paid to the input reconstruction problem because it provides more analytical redundancy and potential for improving a Fault Tolerant Control architecture.

In order to determine conditions for input observability, consider the LTI model in (0.69)-(0.70) and express the system as

$$\begin{bmatrix} -pI + \Phi & \Gamma \\ C & D \end{bmatrix} \begin{bmatrix} x(t) \\ u(t) \end{bmatrix} = \begin{bmatrix} 0 \\ I \end{bmatrix} y(t). \quad (0.73)$$

Now define the matrix

$$M(\lambda) = \begin{bmatrix} -\lambda I + \Phi & \Gamma \\ C & D \end{bmatrix} \quad (0.74)$$

called the matrix pencil [200][139]. Input observability is a necessary and sufficient condition for the existence of an estimator reconstructing inputs [169]. In the case of a controllable and observable system of equations (0.69)-(0.70) with unknown initial conditions, the input $u(t)$ is observable if and only if

$$\text{rank}(M(\lambda)) = \dim(x) + \dim(u), \quad \forall \lambda \in \mathbb{C}. \quad (0.75)$$

If the input observability condition (0.75) is satisfied for a system, then one such input estimator exists of the form

$$\dot{w}(t) = F_1 w(t) + F_2 y(t) \quad (0.76)$$

$$\hat{u}(t) = G_1 w(t) + \sum_{i=0}^k G_{2,i} y^{(i)}(t) \quad (0.77)$$

where $y^{(i)}(t)$ denotes the i^{th} derivative of $y(t)$ [169]. The number k is called the *index* of the estimator and it indicates the highest derivative needed. The methods for input estimation described here and elsewhere require high orders of derivatives on the output measurements, which would make the estimate sensitive to noise. Also, in [268] an iterative algorithm is described for determining an input estimation filter.

Another method for determining the input estimate is derived directly from the state space realization (0.69)-(0.70) and is similar to the system inversion problem in [268], only no iterative process is necessary. It is expressed here in partial-state space form as

$$\dot{\underline{z}}(t) = T^{-1}(\Phi - \Gamma EC)T\underline{z}(t) + T^{-1}\Gamma Ey(t) \quad (0.78)$$

$$\hat{u}(t) = -ECT\underline{z}(t) + Ey(t) \quad (0.79)$$

where all the system matrices are defined in (0.69)-(0.70), the matrix E is defined as

$$E = \begin{cases} D^{-1} & \text{if } n_u = n_y \\ D^\dagger & \text{if } n_y > n_u, \end{cases}$$

and the nonsingular matrix T transforms state $x(t)$ to the partial-state vector $\underline{z}(t)$ as before. Notice that each term in the input estimation equation (0.79) includes the matrix E , which is directly related to the degree of the numerator polynomial $B(p)$ as shown in the equivalent equation (0.71) from the polynomial approach. Once again, in order to

have a proper system inverse, the degree of the numerator polynomial $B(p)$ must be the same as the denominator polynomial $A(p)$ or, in the state space realization $D \neq 0$.

In most cases for fault diagnosis, the number of outputs will be strictly greater than the number of inputs. This implies that D is not square and only some of the eigenvalues of $(A - BEC)$ will depend on E . If D is rank deficient, then the inputs corresponding to a zero column will not have an estimate. Notice that the inverted “output” equation in (0.79) is identical to (0.71), which again shows the equivalence of minimal realizations of a system.

If the system does not satisfy the inversion rank condition, it does not mean that an input estimate cannot be estimated. It only means that the system does not have a proper inverse. An explanation in [73] and [280] shows that if we relax the rank condition to

$$\text{rank}(M'(\lambda)) < \dim(x) + \dim(u) \quad (0.80)$$

where

$$M'(\lambda) = \begin{bmatrix} -\lambda I + \Phi & \Gamma \\ C & 0 \end{bmatrix},$$

and we further assume that a full-state estimate is obtainable and input matrix Γ is full rank (which it will be if the system is controllable), then an input estimation process can be established with derivatives on the output measurements as shown in (0.76)-(0.77). Another way to look at this result is to consider an estimate of the input directly from the dynamic equation (0.32) represented in the partial state as

$$\hat{u}(t) = (T^{-1}\Gamma)^\dagger \dot{\hat{\underline{z}}}(t) - (T^{-1}\Gamma)T^{-1}\Phi T\hat{\underline{z}}(t). \quad (0.81)$$

By comparing equations (0.79) and (0.81), we see that the expression (0.81) shows dependence on derivatives of the partial state, but is independent of D . This relationship shows the similarity of determining the input estimate based on the right fraction transfer matrix representation in (0.72). Finally, recall that an estimate of the partial state is possible even when a full-state estimate is not. Then by extension, an input estimate in this case can still be achieved by adding derivatives as necessary to (0.81).

2. Examples

Two examples are presented to demonstrate input reconstruction on an unknown input observer. The first shows how a bank of unknown input observers successfully estimates the inputs while being systematically independent of each input. From the structured residual set, it can be seen that the indication of the presence of a fault is more prominent using residuals from the input estimate rather than based on the output measurements. In addition, for a certain class of systems the residual signal is an estimate of the fault signal itself. The second example demonstrates an unknown input observer used to estimate nonlinear components of a system.

The first example is a UIO-based structured residual set designed to detect and isolate actuator faults. Suppose a system follows the flow diagram depicted in Figure III.8. The system model shows an input $u(t)$ being subjected to an unknown disturbance η_u with known mean (zero) and variance (σ_u^2) and another completely unknown disturbance $f(t)$. The corrupted signal $u_f(t)$ is the input to the known plant dynamics and its output measurement is also influenced by a zero mean disturbance with variance σ_y^2 . The goal is to determine the characteristics of the unknown disturbance $f(t)$ – that is, determine $\hat{f}(t)$.

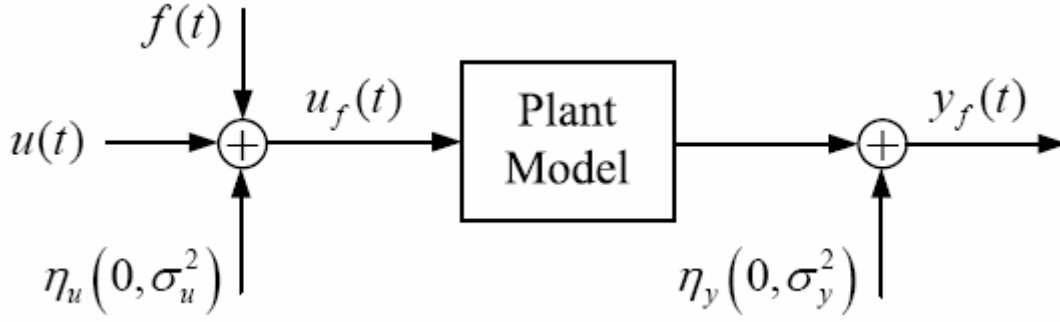


Figure III.8: UIO Example, Signal Flow Diagram

To make the problem more general, suppose the system depicted in Figure III.8 is a MIMO system where $u(t)$ and $y(t)$ are vectors. Let $f(t)$ be a scalar disturbance operating on one of the inputs, but it is not known *a priori* which one. Also let the disturbances η_u and η_y have influence on all the inputs and outputs, respectively. Now, the goal is to determine which input is corrupted by $f(t)$ on the basis of the input residual

$$r_u(t) = u(t) - \hat{u}(t)$$

and, for comparison, the output residual

$$r_y(t) = y(t) - \hat{y}(t) .$$

The problem is solved using unknown input observers with input reconstruction (UIO-IR) in a structured residual set depicted in Figure III.9 where the bank of observers are designed to reject the inputs one at a time. The system used in this example is the

sixth-order, four-input, twelve-output* port bus model for the DC ZEDS system shown in Figure II.6., with parameters listed in Table II.3. For the purpose of this exercise, the bus is assumed to be in Mode 3 (where zones 1, 2, and 3 are energized) and the system is adjusted in time scale using arbitrary inputs

$$\begin{bmatrix} u_1(t) \\ u_2(t) \\ u_3(t) \\ u_4(t) \end{bmatrix} = \begin{bmatrix} \sin(t) \\ \sin(t) + \frac{\pi}{2} \\ \sin(t) + \pi \\ \sin(t) - \frac{\pi}{2} \end{bmatrix}.$$

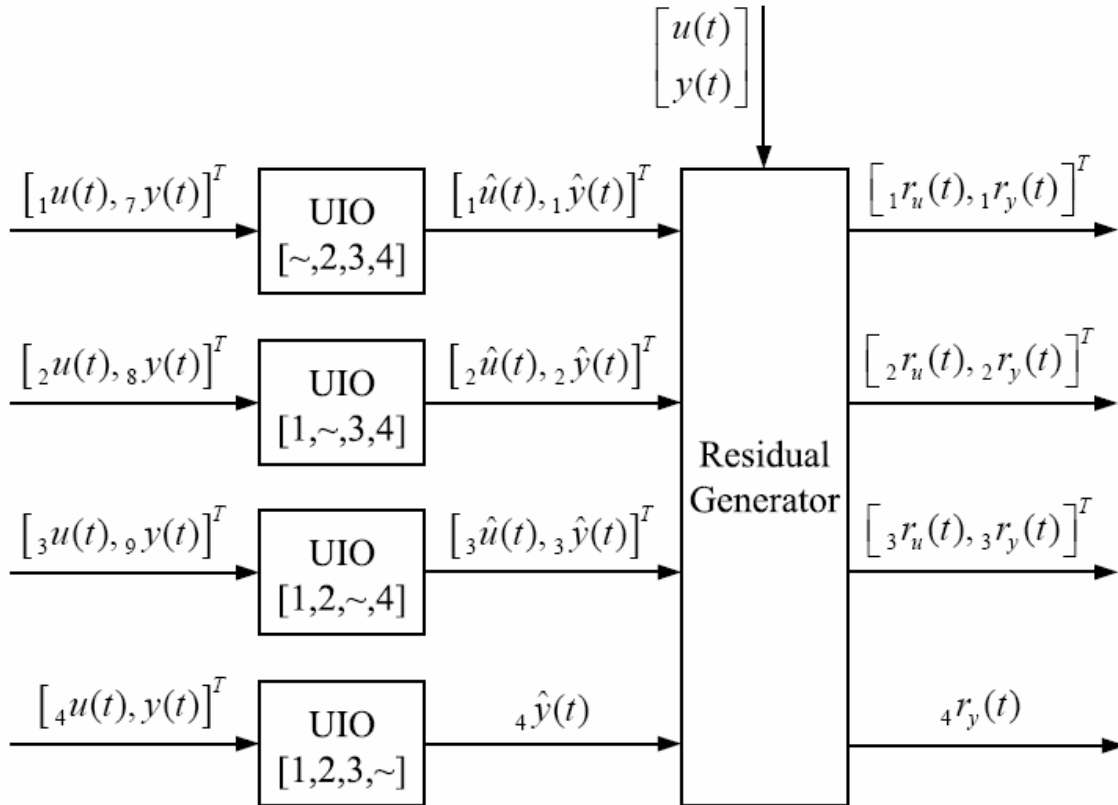


Figure III.9: UIO Example, Structured Residual set for Input FDI

* It turns out that twelve outputs are not necessary for the UIO implementation. A more manageable number is 9 (bus current, bus voltage, and capacitance voltage in each zone), which still meets all criteria for the minimal realization, UIO rank condition and input observability rank condition.

The bank of UIOs (designed using the polynomial parametrization method) in Figure III.9 shows that each of the four observers is designed to be insensitive to $u_1(t)$, $u_2(t)$, $u_3(t)$, and $u_4(t)$, respectively, where the ‘ \sim ’ represents the unknown input. The other inputs to the observer include the outputs y (denoted as $y_f(t)$ in Figure III.8) less the bus voltage sensors where indicated. For this problem, the system is a minimal realization and the UIO rank condition is satisfied for all conditions. If only the bus current, bus voltage, and capacitance voltage for each zone are considered as outputs, then the D matrix, in (0.11) would be

$$D = \begin{bmatrix} 0 & 0 & 0 & 0 \\ 0 & 0 & 0 & 0 \\ 0 & 0 & 0 & 0 \\ 0 & 0 & 0 & 0 \\ 0 & 0 & 0 & 0 \\ 0 & 0 & 0 & 0 \\ -0.1 & 0 & 0 & 0 \\ 0 & -0.1 & 0 & 0 \\ 0 & 0 & -0.1 & 0 \end{bmatrix},$$

and the input observability rank condition in (0.75) is satisfied. From this structure, it can be seen that $\text{rank}(D) = 3 < n_u$ and so a solution to the input estimate can be determined by (0.71) or (0.79) for all except $u_4(t)$, which shows all zeros in the fourth column. In other words, none of the outputs are algebraically dependent on the input $u_4(t)$, which is the output voltage from the power supply in the DC ZEDS system.

Also, since there is input dependence on the last three output measurements, they must be removed from the observer estimate because a fault on the input will also mean a fault on the outputs that are linearly dependent on the inputs. These last three rows of D correspond to the bus voltage sensors.

In this example, a disturbance signal $f(t)$ was arbitrarily chosen to be a triangle waveform added to the input $u_1(t)$ as shown in Figure III.10.

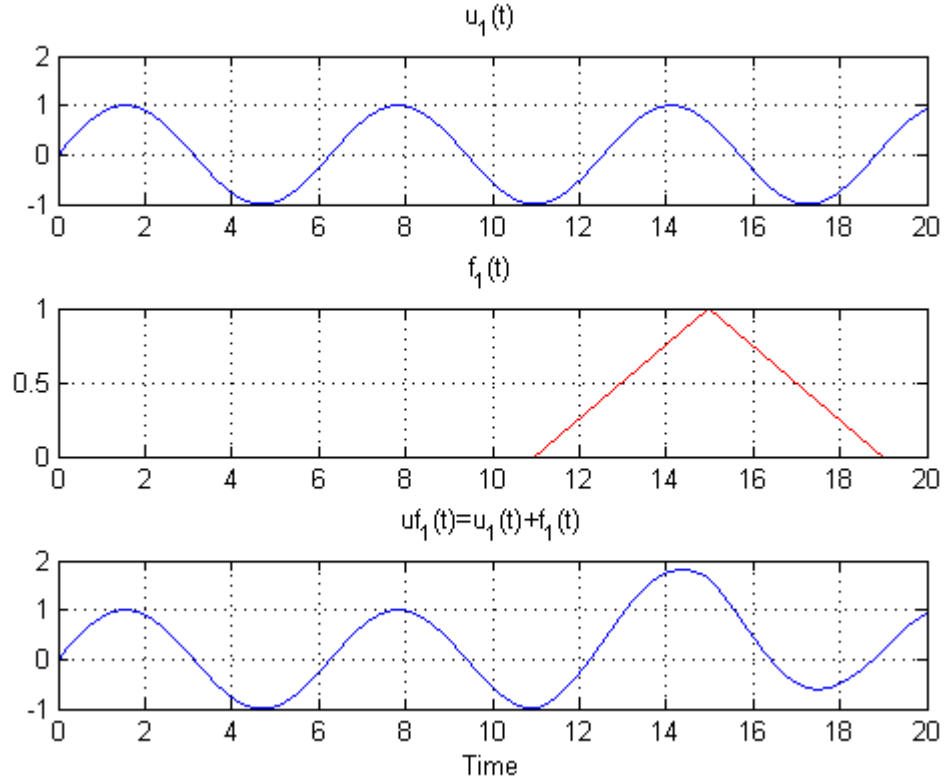


Figure III.10: UIO Example, Input Fault Trajectory

The results from the simulation were obtained through residuals generated from the structured residual set in Figure III.9 and show a fault indication on the far left column of Figures III.11 - III.13. The columns of these figures represent residuals generated from the UIOs insensitive to $u_1(t)$, $u_2(t)$, $u_3(t)$, and $u_4(t)$ from left to right, where the ‘~’ represents the unknown input. The rows in each figure are residuals based on estimates of the inputs or outputs. In Figure III.11, the subscript “ipz*” are the load demands leading to the SSCMs in each zone as shown in Figure II.6 as “ i_{out_s} ”, in Figure III.12, the subscript “ibus*” are the bus currents in each zone and in Figure III.13, the subscript “vb*” is bus voltage in each zone. The fourth input is v_{out} from the power

supply but is not shown in Figure III.11 because an estimate cannot be determined without derivatives to the partial state.

It can be seen that the residual in the very top left corner of Figure III.11 is the estimate of the disturbance $f(t)$ and because it resides in the first column, where no other signatures reside going down the column, the disturbance is on the first input $u_1(t)$. To make the figures more readable, the triangle disturbance signal $f(t)$ is superimposed in red, the actual results are in blue, and the mean is green.

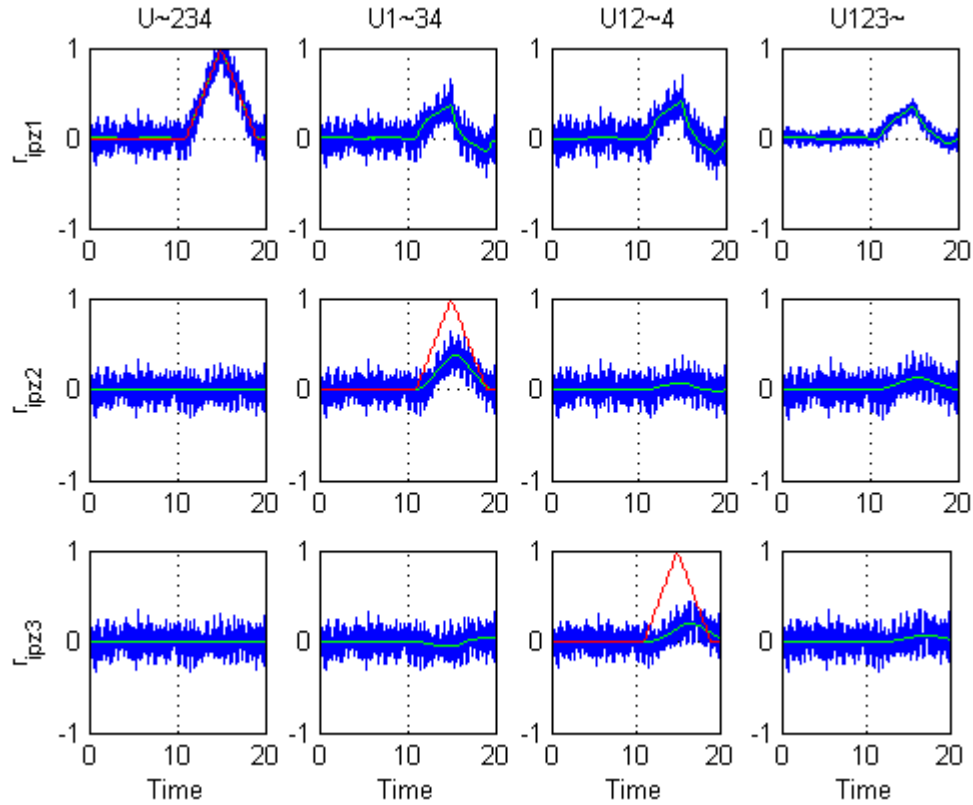


Figure III.11: Input Residuals (Fault on $u_1(t)$)

If the estimate $\hat{u}_1(t)$ is determined from UIO.U~234 (shorthand for the unknown input observer insensitive to $u_1(t)$), then from the consistency between input $u_1(t)$, $u_2(t)$, $u_3(t)$, and $y_f(t)$, an input estimate will be $\hat{u}(t) = \hat{u}_1(t) + \hat{f}(t)$ and the residual ${}_1r_u$

(shorthand for input residual from UIO.U~234) would be ${}_1r_{u_1} = -\hat{f}_1(t)$, which is the opposite of the estimate of the disturbance signal. Any other combination of inputs and outputs will result in some signature in the residuals.

Looking at the other columns in Figure III.11, it is possible to have ambiguous results. For example, column U12~4 shows a similar signature in the top row with very small residual signatures down the column. This is essentially a problem of residual evaluation, but a solution might be that if the disturbance signal (i.e. the fault) is known to have a certain characteristics, then a matched filter can be implemented along with any standard noise reduction scheme to identify signals buried in noise. Another method might be to look for fault characteristics in the frequency domain.

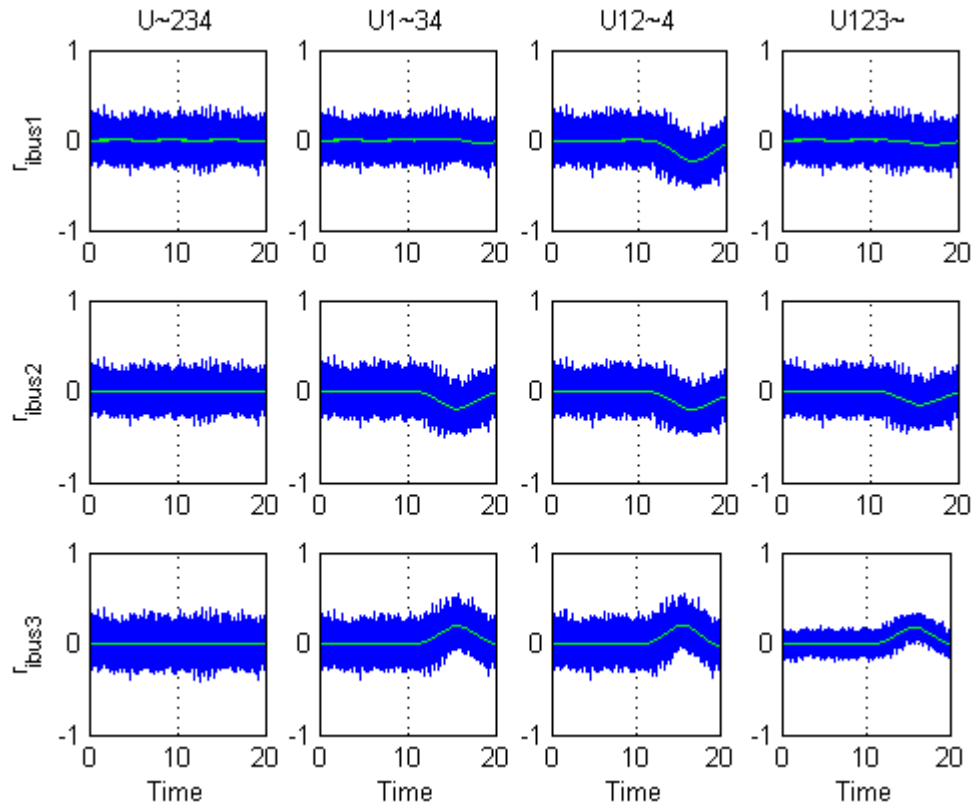


Figure III.12: UIO Example, Output Residuals (Bus Current per Zone)

Looking at Figure III.12 and Figure III.13, we see the residuals based on output measurements. Once again, the very first column has no signature while all the other columns do (except for ${}_1r_{vb_1}$, which will be explained later). This means that the fault indication is associated with $u_1(t)$. Notice in these two figures, the residuals are not nearly as pronounced as they were in the residuals based on input estimation. This can be explained by the linear combination of matrices in generating the residuals from the input estimation is better “tuned”, or simply more suitable, for detecting input faults. Likewise, residuals generated from output estimates are better suited for sensor FDI.

As mentioned before, the only output residual with any signature in the first column is the one in the top left corner of Figure III.13 (${}_1r_{vb_1}$). This is because the bus voltage sensor in zone 1 is linearly dependent on the input $u_1(t)$. Recall that this measurement was removed from UIO.U~234 when determining the state estimate. This means that the estimate will have a $u_1(t)$ fault influence on the output measurement and therefore the row can be discarded.

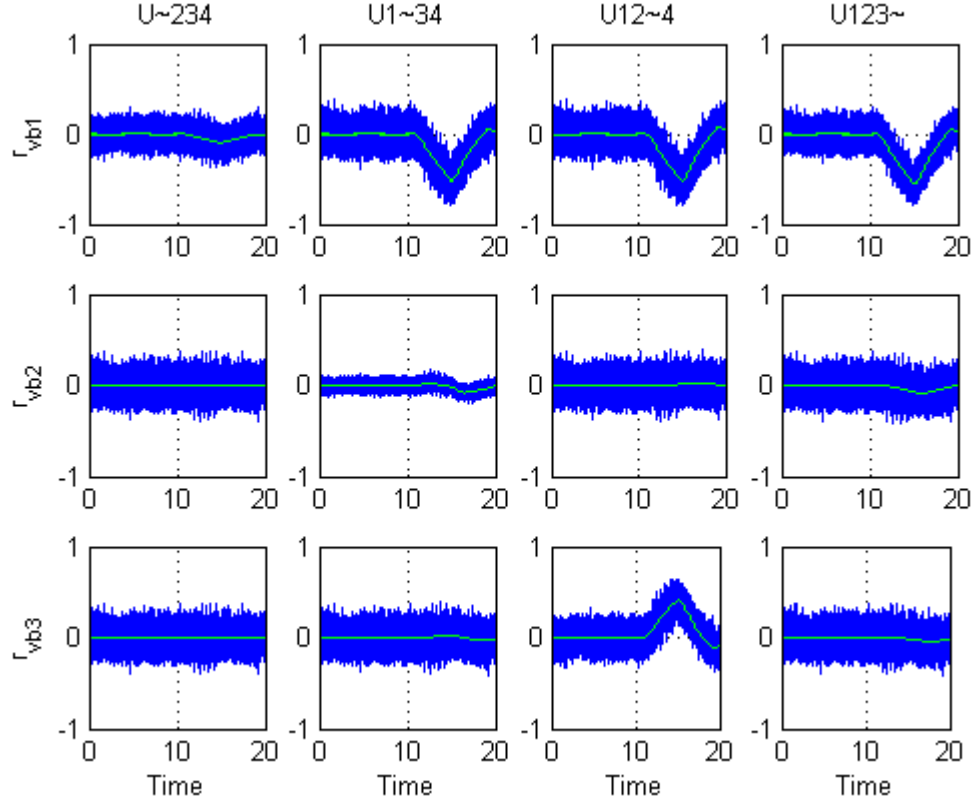


Figure III.13: UIO Example, Output Residuals (Bus Voltage per Zone)

In the second example the purpose is to demonstrate how a UIO can be used to estimate the nonlinear terms in a system and then further estimate unknown input. In this case, the power supply model with buck controller is used where its topology and corresponding parameters are shown in Figure II.3 and Table II.1. Also, its controller design and parameters are shown in Figure II.4 and Table II.2. The power supply model dynamic equation is shown in (0.4) and rewritten here as

$$\dot{x} = A_{ps}x + B_{1,ps} \begin{bmatrix} u_1(t) \\ u_4(t) \end{bmatrix} + B_{2,ps} \begin{bmatrix} u_2(t) \\ u_3(t) \end{bmatrix} \quad (0.82)$$

where the known inputs are $[u_1(t) \ u_4(t)]^T = [\sqrt{2}E \ i_{Load}]^T$ and the “unknown” inputs are the nonlinear terms $[u_2(t) \ u_3(t)]^T = [d \cdot i_{Lout} \ d \cdot v_{dc}]^T$. The UIO design shown in Figure III.14 describes the estimation procedure. The idea is to design an observer independent of the nonlinear dynamics, then estimate the inputs through input reconstruction. Finally, divide the unknown input estimates by the state estimates \hat{v}_{dc} and \hat{i}_{Lout} to determine an estimate on the control input $\hat{d}(t)$. If the input can be measured, then a residual $r_d(t)$ can be formed. In this case, both the UIO rank condition and the input observable condition are satisfied.

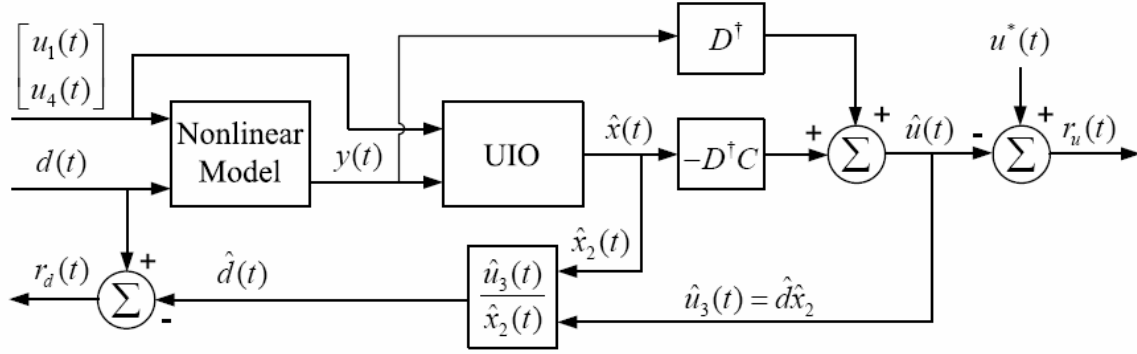


Figure III.14: Input Estimation of a Nonlinear System

The results are shown in Figure III.15. Here, the estimate of the control input $\hat{d}(t)$ is determined in the top graph while the bottom graph only serves to show that the estimate found is consistent with the actual control input trajectory.

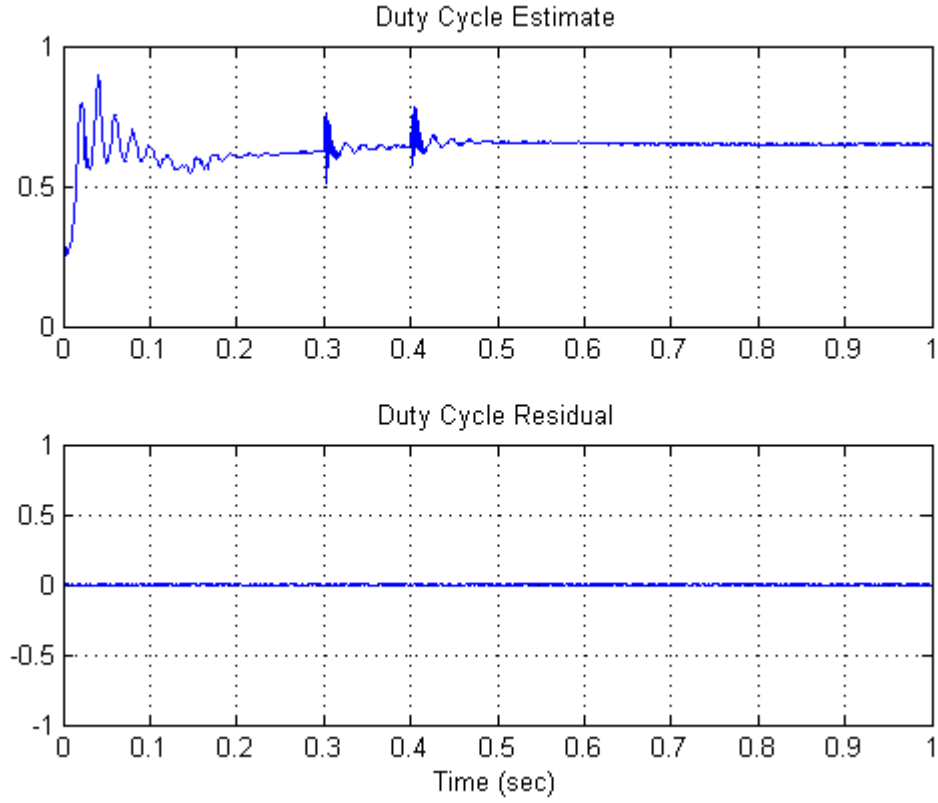


Figure III.15: Results from Polynomial UIO with Input Reconstruction

From the observer point of view, if algebraic equations relating the unknown input to the measured output are included in the output measurements and certain rank conditions similar to the left inverse problem in [268], then input estimation is achievable without additional derivatives on the partial state.

IV. FAULT DIAGNOSIS APPLIED TO THE DC ZEDS SYSTEM

It has been shown in numerous publications that the physics-based models of the DC ZEDS system accurately represent system dynamics [285][335][327][328][336]. Indeed, the DC ZEDS simulation model used herein was developed and tested by the authors of the aforementioned publications and the text [220]. Because the Power Supply, bus, SSCM, and Oring functions in Figure II.1 and described in Chapter II are well-defined, it is reasonable, then, to take a model-based approach to Fault Diagnosis on the DC ZEDS system. Chapter II sought to organize the DC ZEDS system into modules and represent their dynamics in state space form. In cases where the average value models are nonlinear, such as the power supply and SSCM modules, the models are separated into linear and nonlinear parts. Chapter III then developed several unknown input observer approaches that assume a model in state space form for implementation.

The nature of the DC ZEDS system provides high bandwidth system control response, but because it can be controlled so tightly, faults can propagate quickly as well [327] (on the order of tens of milliseconds). The fault diagnosis schemes must distinguish between normal and casualty transients and ultimately be able to dynamically reconfigure under stressful battle conditions [390]. Because time is critical, model based methods to detect the source of a fault rather than trace its effect, is sought.

This chapter applies a variety of model-based observer techniques (including the polynomial approach) to the DC ZEDS simulation model for fault detection and isolation. It is desired to detect faults and classify them according to their characteristics. Some of the means for characterization depends upon the detection method (i.e. structured residual set, unknown input observers, or fault modeling), while others upon the signature itself (i.e. positive or negative, shape, or relative size). The goal for this chapter is to develop a set of methodologies to identify residuals that indicate certain classes of faults.

It is acknowledged here that standalone sensors perform a certain level of analytical redundancy without computations. However, individual sensors do not contribute to a “global” perspective as do a network of sensors connected together by mathematical relationships. One of the presuppositions in this work is to develop ways to

automate the fault detection process quickly, reliably, and accurately – and a hierarchical automated fault detection layer using robust model-based estimation is one such way.

A. MODULAR APPROACH TO INPUT-OUTPUT CONSISTENCY

The DC ZEDS model as a whole contains 68 states, and this does not consider the ac side of the overall power system from prime mover to constant power load. From the input of the power supply to the input to the SSIM in each zone, the DC ZEDS system has many modes and system configurations that make it difficult to estimate as a whole – even under normal operating conditions. A suitable solution to handle the sheer size of the problem is to separate the system into smaller logical subsystems and connect them together with common inputs and outputs. This modular approach to verifying input-output consistency is done for the DC ZEDS system and the topology is shown in Figure IV.1.

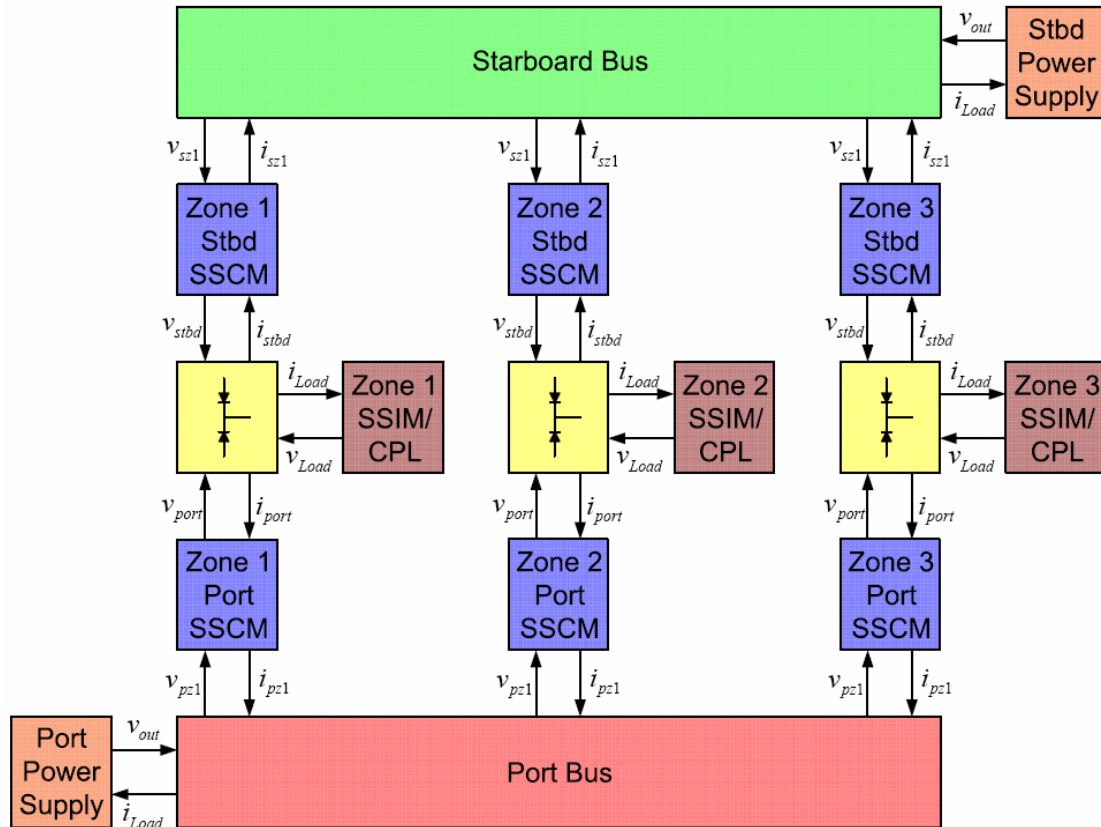


Figure IV.1: DC ZEDS Module Topology

Four representative component module block types are configured so that each input/output pair between them is shared measurements such that the output to one block is the input to the connecting block. Under this method, the entire system is viewed as a dynamic interconnection of subsystems with common inputs and outputs and is consistent with the DC ZEDS simulation model. Notice also in Figure IV.1 that the models show voltages as outputs moving toward the constant power load in each zone and currents as inputs.

Using various types of observers, model consistency is verified by comparing module estimates with measurements. With algebraic equations relating the states and the input in the form of energy conservation laws, the observers become input observable and therefore an estimate of the inputs can be made without derivatives. Taking a closer look at the input/output connections shown in Figure IV.2, we see that redundancy is verified from the input and output measurements of each module block “A”, “B”, and “C”.

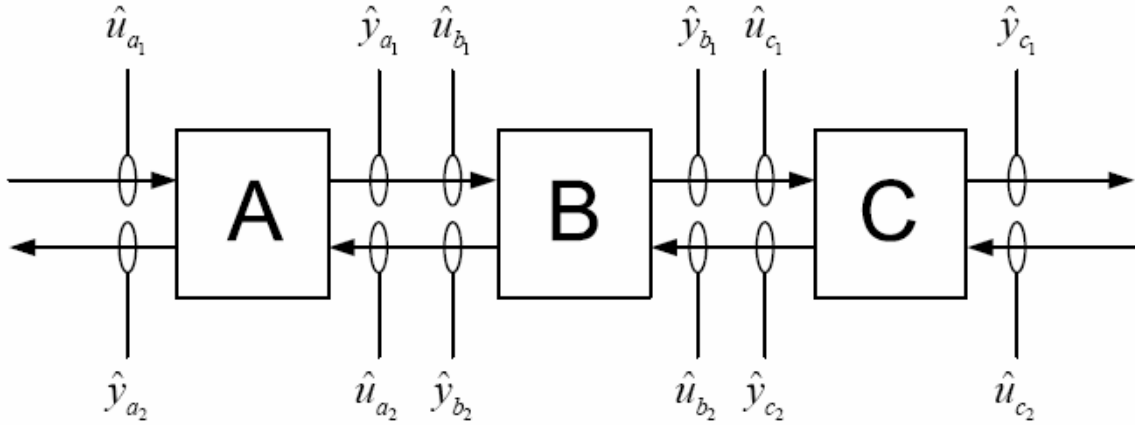


Figure IV.2: System Module Interconnection

Suppose block “B” is the port SSCM in Zone 1 where the external inputs \hat{u}_{b_1} and \hat{u}_{b_2} in (0.19)-(0.20) are the port bus voltage and load current and let \hat{y}_{b_1} and \hat{y}_{b_2} be the SSCM output voltage and the Zone 1 load requirement to the port bus, respectively. To verify analytical redundancy across the entire DC ZEDS system, estimates can be made

on system measurements from both sides of the block and compared to the estimates (or measurements) from each connecting block. In our example, \hat{u}_{a_2} and \hat{y}_{a_1} from the port bus (block “A”) would represent the bus voltage and load current in (0.10)-(0.11), while \hat{u}_{c_1} and \hat{y}_{c_1} from the Oring function (block “C”) would represent input v_{port} and output i_{port} in (0.21)-(0.22). Residuals can be generated by comparing the measurements from each common line as

$$\begin{aligned} r_{AB}(t) &= \hat{u}_{b_1}(t) - \hat{y}_{a_1}(t) \\ r_{BA}(t) &= \hat{u}_{a_2}(t) - \hat{y}_{b_2}(t) \\ r_{BC}(t) &= \hat{u}_{c_1}(t) - \hat{y}_{b_1}(t) \\ r_{CB}(t) &= \hat{u}_{b_2}(t) - \hat{y}_{c_2}(t) \end{aligned} \tag{0.83}$$

Notice that the one estimate in each equation of (0.83) is independent of the other. In this manner, the modular interconnection model shown in Figure IV.2 can zoom down to any desired level in the system, provided its external inputs and outputs are the outputs and inputs to connecting modules.

Among the benefits of this consistency scheme is increased redundancy. For example, if \hat{u}_{a_2} is a control signal input for the controller in Module A, and the signal becomes disconnected or otherwise erroneous, then between the two estimates \hat{u}_{a_2} and \hat{y}_{b_2} the fault can be isolated to one of the modules. In some cases, different methods of FDI can be performed in separate modules that draw the same conclusion and your confidence of the fault indication becomes much stronger.

From Module A, verifying sensor consistency is done using a structured residual set of regular Kalman Filters as shown in Figure IV.3. Here, an observer is designed to minimize the mean squared error of the output residuals using all the inputs and all the outputs less one. Each successive observer in the set performs the same operations until all n_y sensors are removed one at a time for a total of n_y observers. The notation ${}_1y(t)$

indicates the output measurement vector $y(t)$ without sensor 1, and so on. Likewise, ${}_1\hat{y}(t)$ and ${}_1r_y(t)$ are the corresponding output measurements and output residuals based on observer inputs $u(t)$ and $y(t)$ without sensor 1. The residual generator compares the full output vector $y(t)$ with all its estimates for consistency. Suppose for example that the number three output sensor is faulted.

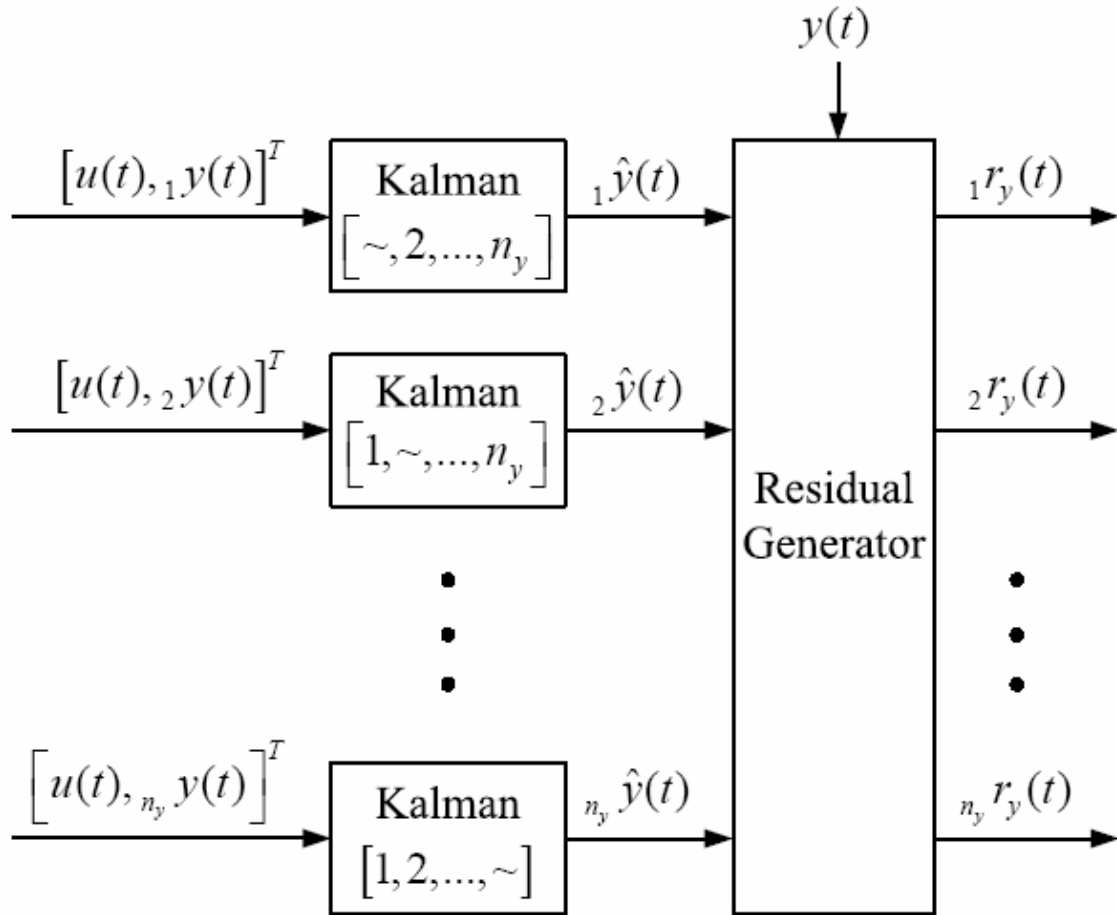


Figure IV.3: Sensor FDI Structured Residual Set

Then by the observer structure in Figure IV.3, the third observer in the set would accurately estimate the faulted output signal 3, while the rest would show a signature in the residuals. This is because all the other observers are dependent on the faulted measurement.

The following DC ZEDS example demonstrates the concept of modular FDI. Consider the nominal operating scenario where the port and starboard power supplies are energizing the port and starboard bus, respectively. The starboard bus is providing power to the load in Zone 1 while the port bus is feeding the load in Zones 2 and 3 with operating parameters according to Table II.5. The power supply controller is regulating a 500 V output voltage through the control input d , which is assumed to be measurable.

Suppose a fault occurs to the load current signal i_{out} in the port power supply controller (shown in Figure II.4) at time $t_{fault} = 0.6$ seconds. In the fault condition the signal i_{out} is a constant zero, thus removing the feedforward path to the PI controller. The local effect of the fault is that the feedforward path will communicate to the controller that there is no required load current, which disables the controller's ability to provide fast response to changes in the load. The fault propagates through to the port bus as a small transient that quickly recovers to the steady state as shown in Figure IV.4 and Figure IV.5. The starboard bus remains unchanged.

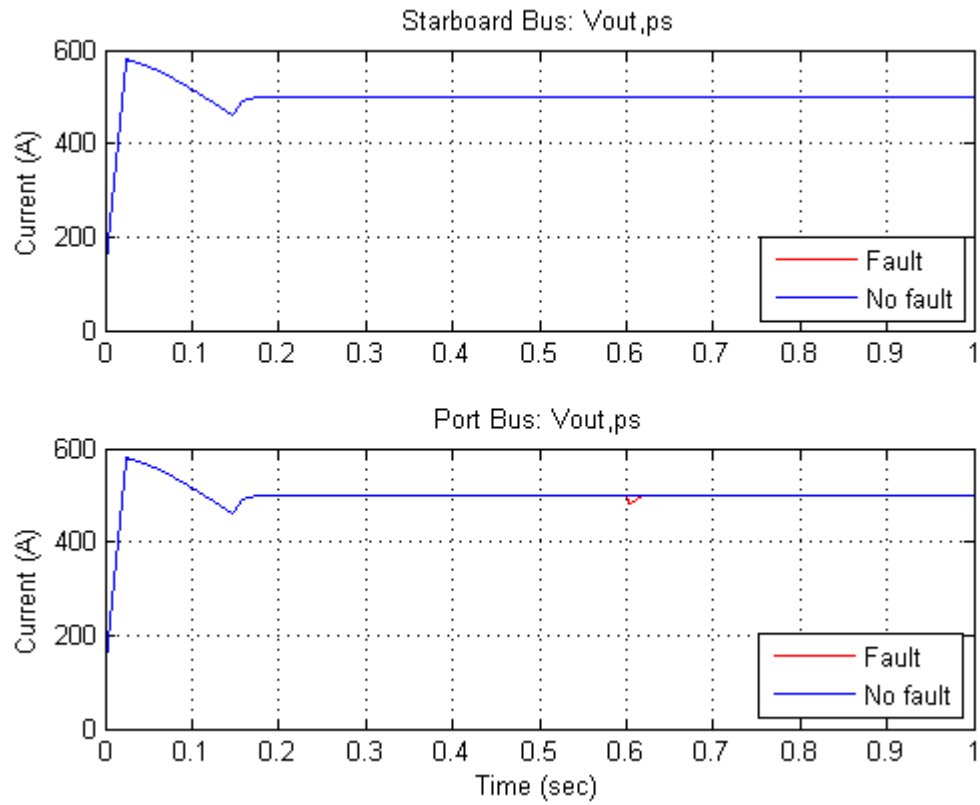


Figure IV.4: Bus Voltage Showing Bus Current Sensor Fault

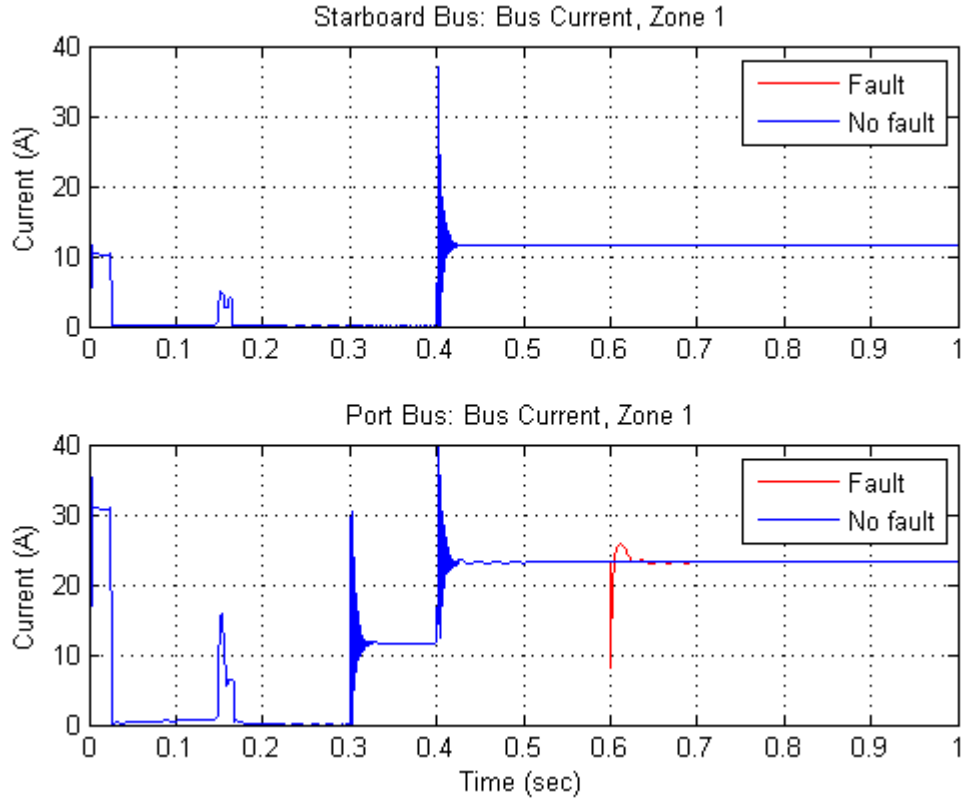


Figure IV.5: Bus Current Showing Bus Current Sensor Fault

The goal here is to use the modular FDI approach to detect the fault and determine in what module the fault originated. Beyond that, it is desirable to gain other fault characteristics, if possible. Looking at the power supply module shown in Figure IV.1 we see that it is connected to the port bus through common signals v_{out} and i_{Load} . The first step to our goal is to conduct sensor FDI on the sensors within the bus module. Developing a structured residual set of Kalman Filters as shown in Figure IV.3 achieves that task. So as to not be unnecessarily exhaustive in showing all the sensor FDI residuals, only the zone current sensors are plotted here since the other residuals are consistent with what is shown here in Figure IV.6.

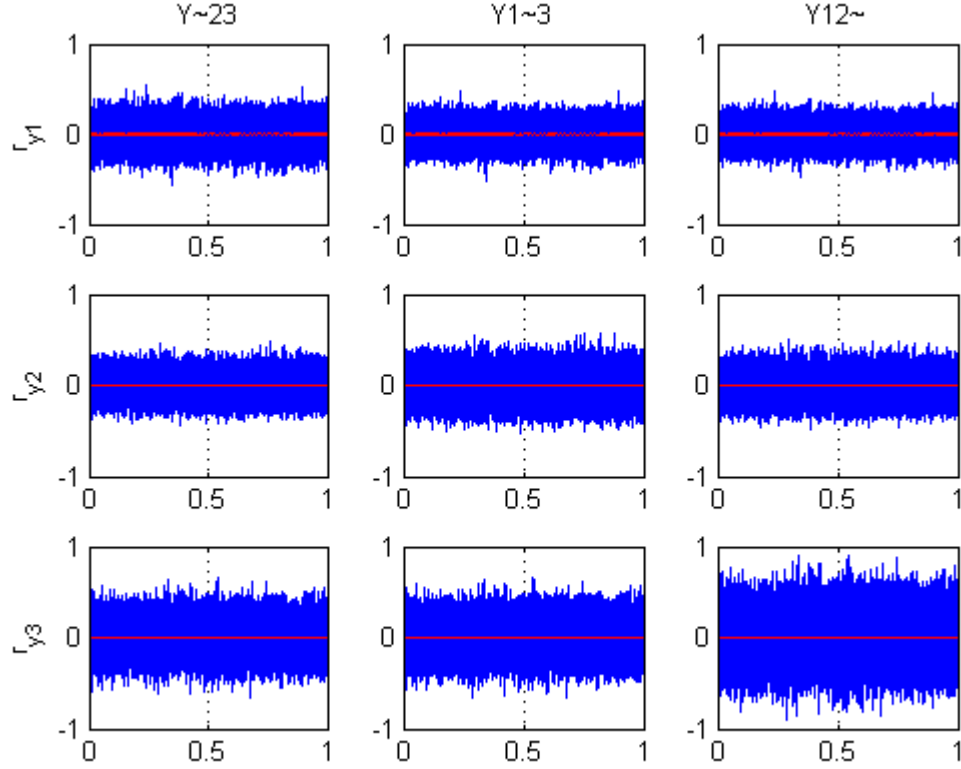


Figure IV.6: Bus Sensor FDI Residuals for Bus Current Sensor Fault in Power Supply

The residuals in Figure IV.6 show that there is consistency between estimates and measurements since they are white and stationary. It can be shown that the other sensors in the set show the same result. Based on this result, we conclude that the sensor fault is not in the bus module. Now we take a look at the structured residual set in the port power supply module. Since the fault in question occurs on the input to the power supply, an actuator fault diagnosis problem similar to the one described in Figure III.8 applies. Applying the structured residual set similar to the one shown in Figure III.9 for the power supply model in (0.4)-(0.5), we receive the following residuals on the input and output estimates as shown in Figures IV.7 and IV.8.

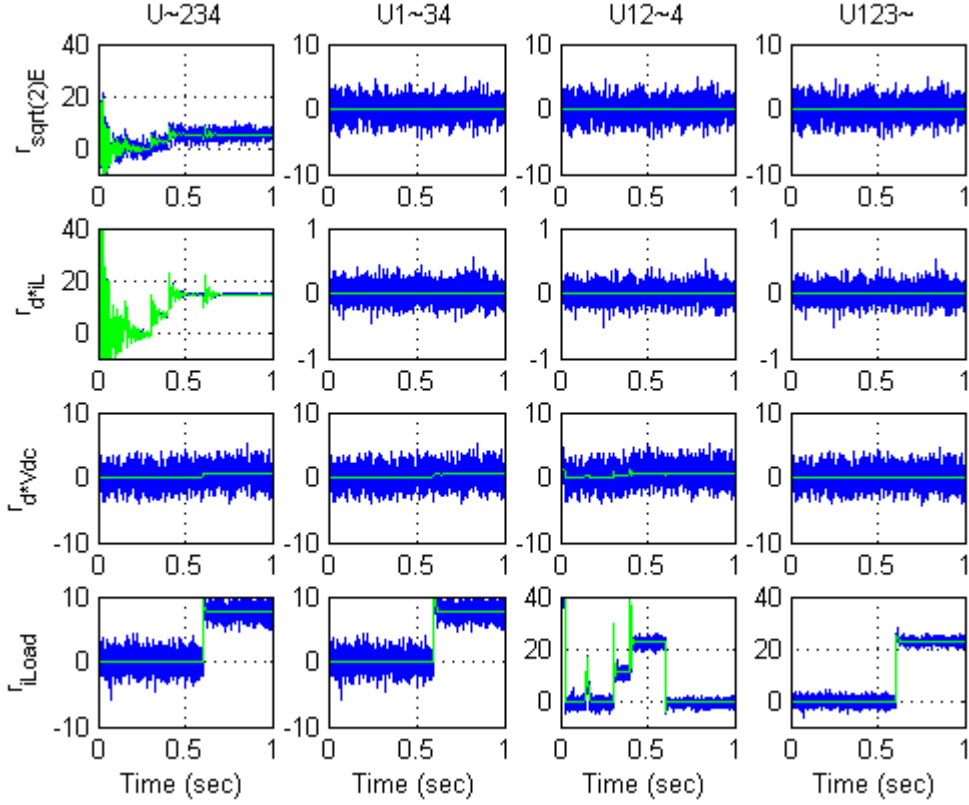


Figure IV.7: Input Residuals for Bus Current Sensor Fault in Power Supply Controller

In contrast to the sensor residuals in the bus module in Figure IV.6, the residuals in Figure IV.7 indicate the presence of a fault. As before, the residuals are generated from the input estimations indicated by row and the unknown input observers by column. Looking down column U123~, it can be seen that the only residual which is not white is in the last row, which corresponds to the signal in question, i_{Load} . This makes sense because the estimates in the column to the far right base their estimate on all inputs except i_{Load} , which is where the fault resides. The residuals down the column indicate input/output consistency, while the input estimate for i_{Load} contains the fault signature. Similar results are shown in the output residuals in Figure IV.8.

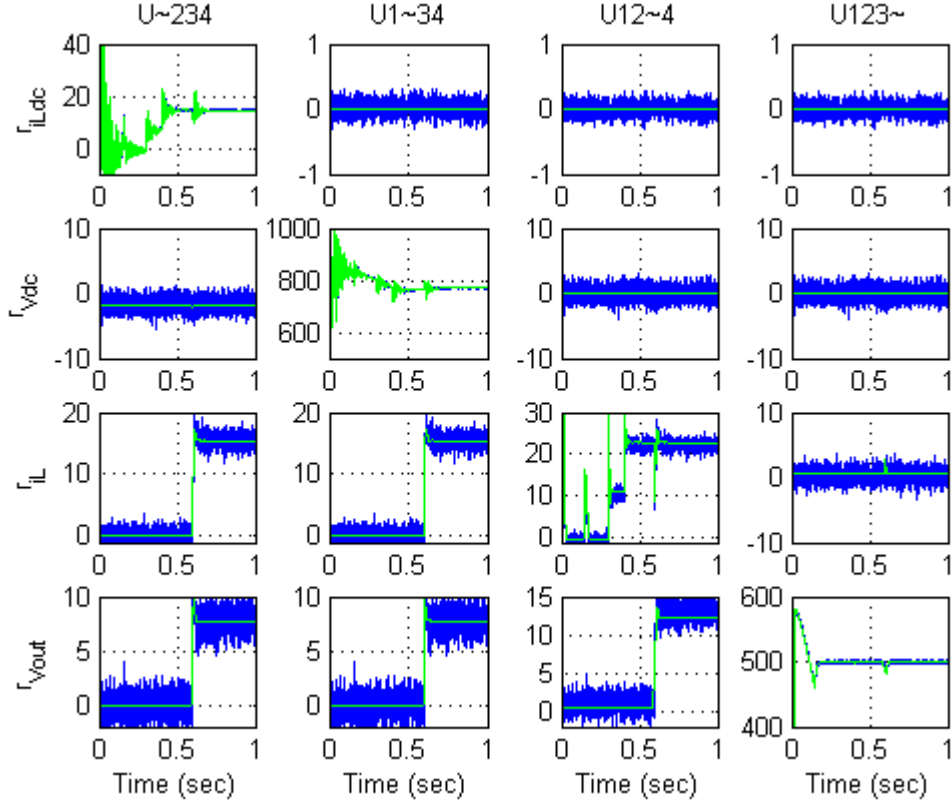


Figure IV.8: Output Residuals for Bus Current Sensor Fault in Power Supply Controller

The result of the bus current sensor fault example shows that first, the fault did not have any indication of originating in the bus module. It did, however, have an indication in the power supply model and, more specifically, the fault showed indication of residing in the bus current sensor somewhere between the bus and the controller.

B. FDI BASED ON FAULT MODELING

In the last section we considered a class of faults where the fault information was due to a difference between measurements and estimates. Using the methodical, structured residual set for both input and output residuals, a fault was detected. The key component to this method is a valid model that accurately represents the input-output relationship. In this section, we consider another means to detect faults using mathematical models specifically “tuned” to a particular class of fault. In this case,

regular Kalman Filters are determined from models which are known to indicate a fault condition in the DC ZEDS system. In this case, indication of a fault in the residuals is exactly opposite of the results from the previous section. A zero residual would indicate a match to the fault model, providing precise fault detection and isolation – provided the fault model is consistent with the actual fault dynamics.

Suppose we have a nominal plant configuration similar to the one described in the last section and we wish to consider what the effects of an SSCM switch failure in the closed position would do to the DC ZEDS system. Then, the goal is to model this failure and simulate the FDI scheme.

For simulating the SSCM switch in the closed position, we first choose the starboard SSCM in Zone 1 depicted in Figure II.1. In the average value model, the fault is triggered by setting the SSCM control signal d to 1. Similarly, in the detailed model, the control switching signal s is set to 1. A simulation of the fault condition was conducted and its effect on the bus is shown in Figures IV.9 and IV.10.

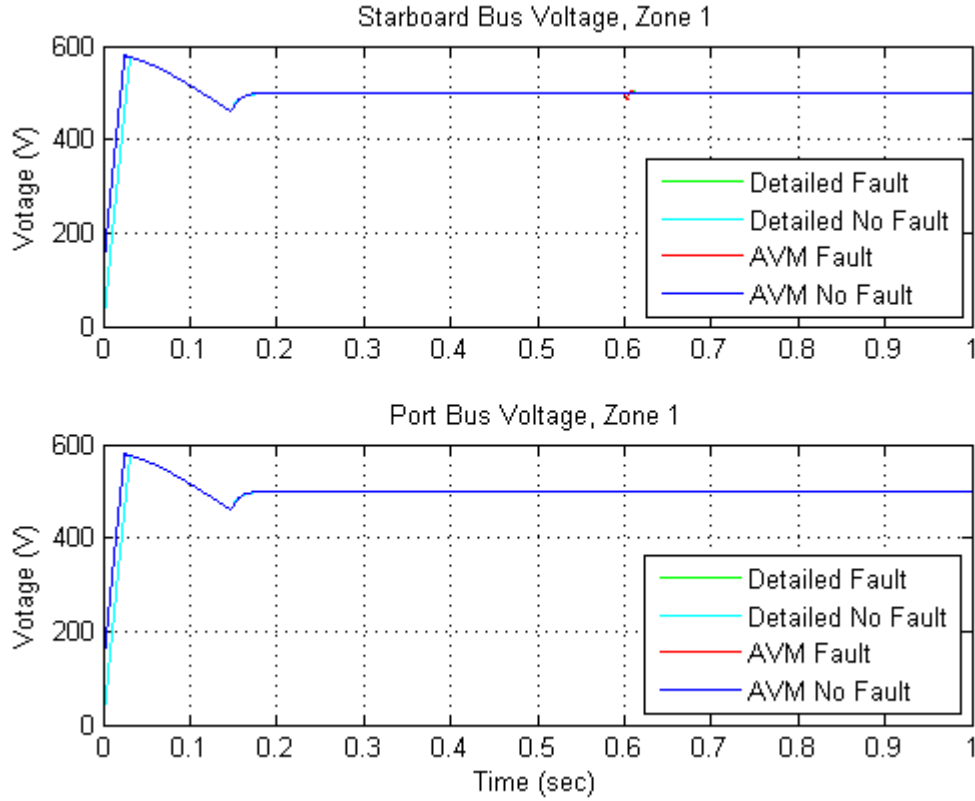


Figure IV.9: SSCM Switch Closed Failure: Port/Stbd Bus Voltage

From Figure IV.9 it can be seen that the SSCM failure has very little effect on the bus voltage. This is due to the sophisticated and robust power converter control elements that provide nearly-ideal load regulation and transient performance [327][332]. The port and starboard bus current is shown in Figure IV.10 where the starboard bus shows a large transient at the time of the fault, but settles back to near the same level as before. It can also be seen on the starboard bus current figure that the average value model follows very closely to the detailed model, even in the fault transient. Notice also that the port bus remains unchanged.

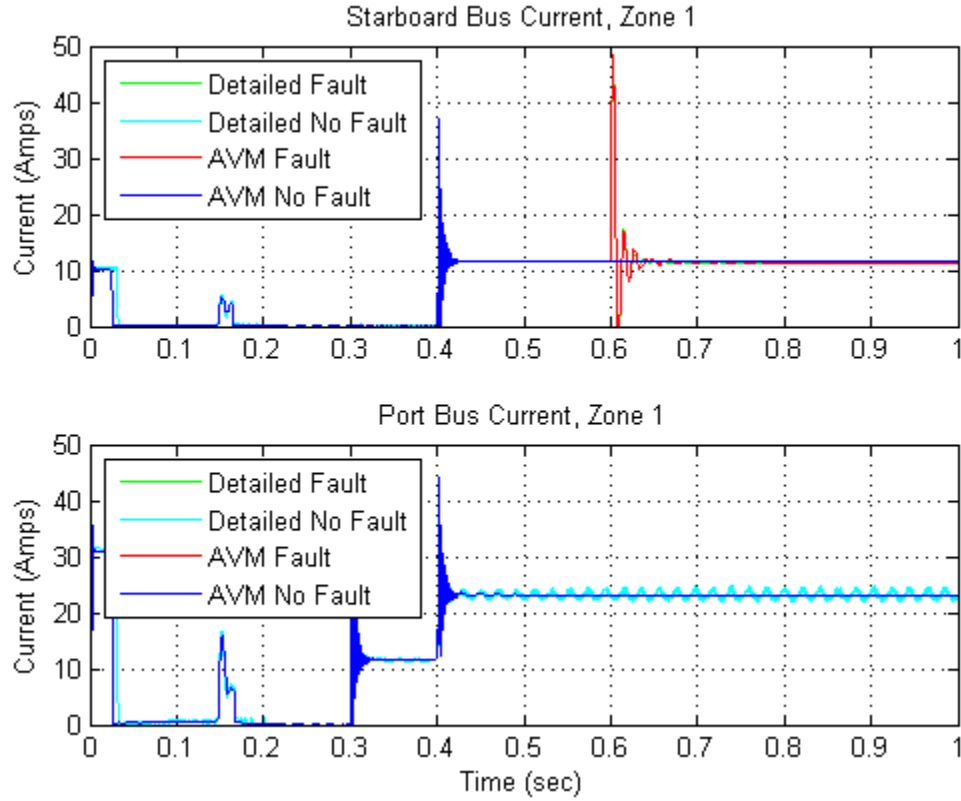


Figure IV.10: SSCM Switch Closed Failure: Port/Stbd Bus Current

The next set of figures shows the inputs and outputs to the SSCM under the switch closed fault condition. Figure IV.11 shows the inputs to the SSCM. The bus voltage is virtually unchanged as before, but the load current demand oscillates very rapidly in the steady state. This is due to the constant power nature of the load that the SSCM is feeding. If the voltage to the load oscillates in the steady state, then so will the current according to the relationship $v_{Load} \cdot i_{Load} = P^*$, where P^* is the constant load requirement shown in Figure II.15. Here again, the average value fault simulation agrees with the detailed simulation.

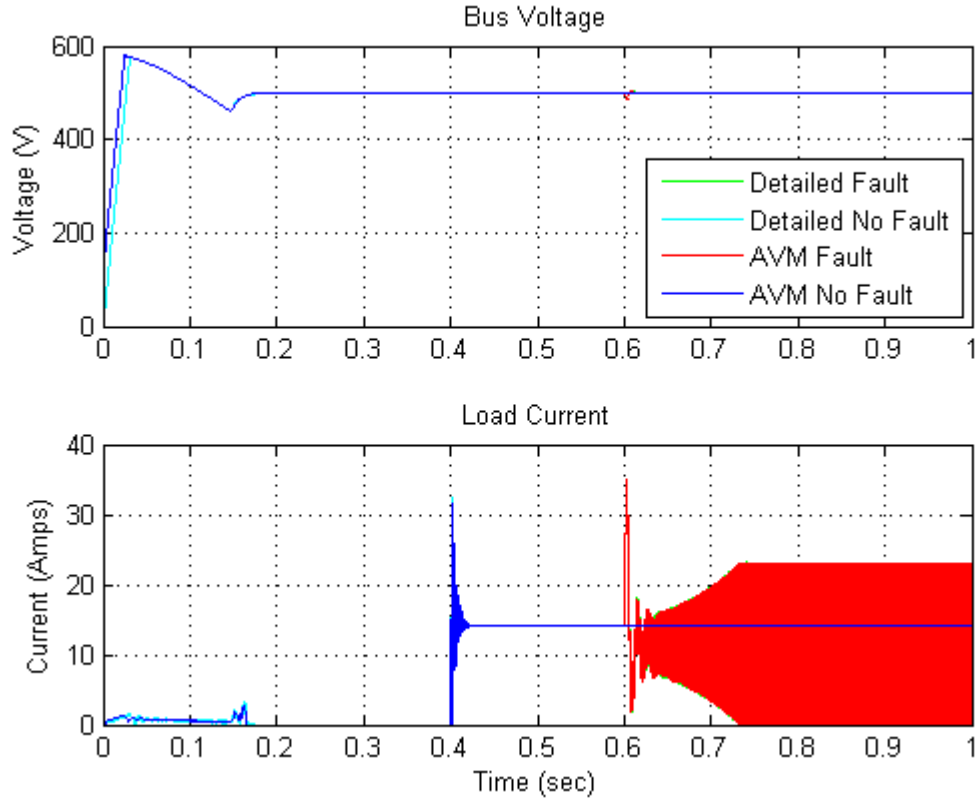


Figure IV.11: SSCM Switch Closed Failure: SSCM Inputs

Looking at the SSCM circuit diagram in Figure II.10, it can be seen that if the switch is closed permanently, then the steady-state output should be very close to the input. This is indeed the case as shown in Figure IV.12 where the dc value of the SSCM output is close to the bus voltage (500 V).

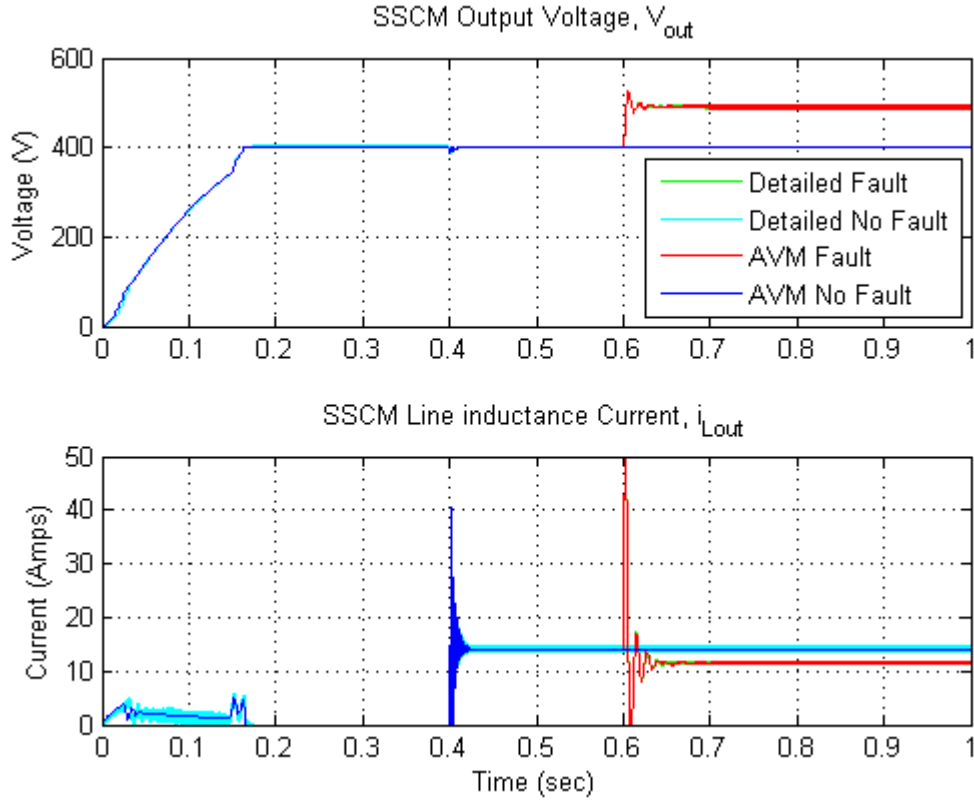


Figure IV.12: SSCM Switch Closed Failure: SSCM Outputs

Next we examine what is happening inside the controller depicted in Figure II.12. As it turns out, the position of the control signal d becomes important for detecting the fault. First, it makes sense that the duty cycle d is around 80% under no-fault conditions because the regulated output voltage is 80% of the input voltage.

If the SSCM switch fails closed, then we see that the output voltage becomes close to the input voltage. The controller in Figure II.12 shows a large error signal between the output voltage (~ 500 V) and the reference voltage (400 V), resulting in the controller commanding the switch to open. This fault condition means that the command signal d is a constant zero, while the actual operating condition of the switch is stuck in the opposite state. These command signal dynamics are shown in Figure IV.13.

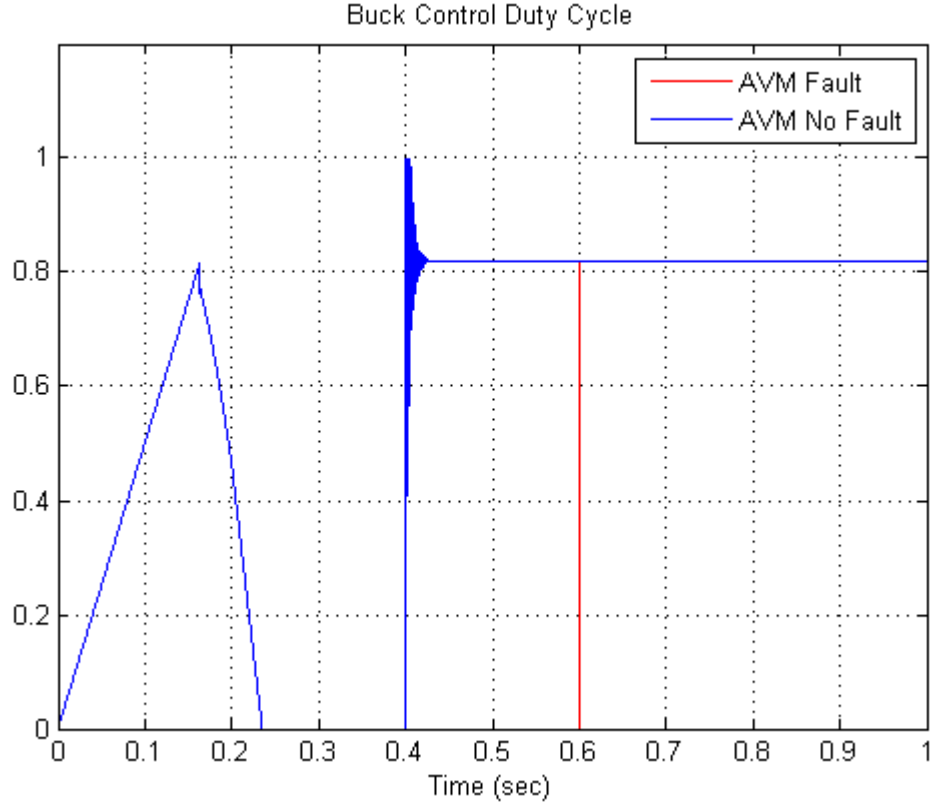


Figure IV.13: SSCM Switch Closed Failure: SSCM Control Signal d

In what follows we derive the equations that model the fault. Consider the SSCM model equations in (0.19)-(0.20) where the dynamic equation is rewritten here as

$$\dot{x} = A_{sscm}x + B_{1,sscm} \begin{bmatrix} u_1 \\ u_4 \end{bmatrix} + B_{2,sscm} \begin{bmatrix} u_2 \\ u_3 \end{bmatrix}. \quad (0.84)$$

Recall that the inputs $u_2(t)$ and $u_3(t)$ are the nonlinear terms relating the control signal d and the states of the system as

$$\begin{aligned} u_2(t) &= d \cdot x_5(t) \\ u_3(t) &= d \cdot x_3(t) \end{aligned} \quad (0.85)$$

Under the SSCM switch closed fault condition, the control signal $d=1$ and the nonlinear terms in (0.84) can now be expressed as a part of the linear dynamics in the new fault dynamics state space equation

$$\dot{x}(t) = A_{sscm}^* x(t) + B_{1,sscm} \begin{bmatrix} u_1(t) \\ u_4(t) \end{bmatrix} \quad (0.86)$$

where

$$A_{sscm}^* = A_{sscm} + \begin{bmatrix} 0 & 0 & 0 & 0 & 0 \\ 0 & 0 & 0 & 0 & 0 \\ 0 & 0 & 0 & 0 & -\frac{1}{C_{f_2}} \\ 0 & 0 & 0 & 0 & 0 \\ 0 & 0 & \frac{1}{L_{out}} & 0 & 0 \end{bmatrix}.$$

The fault model in (0.86) along with the output equations in (0.20) is controllable, observable, and input observable. Therefore, a standard Kalman Filter is applied to the SSCM switch closed fault model and simulated using the detailed model data. The results in Figure IV.14 show the opposite trend in a positive identification of the fault compared to previous methods, which is expected. What we have is essentially a filter that is “tuned” to the particular fault where the residuals will be zero when the fault occurs, which indicates input/output consistency in the fault condition. All five states of the SSCM model reveal a constant near-zero mean residual, but only 4 of the 5 are shown in Figure IV.14.

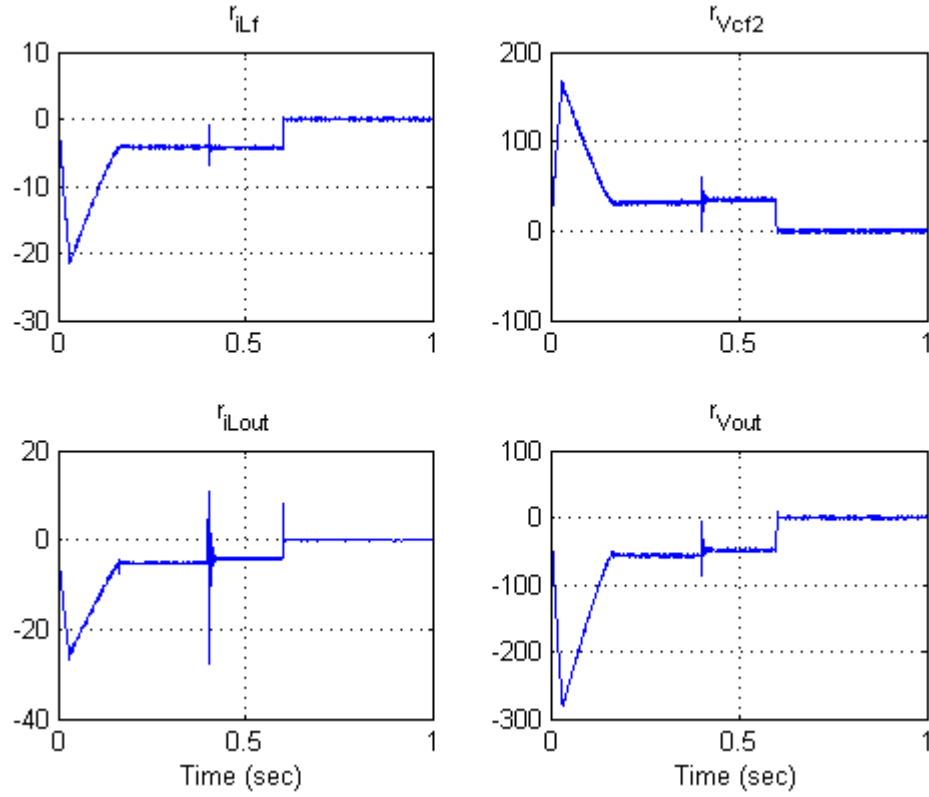


Figure IV.14: SSCM Switch Closed Failure: Fault Model Residuals

Finally, we go back to the nonlinear input estimation problem described in Figure III.14. The SSCM model (0.19) has a similar model equation structure as the power supply model (0.4) and so its control signal d can be estimated in like manner. Recall that in the failed condition where the output voltage is far greater than the reference voltage, the SSCM controller is continuously sending the command to have the switch opened as seen in Figure IV.13. Without the use of the fault model, a fault indication can still be achieved if a UIO scheme is set up such that it estimates the command signal d . If the control signal is measurable, then a residual on the command signal can indicate the presence of an SSCM switching fault as shown in Figure IV.15.

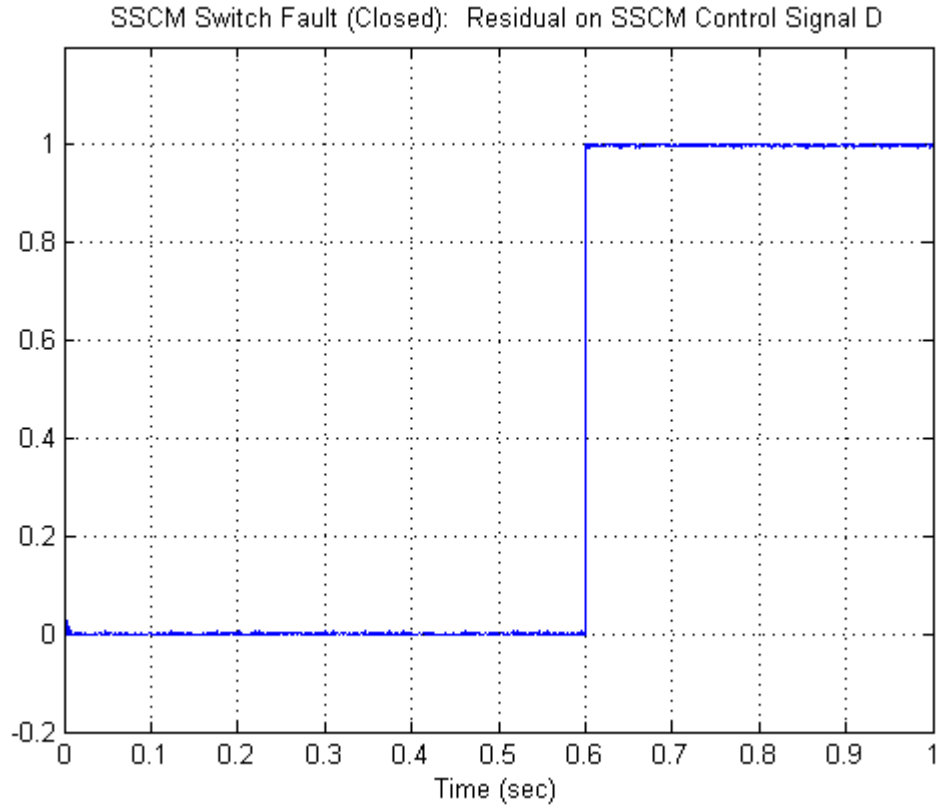


Figure IV.15: SSCM Switch Closed Failure: Residual on Control Signal d

One more example for FDI based on fault modeling is presented. Suppose only the port power supply is on line providing power to all three zones and an open circuit on the bus occurs so that Zone 3 is dead. The scenario was simulated and the results are shown in Figure IV.16. The bus current, is shown to drop from the no fault Mode 3 condition down to the Mode 2 condition. This is consistent with what is expected since the load in Zone 3 is completely dropped.

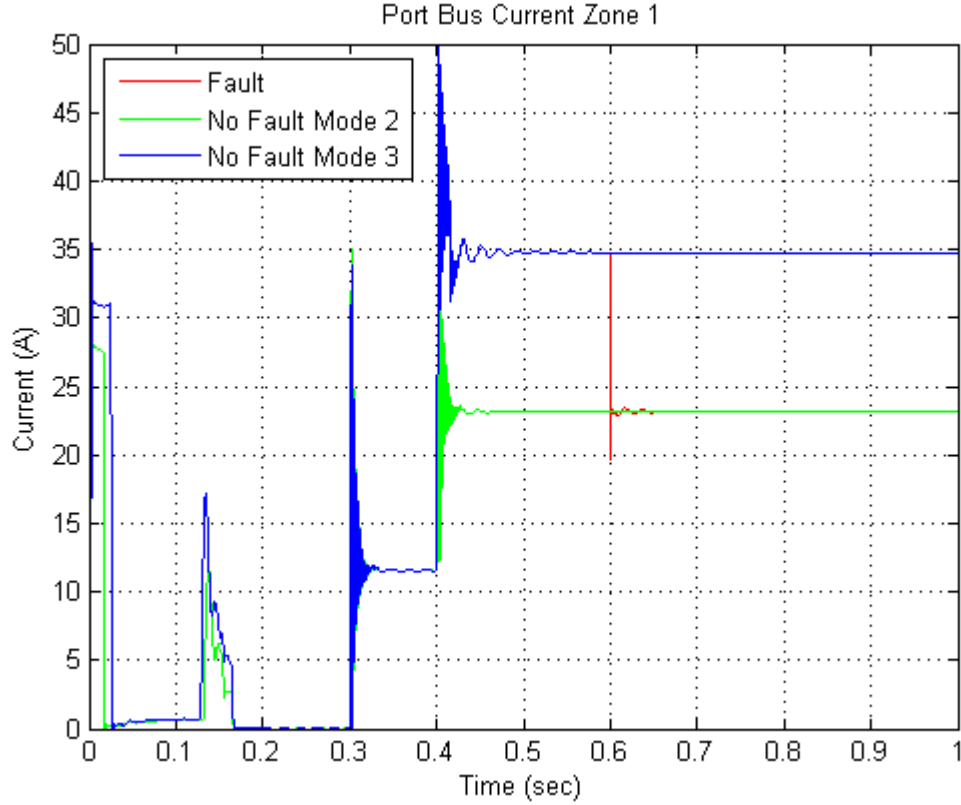


Figure IV.16: Bus Open Circuit in Zone 3: Bus Current

We use the three bus mode models shown in Figure II.6 and Table II.4 as a means to detect the bus open circuit. Using the inputs and output measurements, we process the data through three Kalman Filters tuned to each bus mode configuration. The model that is most consistent with the input and output data will show a zero residual. The observers are based on bus model equations (0.10)-(0.11), and the results are shown in Figure IV.17. From the residuals, it can be seen that the system began in Mode 3 operation (i.e., all zones on line) and then suddenly switched to zone 2, indicating an open circuit in zone 3.

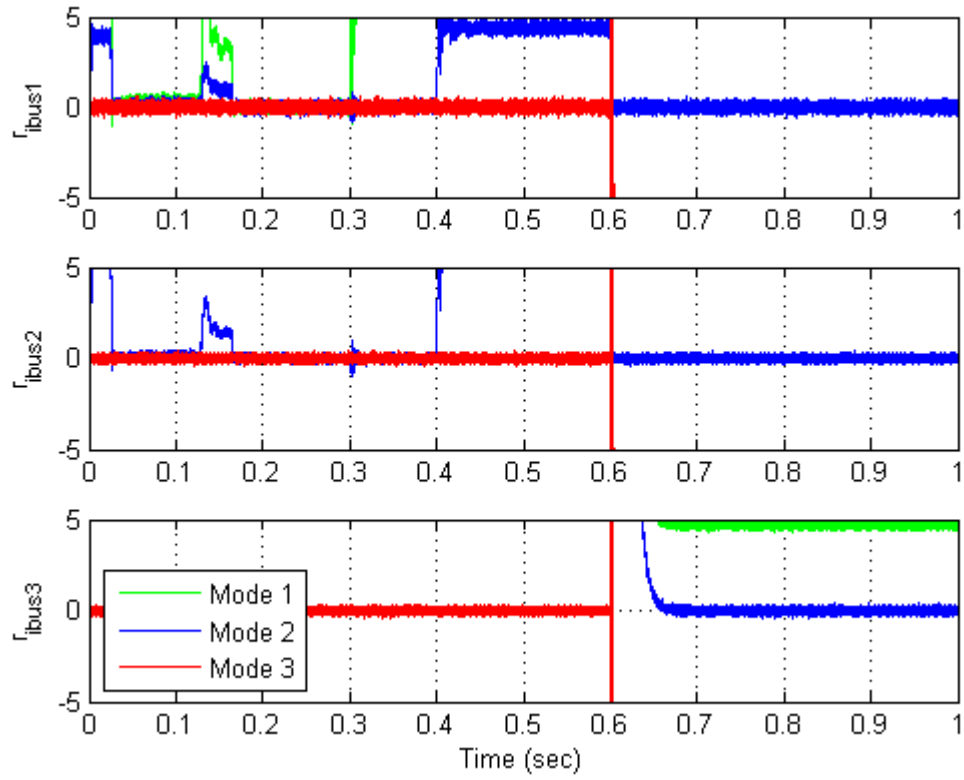


Figure IV.17: Bus Open Circuit: 3 Mode Residuals

To conclude this section, it is shown that FDI using fault models shows good results. But like all model-based methods, they are dependent on the accuracy of the model. Fortunately, these models have been proven to be accurate.

V. CONCLUSION

A. SUMMARY OF FAULT DIAGNOSIS RESULTS TO THE DC ZEDS MODEL

Model-based Fault Diagnosis is an excellent method for validating system input/output consistency and to detect fault indicators in the residuals, which is the fundamental principle of analytical redundancy. However, these methods are only as good as the models upon which they are based. Fortunately, it has been shown that the DC ZEDS model is an accurate power electronics-based distribution system and is very similar in design to the reduced scale hardware model implemented in the Naval Combat Survivability (NCS) Testbed located at Purdue University, which is specifically designed for concept studies such as the ones in this work [335]. The DC ZEDS system is a reduced-scale model, yet it contains enough of the complex, nonlinear, dynamically interdependent nature to make it quite suitable for scholarly research [56][327][328][245][246][335][285].

Two models were used side-by-side for the results of this research: the average value model and the more accurate detailed model. The difference between the two models is the 20 kHz switching dynamics of the power supply and SSCM. The average value models are nonlinear, but the switching dynamics are removed and, through the use of unknown input observers, accurate state and input estimates are determined for robust residual generation. In these fault scenarios, most of the FDI results aim at detecting the source of a fault rather than studying its propagation effects.

Based on the results, the average value model accurately matched the detailed model for the fault scenarios studied herein – even in the transients. It is acknowledged, however, that a class of faults caused by switching dynamics may not be accurately modeled (and therefore not accurately estimated) using the average value model and so they were not addressed.

The closest one of the fault scenarios came to studying switching dynamic faults is the one with the SSCM switch failure in the closed position. Here, the nonlinear dynamics are essentially removed by a constant connection, and a model of the fault is

formed. The FDI scheme in this scenario used an observer based on the fault model to generate a residual. Similarly, another fault model scheme presented in the results uses a bank of Kalman Filters specifically “tuned” to detect an open circuit in various places along the bus. Again, the indication of this fault will be a zero in the residuals, meaning that there is input/output consistency in the fault condition. As long as the models accurately represent the system and the fault, the fault model FDI scheme works quite well. One drawback to this method might be that it is specifically designed to detect a particular fault while other FDI methods (using a structured residual set, for example) are able to detect a broader class of faults. This might not be undesirable, though, if several FDI methods are applied concurrently; for example, one FDI method might be used for detecting a broader class of faults with less accuracy and the other method might be used for detecting (with greater accuracy) a very specific fault that is known to produce grave consequences.

For a more general FDI scheme, it is shown that model consistency for the overall large-scale system can be successfully subdivided into modules with common inputs to and outputs from connecting modules. In this manner, classes of faults (such as sensor faults or communication faults between modules) can be isolated to a particular module by verifying input/output consistency between modules. This modular FDI approach has the effect of being able to subdivide into arbitrarily small submodules, provided that the inputs and outputs are common to the connecting modules.

B. SUMMARY OF POLYNOMIAL UIO RESULTS

A special type of observer that can be made insensitive to any combination of inputs (provided certain conditions are satisfied) is used extensively for the FDI application. It is shown in several examples that a structured residual set of unknown input observers can accurately detect and isolate actuator faults and in some cases can estimate the fault signal itself. Here, two UIO methods based on a polynomial representation of a system are developed and compared to the subspace projection UIO method. Since these methods take advantage of the partial-state representation of a system, it is shown that in some cases an estimate of the partial state can still be determined even if the UIO rank condition is not satisfied, which is a necessary condition

for the subspace projection UIO method. For the purpose of residual generation, a partial-state representation could possibly be all that is needed. If the full-state estimate is required, then it can still be done by taking derivatives of the partial state – a process that is sensitive to noise.

The input replacement UIO method is straightforward to implement, but is restricted to a smaller class of systems where higher degrees of the numerator polynomial is necessary. One way to ensure the higher numerator polynomial degree is to include output measurements that are dependent on the states and inputs. In the state space realization, this implies that the D matrix is nonzero. The input replacement UI method is also similar to the input inversion problem.

The parametrization UIO method is comparable in performance to the subspace projection method and applies to a larger class of systems. It is based on the nonunique solution of the Diophantine equation, where the particular solution we choose separates the known system dynamics from the unknown. It is believed that this concept can be extended to an adaptive polynomial UIO method where the parameter vector is determined adaptively by minimizing the output residual. However, precise conditions for existence of a solution still have to be determined. In some applications to the DC ZEDS models, the parametrized solution of the UIO provided a nonrealizable estimator.

Having a feed-through D matrix in the system of equations of the state space realization (which implies higher order numerator polynomials in the right matrix polynomial realization) also allows for input estimation without having to take derivatives of the partial state. Input estimation is quite useful for fault diagnosis as shown in several examples where the input to a nonlinear model was estimated. It is also a key element to the modular approach to FDI as it enables each module to estimate both outputs and inputs for consistency validation. It has also been shown that in some cases an estimate of the fault signal itself can be determined.

C. FUTURE WORK

For follow-on work, other non-model based fault diagnosis strategies could be developed and compared to these results. It would also be valuable to validate the fault diagnosis schemes using the Naval Combat Survivability (NCS) Testbed; it is very similar in design to the DC ZEDS model described in Chapter II and has been developed by the same team of engineers at Purdue University [335]. Here, real-time FDI on an actual hardware DC ZEDS system could be compared with simulation results. The work would require modeling and simulation on a validated truth model using Advanced Continuous Simulation Language (ACSL).

At the reconfiguration level shown in Figure I.1, raw residual data is analyzed and decisions are made about positive fault identification. From the innovations determined in Chapter IV on the stochastic models described in Chapter II, residual evaluation techniques can be applied to determine fault probabilities or to develop an intelligent fault decision-making process. Methods for residual evaluation may include:

- Generalized likelihood ratio (GLR) testing
- Fuzzy logic
- Adaptive thresholds (time and/or freq domain)
- Hypothesis testing
- Multiple Model Adaptive Estimation (MMAE)

In this systematic manner of evaluating residuals, a positive fault indication can then be sent to a control reconfiguration scheme to achieve the ultimate goal: continuity of service despite combat damage involving cascading failures.

Other areas for FDI research could be to introduce multiple simultaneous faults or conduct similar fault simulations on the DC ZEDS system with a droop a mode capability where power in each zone is brokered between the port and starboard busses.

In [60], authors Chen and Patton note that robust FDI is still an “open problem” where the most significant challenge is due to conflicting criteria in model-based robust residual generation. Specifically, residual generation methods must be sensitive to faults, yet insensitive to modeling uncertainties. In order to account for this in the residuals, a multicriteria optimization approach can be investigated where fault effects are maximized and modeling uncertainties are minimized. Some general optimal FDI work has been studied using a single objective function codified as a weighted sum of objectives [59][60]. In many of these cases, however, the solutions do not adequately address the original problem [322]. What’s more, FDI is most often considered separately from the rest of the system design. A better approach might be to develop a multicriteria optimal solution by investigating trade offs between design variables, system constraints, control laws, sensor allocation, and fault sensitivity.

THIS PAGE INTENTIONALLY LEFT BLANK

APPENDIX A: IFAC SAFEPROCESS FAULT DIAGNOSIS DEFINITIONS

The following keywords are common terms applied to the field of Fault Diagnosis and Fault Tolerant Control. They were developed by the Fault Detection, Supervision, and Safety for Technical Processes (SAFEPROCESS) Technical Committee and published in Isermann and Balle, 1997; [178]. The definitions are widely accepted in published books on the subject (Blanke et. al., 2003; [44], Chen and Patton, 1997; [60]).

Active fault-tolerant control system	A fault-tolerant system where faults are explicitly detected and accommodated. Opposite of a passive fault-tolerant system.
Analytical redundancy	Use of two or more, but not necessarily identical ways to determine a variable where one way uses a mathematical process model in analytical form.
Availability	Probability of that a system or equipment will operate satisfactorily and effectively at any point in time.
Constraint	The limitation imposed by nature (physical laws) or man. It permits the variables to take certain values in the variable space.
Dependability	A form of availability that has the property of always being available when required. It is the degree to which a system is operable and capable of performing its required function at any randomly chosen time during its specified operating time, provided that the item is available at the start of that period.
Diagnostic model	A set of static or dynamic relations which link specific input variables - the symptoms - to specific output variables - the faults.
Discrepancy	An abnormal behavior of a physical value or inconsistency between more physical values and the relationship between them.
Disturbance	An unknown (and uncontrolled) input acting on a system
Error	Deviation between a measured or computed value (of an output variable) and the true, specified, or theoretically correct value.
Fail safe	The ability to sustain a failure and retain the capability to make a safe close-down. A system where the occurrence of a single fault can be determined but not isolated and where the fault cannot be accommodated to continue operation.

Fail-operational	A fault-tolerant system has the property that a single fault does not develop into a failure of the closed-loop system. A Fail-operational system is one that the performance of the faulted system remains the same (original objective of the nominal system is met).
Failure	Permanent interruption of a systems ability to perform a required function under specified operating conditions.
Failure effect	The consequence of a failure mode on the operation, function, or status of an item.
Failure mode	Particular way in which a failure can occur.
Fault	Unpermitted deviation of at least one characteristic property or parameter of a system from its acceptable/usual/standard condition.[Blanke et. al. adds: A fault is the occurrence of a failure mode (Blanke, 2003)]
Fault accommodation	A correcting action (reconfiguration or a change in the operation of a system) that prevents a certain fault to propagate into an undesired end-effect.
Fault detection	Determination of faults present in a system and time of detection.
Fault detector	An algorithm that performs fault detection and isolation.
Fault diagnosis	Determination of kind, size, location, and time of occurrence of a fault. Fault diagnosis includes fault detection, isolation, and estimation.
Fault estimation	Determination of the size and behavior of a fault over time.
Fault identification	Determination of the size and time-variant behavior of a fault. Follows fault isolation
Fault isolation	Determination of kind, location, and time of detection of a fault. Follows fault detection.
Fault modeling	Determination of a mathematical model to describe specific fault effect.
Fault propagation analysis	Analysis to determine how certain fault effects propagate through the considered system.
Fault tolerant control	Aims at changing the control law so as to cancel the effects of the faults or to attenuate them to an acceptable level.

Fault tolerant system	A system where a fault is accommodated with or without performance degradation, but a single fault does not develop into a failure on subsystem or system level. Fault tolerant system has the property that a single fault does not develop into a failure of the closed-loop system (p. 9).
Hardware redundancy	Use of more than one independent instrument to accomplish a given function
Incipient fault	A fault where the effect develops slowly e.g. clogging of a valve. In opposite to an abrupt fault.
Malfunction	An intermittent irregularity in the fulfillment of a system's desired function.
Monitoring	A continuous real-time task of determining the conditions of a physical system, by recording information, recognizing and indicating anomalies in the behavior
Passive fault-tolerant system	A fault-tolerant system where faults are not explicitly detected and accommodated, but the controller is designed to be insensitive to a certain restricted set of faults. Contrary to an active fault-tolerant system.
Perturbation	An input acting on a system, which results in a temporary departure from the current state.
Protection	Means by which a potentially dangerous behavior of the system is suppressed if possible or means by which the consequences of a dangerous behavior are avoided.
Qualitative model	Use of static and dynamic relations among system variables and parameters in order to describe a system's behavior in qualitative terms such as causalities or if-then rules.
Quantitative model	Use of static and dynamic relations among system variables and parameters in order to describe a system's behavior in quantitative mathematical terms.
Recoverability	Possibility to accommodate the fault or to reconfigure the system if fault occurs.
Reliability	Ability of a system to perform a required function under stated conditions, within a given scope, during a given period of time.
Remedial action	A correcting action (reconfiguration or a change in the operation of a system) that prevents a certain fault to propagate into an undesired end-effect. Synonymous to fault accommodation.

Residual	A fault indicator, based on a deviation between measurements and model-equation-based computations
Safety	Ability of a system not to cause danger to persons or equipment or the environment
Safety system	Electronic system that protects local subsystems from permanent damage or damage to environment when potential dangerous events occur.
Sensor fusion	Integration of correlated signals from different [sources].
Supervision	Monitoring of a physical system and taking appropriate actions to maintain the operation in the case of faults.
Symptom	A change of an observable quantity from normal behavior.
Threshold	Limit value of a residual's deviation from zero, so if exceeded, a fault is declared as detected.

APPENDIX B: POWER SUPPLY AVM TRANSFORMATION

The average value model begins with several reference frame transformations of the input voltage to obtain the time-dependent rms voltage of the input. The source for the transformation is shown in Krause *et al* [220].

The 3-phase ac input voltage is expressed as

$$v_{ag} = \sqrt{2}E \cos(\theta_g) \quad (.87)$$

$$v_{bg} = \sqrt{2}E \cos\left(\theta_g - \frac{2\pi}{3}\right) \quad (.88)$$

$$v_{cg} = \sqrt{2}E \cos\left(\theta_g + \frac{2\pi}{3}\right) \quad (.89)$$

and the arbitrarily rotating real and reactive (q-d) axis representation is expressed as

$$v_{qd0s} = K_s v_{abc}, \quad (.90)$$

where

$$K_s = \frac{2}{3} \begin{bmatrix} \cos \theta_g & \cos(\theta_g - 2\pi/3) & \cos(\theta_g + 2\pi/3) \\ \sin \theta_g & \sin(\theta_g - 2\pi/3) & \sin(\theta_g + 2\pi/3) \\ 1/2 & 1/2 & 1/2 \end{bmatrix}.$$

If the input deviates from being balanced, then the third of 3 outputs of the transformation will be nonzero.

A second transformation is applied to the arbitrarily rotating orthogonal q-d axis to a reference frame where the reactive voltage is identically equal to zero. In doing so, the transformation calculates the rms voltage of the input, $\sqrt{2}E$.

$$\begin{bmatrix} v_q^g \\ v_d^g \end{bmatrix} = \begin{bmatrix} \sqrt{2}E \\ 0 \end{bmatrix} = {}_a K_g v_{qd0s} \quad (.91)$$

where

$${}_a K_g = \begin{bmatrix} \cos(\varphi_g) & \sin(\varphi_g) & 0 \\ -\sin(\varphi_g) & \cos(\varphi_g) & 0 \\ 0 & 0 & 1 \end{bmatrix}$$

and

$$\varphi_g = \tan^{-1} \left(\frac{v_q^g}{v_d^g} \right). \quad (.92)$$

The average value model of the 3-phase bridge rectifier is developed in [Krause, et al] and the schematic of the Port Power Supply in the DC ZEDS model is shown in Figure 1 along with its Buck Converter controller. The input voltage expression takes into account the line-to-line voltage of the balanced 3-phase ac input and represents it with the rms voltage. The 3 phase full wave rectifier equipped with thyristors allows for full control of the output dc voltage through the control input firing angle α .

APPENDIX C: SUBSPACE PROJECTION UNKNOWN INPUT OBSERVER

The purpose of Appendix C is to develop the subspace method Hui and Zak's unknown input observer from a slightly different approach presented in [175]. The resulting observer design allows for any combination of inputs to be made insensitive to the observer – or all of them – provided that certain rank conditions are met. This design freedom makes this observer type useful for Fault Diagnosis. The paper does not explicitly address output measurements that are dependent on the inputs (i.e. $D \neq 0$), only to the extent that the input can be subtracted from the output measurements before the UIO is implemented and then added back to obtain an output estimate.

The class of dynamical models considered herein is of the form

$$\dot{x} = Ax + Bu \quad (.93)$$

$$y = Cx \quad (.94)$$

where state vector $x \in \mathbb{R}^{n_s}$, input $u \in \mathbb{R}^{n_u}$, and output $y \in \mathbb{R}^{n_y}$ and matrices A , B and C are completely known with appropriate dimensions. For a system where at least one of n_u inputs is unknown, the input matrix B and corresponding input vector function u are partitioned into known and unknown inputs as

$$Bu = \begin{bmatrix} B_1 & B_2 \end{bmatrix} \begin{bmatrix} u_1 \\ u_2 \end{bmatrix}$$

where the first n_{u_1} known inputs are separated from the remaining $n_{u_2} = n_u - n_{u_1}$ unknown inputs. In this manner, the inputs of (.93) can be represented with separated known and unknown inputs with the same output equations as

$$\dot{x} = Ax + B_1 u_1 + B_2 u_2 \quad (.95)$$

$$y = Cx$$

where $B_1 \in \mathbb{R}^{n_{u_1}}$ and $B_2 \in \mathbb{R}^{n_{u_2}}$. It should be noted up front that the well-known rank condition must be satisfied in order to check for the existence of the observer [230]. For the observer to exist, $\text{rank}(CB_2) = \text{rank}(B_2)$, which implies that there must be at least as many independent outputs as there are unknown inputs.

The Hui and Zak UIO algorithm is based on the idea that we want to project the unknown component in \mathbb{R}^{n_s} onto the subspace of known state components. Then, an observer is constructed within this subspace to estimate the entire state. Let P be a projection matrix such that

$$P = MC \quad (.96)$$

where $P \in \mathbb{R}^{n_s}$ and $M \in \mathbb{R}^{n_y}$. The projection matrix has two important properties. First, P is symmetric ($P^T = P$). Second, the square of P is itself ($P^2 = P$). The second property also implies that

$$P^n = P \quad \forall n \geq 1$$

since any positive integer exponent n can either be divided by two with a remainder of 0 or 1. When expanding the exponents of P the result will always be a series of

multiplications of the projection matrix raised to the first or second power, which will always reduce to the second property of the projection matrix. Using the projection matrix, the state vector can be separated as

$$x = (I - P)x + Px \quad (.97)$$

Notice that the expression $(I - P)$ is a projection matrix itself because it is symmetric and

$$\begin{aligned} (I - P)^2 &= I^2 - 2P + P^2 \\ &= I - 2P + P \\ &= (I - P). \end{aligned}$$

We can also conclude that

$$P(I - P) = P - P^2 = 0.$$

Substituting the output equation (.94) and (.96) into equation (.97) we get

$$x = q + My \quad (.98)$$

where

$$q = (I - MC)x. \quad (.99)$$

The projection matrix $I - MC$ is constant so the derivative of (.99) is simply

$$\dot{q} = (I - MC)\dot{x} \quad (.100)$$

Notice that q can be viewed as the projection (not necessarily orthogonal) of x onto the subspace of known components in \mathbb{R}^{n_s} . If the subspace state q can be estimated, then an estimate of the entire state x can be determined by equation (.98) since the output measurement vector y is known. To determine M , the constraint

$$(I - MC)B_2 = 0 \quad (.101)$$

must be met, which essentially removes the influence of the unknown input in (.95). An observer is then designed within the subspace. Provided that the rank condition $\text{rank}(CB_2) = \text{rank}(B_2)$ is met (Kudva *et al* [230]), the known state subspace exists and the matrix M is determined to be

$$M = B_2 \left((CB_2)^\dagger + H_0 \left(I_r - (CB_2)(CB_2)^\dagger \right) \right) \quad (.102)$$

where the superscript \dagger denotes the Moore-Penrose pseudo-inverse operation and H_0 is $(n_{u_2} \times n_y)$ is a design parameter matrix introduced in [175] (default is zero). To determine the dynamic state space model for the subspace state q , we substitute equation (.95) into (.100) to get

$$\dot{q} = (I - MC)A(q + My) + (I - MC)B_1u_1 + (I - MC)B_2u_2 \quad (.103)$$

Recall that M is chosen such that the constraint (.101) is met and so the last term in equation – the term containing all unknown inputs – is zero. The resulting state space equation is of the form

$$\dot{q} = \tilde{A}q + \tilde{B}\tilde{u} \quad (.104)$$

$$\tilde{y} = Cq \quad (.105)$$

where

$$\begin{aligned} \tilde{A} &= (I - MC)A \\ \tilde{B} &= (I - MC)[AM \quad B_1] \\ \tilde{u} &= \begin{bmatrix} y \\ u_1 \end{bmatrix} \text{ and} \\ \tilde{y} &= y - CM y \end{aligned}$$

Notice the new input \tilde{u} is the vector function of output measurements and known inputs, which is fully known. From here, it can be shown that a standard proportional gain observer can be applied to equations (.104)-(.105) provided the pair (\tilde{A}, C) is fully observable. Note that it is possible that the original system might be fully observable while the pair (\tilde{A}, C) is not. Choosing the closed loop gain matrix \tilde{L} to be

$$\tilde{L} = (I - MC)L,$$

where L is the observer gain matrix chosen for the original system in (.93) and (.94). Finally, the estimate of the subspace state \hat{q} is determined to be

$$\dot{\hat{q}} = \tilde{A}\hat{q} + \tilde{B}\tilde{u} + \tilde{L}(\tilde{y} - C\hat{q}). \quad (.106)$$

Now to show convergence of the subspace method, choose the state error to be $e = q - \hat{q}$ so that the error dynamics are determined by the equation

$$\dot{e} = (\tilde{A} - \tilde{L}C)e.$$

Knowing that $\tilde{A} = (I - MC)A$ and $\tilde{L} = (I - MC)L$ defined in equations (.104) and (.105), the error dynamics can be expressed as the error of the original observer projected onto the known system subspace as

$$\dot{e} = (I - MC)(A - LC)e. \quad (.107)$$

Looking at equation (.107), it is not readily apparent that the error converges to zero. With a few observations, though, it can be shown that it does. First, pre-multiply equation (.107) by the projection matrix MC , which yields

$$MC\dot{e}(t) = 0 \quad \forall t \quad (.108)$$

since

$$MC(I - MC) = MC - (MC)^2 = MC - MC = 0,$$

which implies that

$$MCe(t) = \text{constant} \quad \forall t .$$

Next, pre-multiply the projection matrix MC on q in equation (.99) , yielding

$$MCq(t) = 0 \quad \forall t$$

for the same reason as in (.108). Choose the initial condition on the estimate \hat{q} in the expression as

$$MC\hat{q}(0) = 0 ,$$

then

$$MCe(t) = 0 \quad \forall t .$$

For simplicity, define a projection matrix P' and system matrix A' as

$$\begin{aligned} P' &= I - MC \quad \text{and} \\ A' &= A - LC \end{aligned}$$

then the expression for the error equation in (.107) can be expanded as

$$\begin{aligned}
P'e(t) &= P' \left(I + P'A't + \frac{P'^2 A'^2 t^2}{2!} + \dots \right) e(0) \\
&= P' \left(I + A't + \frac{A'^2 t^2}{2!} + \dots \right) e(0) \\
&= P'e^{A't} e(0)
\end{aligned}$$

Now choose L so that the desired plant characteristics $A' = (A - LC)$ converge to zero so that $(I - MC)e(t) \rightarrow 0$. Putting it all together, it can be seen that the error $e(t)$ approaches zero because

$$\begin{aligned}
(I - MC)e(t) &= e(t) - MCe(t) \rightarrow 0 \\
\Rightarrow e(t) &\rightarrow 0.
\end{aligned}$$

Finally, since it has been shown that the estimate \hat{q} of the known component subspace state converges to the actual state q , an estimate \hat{x} for the whole state can be determined based on the relationship between q and x in equation (.98) as

$$\hat{x} = \hat{q} + My.$$

APPENDIX D: POLYNOMIAL MATRIX DEFINITIONS AND THEOREMS

The purpose of Appendix D is to provide definitions to polynomial matrices for which the multivariable unknown input observer method is based. Most of the definitions herein are documented in [61],[200], and [229].

Definitions

Definition D.1 (field). *A field consists of a set, denoted by \mathcal{F} , of elements called scalars and two operations called addition "+" and multiplication "·"; the two operations are defined over \mathcal{F} such that they satisfy the following conditions:*

1. *To every pair of elements α and β in \mathcal{F} , there correspond an element $\alpha + \beta$ in \mathcal{F} called the sum of α and β , and an element $\alpha \cdot \beta$ or $\alpha\beta$ in \mathcal{F} , called the product of α and β .*

2. *Addition and multiplication are respectively commutative: For any α, β in \mathcal{F} ,*

$$\alpha + \beta = \beta + \alpha \quad \alpha \cdot \beta = \beta \cdot \alpha$$

3. *Addition and multiplication are respectively associative: For any α, β, γ in \mathcal{F} ,*

$$(\alpha + \beta) + \gamma = (\alpha \cdot \beta) \cdot \gamma \quad (\alpha \cdot \beta) \cdot \gamma = \alpha \cdot (\beta \cdot \gamma)$$

4. *Multiplication is distributive with respect to addition: For any α, β, γ in \mathcal{F} ,*

$$\alpha \cdot (\beta + \gamma) = (\alpha \cdot \beta) + (\alpha \cdot \gamma)$$

5. *\mathcal{F} contains an element, denoted by 0, and an element, denoted by 1, such that*

$$\alpha + 0 = \alpha, 1 \cdot \alpha = \alpha \text{ for every } \alpha \text{ in } \mathcal{F}.$$

6. *To every α in \mathcal{F} , there is an element β in \mathcal{F} such that $\alpha + \beta = 0$. The element β is called the additive inverse.*

7. To every α in \mathcal{F} which is not the element 0, there is an element γ in \mathcal{F} such that $\alpha \cdot \gamma = 1$. The element γ is called the multiplicative inverse.

Note 1: The symbol \mathbb{R} and \mathbb{C} is used to denote the field of real numbers and the field of complex numbers, respectively.

Note 2: The set of integers and the set of polynomials do not form a field because they have no multiplicative inverse defined within the field.

Definition D.2 (ring). *More precisely: a commutative ring with multiplicative identity. A set with all properties of a field except for property 7 in Definition D.1.*

Note: The set of integers and the set of polynomials with real coefficients form a ring.

Definition D.3 (linear space over a field). *A linear space over a field \mathcal{F} , denoted by $(\mathcal{H}, \mathcal{F})$, consists of a set, denoted by \mathcal{H} , of elements called vectors, a field \mathcal{F} , and two operations called vector addition and scalar multiplication. The two operations are defined over \mathcal{H} and \mathcal{F} such that they satisfy all the following conditions*

1. To every pair of vectors x_1 and x_2 in \mathcal{H} , there corresponds a vector $x_1 + x_2$ in \mathcal{H} , called the sum of x_1 and x_2 .

2. Addition is commutative: For any x_1, x_2 in \mathcal{H} , $x_1 + x_2 = x_2 + x_1$.

3. Addition is associative: For any x_1, x_2, x_3 in \mathcal{H} , $(x_1 + x_2) + x_3 = x_1 + (x_2 + x_3)$

4. \mathcal{H} contains a vector, denoted by 0, such that $0 + x = x$ for every x in \mathcal{H} .

The vector 0 is called the zero vector or the origin.

5. To every x in \mathcal{H} , there is a vector \bar{x} in \mathcal{H} , such that $x + \bar{x} = 0$.

6. To every α in \mathcal{F} , and every x in \mathcal{H} , there corresponds a vector αx in \mathcal{H} called the scalar product of α and x .

7. *Scalar multiplication is associative: For any α, β in \mathcal{F} and any x in \mathcal{H} , $\alpha(\beta x) = (\alpha\beta)x$.*
8. *Scalar multiplication is distributive with respect to vector addition: For any α in \mathcal{F} and any x_1, x_2 in \mathcal{H} , $\alpha(x_1 + x_2) = \alpha x_1 + \alpha x_2$.*
9. *Scalar multiplication is distributive with respect to scalar addition: For any α, β in \mathcal{F} and any x in \mathcal{H} , $(\alpha + \beta)x = \alpha x + \beta x$.*
10. *For any x in \mathcal{H} , $1x = x$, where 1 is the element 1 in \mathcal{F} .*

Note 1: If $\mathcal{F} = \mathbb{R}$, then $(\mathbb{R}^n, \mathbb{R})$ is called the n -dimensional *real vector space*. For brevity, the field of real numbers is implied and therefore is denoted as \mathbb{R}^n .

Note 2: $\mathbb{R}_n[p]$ is the set of all polynomials of degree less than n with real coefficients.

Note 3: If a field is replaced by a ring \mathbb{R}_i , then $(\mathcal{H}, \mathbb{R}_i)$ is called a *module* over the ring. A $n \times 1$ or $1 \times n$ polynomial vector can be considered as an element of the rational vector space $(\mathbb{R}^n(p), \mathbb{R}(p))$, or an element of the module $(\mathbb{R}^n[p], \mathbb{R}[p])$. A set of polynomial vectors is linearly independent over the field $\mathbb{R}(p)$ if and only if the set is linearly independent over the ring $\mathbb{R}[p]$.

Definition D.4 (normal rank). *The normal rank of a polynomial matrix*

$A(p) \in \mathbb{R}^{m \times n}[p]$ *is defines as e.g.*

1. *The number*

$$\text{rank } A(p) = \max_{s \in \mathbb{C}} \text{rank } A(s)$$

2. *The number of linearly independent columns (or rows) of $A(p)$*
3. *The number of invariant polynomials of the Smith form of $A(p)$*

4. *The dimension of the space spanned by the rows/columns*

Definition D.5 (rank of a rational matrix). *The rank of a matrix $M(p) \in \mathbb{R}^{m \times n}(p)$ is defined as e.g.*

1. *The number of linearly independent rows/columns with rational coefficients*
2. *The (normal) rank of $N(p)$ where $N(p)$ is the numerator in a left or right MFD of $M(p)$*
3. *The dimension of the space spanned by the rows/columns*

Definition D.6 (matrix pencil). *A matrix pencil is a polynomial matrix $M(p)$ of degree one. It is often written as*

$$M(p) = pE + F$$

where E and F are constant matrices and p is a differential/difference operator in the Laplace/Z domain in continuous/discrete time.

Definition D.7 (regular matrix pencil). *A matrix pencil $M(p)$ is said to be regular if $M(p)$ is square and full (normal) rank.*

Definition D.8 (controllability index). *The fact that the controllability matrix*

$$C = [B \ AB \ \cdots \ A^{n-1}B]$$

has rank n means that there are n linearly independent columns in C . It could be that n such columns in the partial controllability matrix

$$C_q = [B \ AB \ \cdots \ A^{q-1}B], \quad 1 \leq q \leq n$$

can be found and that the smallest q is denoted as μ . The controllability index μ of the pair (A, B) is said to be the smallest q such that C_q has rank n .

Definition D.9 (unimodular matrix). A square polynomial matrix $M(p)$ is called unimodular if its determinant is nonzero and independent of p .

Definition D.10 (right/left divisor, right/left multiple). Consider the polynomial matrix equation

$$A(p) = B(p)C(p)$$

where $A(p)$, $B(p)$, and $C(p)$ are polynomial matrices of appropriate orders.

1. $C(p)$ is a right divisor of $A(p)$
2. $B(p)$ is a left divisor of $A(p)$
3. $A(p)$ is a left multiple of $C(p)$
4. $A(p)$ is a right multiple of $B(p)$

Definition D.11 (greatest common right divisor (gcrd)). A square polynomial matrix $R(p)$ is a greatest common right divisor (gcrd) of $N(p)$ and $D(p)$ if $R(p)$ is a common right divisor of $N(p)$ and $D(p)$ and is a left multiple of every common right divisor of $N(p)$ and $D(p)$.

Definition D.12 (greatest common left divisor (gclid)). A square polynomial matrix $Q(p)$ is called a greatest common left divisor (gclid) of $A(p)$ and $B(p)$ if $Q(p)$ is a common left divisor of $A(p)$ and $B(p)$ and $Q(p)$ is a right multiple of every common left divisor $Q_1(p)$ of $A(p)$ and $B(p)$.

Definition D.13 (right coprime). *If a square polynomial matrix $R(p)$ is a gcd of $N(p)$ and $D(p)$ and $R(p)$ is a unimodular matrix, then $N(p)$ and $D(p)$ are said to be right coprime.*

Definition D.14 (left coprime). *If a square polynomial matrix $Q(p)$ is a gcd of $A(p)$ and $B(p)$ and $Q(p)$ is a unimodular matrix, then $A(p)$ and $B(p)$ are said to be left coprime.*

Definition D.15 (Sylvester matrix). *Let $W(p)$ be a polynomial matrix of degree d such that*

$$W(p) = \sum_{i=0}^d W_i p^i$$

with $W_d \neq 0$. Then the q^{th} order Sylvester matrix for $W(p)$ is defined as

$$S(W(p), q) \triangleq \begin{bmatrix} W_0 & W_1 & \dots & W_d & 0 & 0 & 0 \\ 0 & W_0 & W_1 & \dots & W_d & 0 & 0 \\ 0 & 0 & \ddots & \ddots & & \ddots & 0 \\ 0 & 0 & 0 & W_0 & W_1 & \dots & W_d \end{bmatrix}$$

Definition D.16 (characteristic polynomial). *The characteristic polynomial of a proper rational matrix $\hat{G}(p)$ is defined as*

1. *The least common denominator of all minors of $\hat{G}(p)$. The degree of the characteristic polynomial is defined as the McMillan or, simply, the degree of $\hat{G}(p)$ and is denoted by $\delta\hat{G}(p)$.*
2. *Consider the proper rational matrix $\hat{G}(p)$ factored as*

$$\hat{G}(p) = N(p)D^{-1}(p) = \bar{D}^{-1}(p)\bar{N}(p)$$

where $N(p)$ and $D(p)$ are right coprime, and $\bar{N}(p)$ and $\bar{D}(p)$ are left coprime. Then the characteristic polynomial of $\hat{G}(p)$ is defined as

$$\det D(p) \text{ or } \det \bar{D}(p)$$

and the degree of $\hat{G}(p)$ is defined as

$$\delta \hat{G}(p) = \delta(\det D(p)) = \delta(\det \bar{D}(p))$$

Definition D.17 (Right polynomial fraction). Every $q \times p$ proper rational matrix $\hat{G}(p)$ can be expressed as

$$\hat{G}(p) = N(p)D^{-1}(p)$$

where $N(p)$ and $D(p)$ are $q \times p$ and $p \times p$ polynomial matrices, respectively. $\hat{G}(p)$ in this form is called a right polynomial fraction or, simply, right fraction.

Definition D.18 (Left polynomial fraction). The dual expression of $\hat{G}(p)$ in Definition D.16 where the same proper rational matrix can be equally expressed as

$$\hat{G}(p) = \bar{D}^{-1}(p)\bar{N}(p)$$

where $\bar{D}(p)$ and $\bar{N}(p)$ are $q \times q$ and $q \times p$ polynomial matrices, respectively. $\hat{G}(p)$ in this form is called a left polynomial fraction or, simply, left fraction.

Definition D.19 (column/row reduced). A nonsingular polynomial matrix $M(p)$ is column reduced if

$$\delta(\det M(p)) = \text{sum of all column degrees}$$

It is row reduced if

$$\delta(\det M(p)) = \text{sum of all row degrees}$$

Definition D.20 (**Bezout Equation**). Consider two polynomial matrices $A(p), B(p)$ and four polynomial matrices $P(p), Q(p), R(p), S(p)$ such that

$$\begin{bmatrix} P(p) & Q(p) \\ R(p) & S(p) \end{bmatrix} \begin{bmatrix} A(p) \\ B(p) \end{bmatrix} = \begin{bmatrix} G(p) \\ 0 \end{bmatrix}$$

then the following can be said:

1. $A(p), B(p)$ are left coprime if and only if $G(p)$ is unimodular
2. $R(p)$ and $S(p)$ are right coprime
3. $B(p)A^{-1}(p) = -S^{-1}(p)R(p)$

This implies that if $G(p)$ is unimodular, then right and left polynomial fractions of the same proper rational matrix are equivalent as

$$H(p) = B(p)A^{-1}(p) = \bar{A}^{-1}(p)\bar{B}(p)$$

where

$$\begin{aligned} \bar{A}(p) &= -S(p) \\ \bar{B}(p) &= R(p). \end{aligned}$$

Definition D.21 (**Diophantine Equation**). Given three polynomial matrices $A(p), B(p), C(p)$ that are mutually right coprime and deriving equations in a Bezout Equation form, define the Diophantine Equation as

$$C(p) = E(p)A(p) + F(p)B(p)$$

from the top row of the Bezout equation and a left coprime representation such that

$$R(p)A(p) + S(p)B(p) = 0$$

from the bottom row of the Bezout equation. A solution $E_0(p), F_0(p)$ exists such that all solutions (nonunique) can be expressed as

$$\begin{aligned} E(p) &= E_0(p) + W(p)R(p) \\ F(p) &= F_0(p) + W(p)S(p) \end{aligned}$$

with $W(p)$ an arbitrary matrix of appropriate dimensions.

Definition D.22 (polynomial degree operator). *Given a polynomial matrix $M(p)$, define*

$$\begin{aligned}\delta_{ci}M(p) &= \text{degree of } i^{\text{th}} \text{ column of } M(p) \\ \delta_{ri}M(p) &= \text{degree of } i^{\text{th}} \text{ row of } M(p).\end{aligned}$$

Denote δ_{ci} the column degree and δ_{ri} the row degree.

Definition D.23 (right polynomial transfer matrix and control canonical form)

Let a minimal realization of the system

$$px(t) = \Phi x(t) + \Gamma u(t) \quad (.109)$$

$$y(t) = Cx(t) + Du(t) \quad (.110)$$

where $x(t) \in \mathbb{R}^{n_x}$, $u(t) \in \mathbb{R}^{n_u}$, $y(t) \in \mathbb{R}^{n_y}$ and (Φ, Γ, C, D) are of appropriate dimensions. Because the system is a minimal realization, an equivalent representation of (.109)-(.110) is the right polynomial transfer matrix form as $\hat{G}(p) = B(p)A^{-1}(p)$. Let $\mu_1, \mu_2, \dots, \mu_{n_u}$ be the *column degrees* (i.e. the maximum degree of the polynomials in each column) of the matrix $A(p)$ and p is the differential operator in continuous time or the time shift operator in discrete time. If $z(t)$ is defined as the *partial state* [200] (or sometimes called the *pseudo state* [61]), then it is easy to see that it can be related to the input $u(t)$ and output $y(t)$ as

$$u(t) = A(p)z(t) \quad (.111)$$

$$y(t) = B(p)z(t). \quad (.112)$$

The partial-state equations in (.111)-(.112) can be expressed in state space form by first defining the matrices

$$\Sigma_{\mu}(p) = \text{diag} \left\{ p^{\mu_1}, p^{\mu_2}, \dots, p^{\mu_{n_u}} \right\} \in R^{n_u \times n_u} \quad (.113)$$

$$L_{\mu}(p) = \text{diag} \left\{ \begin{bmatrix} 1 \\ p \\ \vdots \\ p^{\mu_1-1} \end{bmatrix}, \begin{bmatrix} 1 \\ p \\ \vdots \\ p^{\mu_2-1} \end{bmatrix}, \dots, \begin{bmatrix} 1 \\ p \\ \vdots \\ p^{\mu_{n_u}-1} \end{bmatrix} \right\} \in R^{(\mu_1+\mu_2+\dots+\mu_{n_u}) \times n_u} \quad (.114)$$

and expressing the polynomial matrices of (.111)-(.112) as

$$A(p) = A_h \Sigma_{\mu}(p) + A_l L_{\mu}(p) \quad (.115)$$

$$B(p) = B_h \Sigma_{\mu}(p) + B_l L_{\mu}(p) \quad (.116)$$

where (A_h, B_h) are matrices of high degree coefficients whose dimensions are $n_u \times n_u$ and $n_y \times n_u$, respectively, and (A_l, B_l) are the matrices of all lower order coefficients with dimension $n_u \times n_s$ and $n_y \times n_s$, respectively. The partial-state vector with dimension $n_s = \mu_1 + \dots + \mu_{n_u}$, can now be expressed as

$$\underline{z}(t) = \left[z_1(t), \dots, p^{\mu_1-1} z_1(t) \dot{z}_2(t), \dots, p^{\mu_2-1} z_1(t) \dot{z}_2(t) \dots \dot{z}_{n_u}(t), \dots, p^{\mu_{n_u}-1} z_{n_u}(t) \right]^T \quad (.117)$$

can now be expressed as

$$\underline{z}(t) = L_{\mu}(p) z(t) . \quad (.118)$$

Substitute (.115)-(.116) into (.111)-(.112) and assume A_h is nonsingular to obtain the state space realization of the original system in (0.32) and (0.33) as

$$\begin{bmatrix} p^{\mu_1} z_1(t) \\ \vdots \\ p^{\mu_{n_u}} z_{n_u}(t) \end{bmatrix} = -A_h^{-1} A_l \underline{z}(t) + A_h^{-1} u(t) \quad (.119)$$

$$y(t) = (B_l - B_h A_h^{-1} A_l) \underline{z}(t) + B_h A_h^{-1} u(t) \quad (.120)$$

It can be shown [61] that the ensuing state space structure of (.119)-(.120) is in controllable canonical form for which the nonsingular matrix T can be found for MIMO systems using a method such as the one published in (Zak, 2003; [386]).

Theorems

Note: Theorems herein are stated without proof. Source information is provided.

Theorem D.1 ([61];Theorem G-6). *A square polynomial matrix is unimodular if and only if its inverse is a polynomial matrix*

Theorem D.2 ([61]; Theorem 7.1). *The controllable canonical form is observable if and only if $D(p)$ and $N(p)$ are coprime.*

Theorem D.3 ([61]; Theorem 7.M2). *A state equation (A, B, C, D) is a minimal realization of a proper rational matrix $\hat{G}(p)$ if and only if the (A, B) is controllable and the (A, C) is observable or if and only if*

$$\dim(A) = \delta \hat{G}(p).$$

Theorem D.4 ([61]; Theorem 7.8). *Let $N(p)$ and $D(p)$ be $q \times p$ and $p \times p$ polynomial matrices, and let $D(p)$ be column reduced. Then the rational matrix $N(p)D^{-1}(p)$ is proper (strictly proper) if and only if*

$$\delta_{ci} N(p) \leq \delta_{ci} D(p) \quad (\delta_{ci} N(p) < \delta_{ci} D(p))$$

for $i = 1, 2, \dots, p$.

Theorem D.5 ([61]; Theorem 7.M3). *All minimum realizations of $\hat{G}(p)$ are equivalent.*

LIST OF REFERENCES

- [1] K. Abed-Meraim, J. -. Cardoso, A. Y. Gorokhov, P. Loubaton and E. Moulines, "On subspace methods for blind identification of single-input multiple-output FIR systems," *Signal Processing, IEEE Transactions on [See also Acoustics, Speech, and Signal Processing, IEEE Transactions on]*, vol. 45, pp. 42-55, 1997.
- [2] K. Abed-Meraim, Y. Hua, P. Loubaton and E. Moulines, "Subspace method for blind identification of multichannel FIR systems in noise field with unknown spatial covariance," *Signal Processing Letters, IEEE*, vol. 4, pp. 135-137, 1997.
- [3] K. Abed-Meraim, P. Loubaton and E. Moulines, "A subspace algorithm for certain blind identification problems," *Information Theory, IEEE Transactions on*, vol. 43, pp. 499-511, 1997.
- [4] K. Abed-Meraim, Wanzhi Qiu and Yingbo Hua, "Blind system identification," *Proceedings of the IEEE*, vol. 85, pp. 1310-1322, 1997.
- [5] K. Abed-Meraim and Yingbo Hua, "Blind identification of multi-input multi-output system using minimum noise subspace," *Signal Processing, IEEE Transactions on [See also Acoustics, Speech, and Signal Processing, IEEE Transactions on]*, vol. 45, pp. 254-258, 1997.
- [6] E. Alcorta Garcia and P. M. Frank, "A novel design of structured observer-based residuals for FDI," in 1999, pp. 1341-1345 vol.2.
- [7] C. Alexander and M. N. O. Sadiku, *Fundamentals of Electric Circuits*. ,1st ed. Boston: McGraw Hill, 2000, pp. 940.
- [8] J. T. Alt, S. D. Sudhoff and B. E. Ladd, "Analysis and average-value modeling of an inductorless synchronous machine load commutated converter system," *Energy Conversion, IEEE Transactions on*, vol. 14, pp. 37-43, 1999.
- [9] A. M. R. Amaral and A. J. M. Cardoso, "Fault diagnosis on switch-mode power supplies operating in discontinuous mode," in 2004, pp. 197-202 Vol.1.
- [10] F. Amoozegar and S. H. Sadati, "Target tracking by neural network maneuver detection and input estimation," in 1995, pp. 143-148.
- [11] J. V. Amy Jr, "Considerations in the design of naval electric power systems," in 2002, pp. 331-335 vol.1.
- [12] P. Anselone and J. Lee, *Multivariable Calculus with Engineering and Science Applications*. ,1st ed. Upper Saddle River, N.J.: Prentice Hall, 1996, pp. 577.

- [13] M. S. Arulampalam, S. Maskell, N. Gordon and T. Clapp, "A tutorial on particle filters for online nonlinear/non-Gaussian Bayesian tracking," *Signal Processing, IEEE Transactions on [See also Acoustics, Speech, and Signal Processing, IEEE Transactions on]*, vol. 50, pp. 174-188, 2002.
- [14] R. W. Ashton and J. G. Ciezki, "The analysis of tradeoffs between power section hardware and feedback gains for a dc distribution system dc-to-dc converter [on ships]," *IEEE 0-7803-4455-3*, 1998, pp. 387-390 vol.3.
- [15] R. W. Ashton and J. G. Ciezki, "The design and fabrication of a reconfigurable hardware testbed for the interaction analysis of power converters in a reduced-scale navy dc distribution system," *IEEE 0-7803-4455-3*, 1998, pp. 379-382 vol.3.
- [16] R. W. Ashton, J. G. Ciezki and M. G. Badorf, "The synthesis and hardware validation of DC-to-DC converter feedback controls," *IEEE 0-7803-4489-8*, 1998, pp. 65-71 vol.1.
- [17] R. W. Ashton, J. G. Ciezki and C. Mak, "The formulation and implementation of an analog/digital control system for a 100-kW dc-to-dc buck chopper," *Circuits and Systems II: Analog and Digital Signal Processing, IEEE Transactions on [See also Circuits and Systems II: Express Briefs, IEEE Transactions on]*, vol. 46, pp. 971-974, 1999.
- [18] K. Astrom and B. Wittenmark, *Computer-Controlled Systems*. ,3rd Edition ed. Upper Saddle River, New Jersey: Prentice Hall, 1997, pp. 557.
- [19] E. Athanasopoulou and C. N. Hadjicostis, "Probabilistic approaches to fault detection in networked discrete event systems," *Neural Networks, IEEE Transactions on*, vol. 16, pp. 1042-1052, 2005.
- [20] E. Athanasopoulou and C. N. Hadjicostis, "Maximum likelihood diagnosis in partially observable finite state machines," *Proceedings of the 13th Mediterranean Conference on Control and Automatin*, 2005, pp. 896-901.
- [21] E. Athanasopoulou and C. N. Hadjicostis, "Synchronization-based fault detection in discrete event systems," *43rd IEEE Conference on Decision and Control*, 2004, pp. 57-62 Vol.1.
- [22] M. Babaali, "Switched Linear Systems: Observability and Observers," *Georgia Institute of Technology*, pp. 1-93, 2004.
- [23] C. Bakiotis, J. Raymond and A. Rault, "Parameter and discriminant analysis for jet engine mechanical state diagnosis," in *Proc. of the 1979 IEEE Conf. on Decision and Control*, 1979,

- [24] P. Balle, D. Juricic, A. Rakar and S. Ernst, "Identification of nonlinear processes and model based fault isolation using local linear models," *Proceedings of the American Control Conference*, 1997, pp. 47-51 vol.1.
- [25] M. E. Baran and N. Mahajan, "System reconfiguration on shipboard DC zonal electrical system," 2005 *IEEE Electric Ship Technologies Symposium*, pp. 86-92.
- [26] Y. Bar-Shalom, K. C. Chang and H. A. P. Blom, "Tracking a maneuvering target using input estimation versus the interacting multiple model algorithm," *Aerospace and Electronic Systems, IEEE Transactions on*, vol. 25, pp. 296-300, 1989.
- [27] Y. Bar-Shalom, X. Li and T. Kirubarajan, *Estimation with Applications to Tracking and Navigation*. New York: Wiley, 2001, pp. 558.
- [28] J. C. Babilio and M. V. Moreira, "A Robust Solution of the Generalized Polynomial Bezout Identity," *Linear Algebra and its Applications*, vol. 385, pp. 287-303, 2004.
- [29] M. Basseville, "Detecting Changes in Signals and Systems - A Survey," *Automatica*, vol. 24, pp. 309-326, 1988.
- [30] R. V. Beard, "Failure Accommodation in Linear System Through Self Reorganization," *Massachusetts Institute of Technology, Cambridge, MA*, 1971.
- [31] S. B. Bekiarov and A. Emadi, "Uninterruptible power supplies: Classification, operation, dynamics, and control," *IEEE-7803-7404-5/02*, in 2002, pp. 597-604 vol.1.
- [32] P. Balle, D. Fussel and O. Hecker, "Detection and isolation of sensor faults on nonlinear processes based on local linear models," *Proceedings of the American Control Conference*, 1997, pp. 468-472 vol.1.
- [33] C. L. Benner and B. D. Russell, "Automated shipboard diagnostics and health evaluation for power equipment and systems: Advanced techniques developed for terrestrial power systems," *IEEE Electric Ship Technologies Symposium* 2005, pp. 407-412.
- [34] B. S. Bhangu, P. Snary, C. M. Bingham and D. A. Stone, "Sensorless control of deep-sea ROVs PMSMs excited by matrix converters," *EPE* 2005, ISBN: 90-75815-08-5, pp. 8.
- [35] S. Bhattacharyya, "Observer design for linear systems with unknown inputs," *Automatic Control, IEEE Transactions on*, vol. 23, pp. 483-484, 1978.

- [36] Bing Liang and Guangren Duan, "Observer-based H_{∞} fault-tolerant control against actuator failures for descriptor systems," *Proceedings of the 5th World Congress on Intelligent Control and Automation*, 2004, pp. 1007-1011 Vol.2.
- [37] Bing Liang and Guangren Duan, "Observer-based H_{∞} fault-tolerant control for descriptor linear systems with sensor failures," *Proceedings of the 5th World Congress on Intelligent Control and Automation*, 2004, pp. 1012-1016 Vol.2.
- [38] Bing Liang and Guang-Ren Duan, "Observer-based fault-tolerant control for descriptor systems," *8th International Conference on Control, Automation, Robotics and Vision*, 2004, pp. 2233-2237 Vol. 3.
- [39] M. Bisiacco and M. E. Valcher, "Observer-based fault detection and isolation for 2D state-space models," *Multidimensional Systems and Signal Processing*, vol. 17, pp. 219-242, 2006.
- [40] M. Bisiacco and M. E. Valcher, "A behavioral approach to the estimation problem and its applications to state-space models," *44th IEEE Conference on Decision and Control, and the European Control Conference*, 2005, pp. 167-172.
- [41] M. Bisiacco, M. E. Valcher and J. C. Willems, "A Behavioral Approach to Estimation and Dead-Beat Observer Design With Applications to State-Space Models," *Automatic Control, IEEE Transactions on*, vol. 51, pp. 1787-1797, 2006.
- [42] M. Blanke, R. Izadi-Zamanabadi, S. Bogh and C. Lunau, "Fault-Tolerant Control Systems: A Holistic View," *Control Engineering Practice*, vol. 5, pp. 693-702, 1997.
- [43] M. Blanke, M. Staroswiecki and N. E. Wu, "Concepts and methods in fault-tolerant control," *Proceedings of the American Control Conference*, 2001, pp. 2606-2620 vol.4.
- [44] M. Blanke, *Diagnosis and Fault-Tolerant Control*. Berlin ; New York: Springer, 2003, pp. 571.
- [45] P. L. Bogler, "Tracking a Maneuvering Target Using Input Estimation," *Aerospace and Electronic Systems, IEEE Transactions on*, vol. AES-23, pp. 298-310, 1987.
- [46] S. Bousghiri-Kratz, O. Malasse and W. Nuninger, "Fault detection using state estimation. application to an electromechanical process," *Proceedings of the 34th Conference on Decision and Control*, 1995, pp. 2397-2402 vol.3.

- [47] R. G. Brown and P. Y. C. Hwang, *Introduction to Random Signals and Applied Kalman Filtering : With MATLAB Exercises and Solutions*. ,3rd ed. New York: Wiley, 1997, pp. 484.
- [48] J. B. Burl, *Linear Optimal Control*. Menlo Park, CA: Addison Wesley Longman, Inc., 1999,
- [49] Z. C., M. Fan and V. Chellaboina, "Adaptive Input Estimation Methods for Improving the Bandwidth of Microgyroscopes," *Sensors Journal, IEEE*, vol. 7, pp. 562-567, 2007.
- [50] F. Caccavale and L. Villani, *Fault Diagnosis and Fault Tolerance for Mechatronic Systems : Recent Advances*. , vol. 1, Berlin ; New York: Springer, 2003, pp. 191.
- [51] J. Calado and Sa Da Costa, Jose, "An Expert System Coupled with a Hierarchical structure of Fuzzy Neural Networks for Fault Diagnosis," *Int. J. Appl. Math. and Comp. Sci.*, vol. 9, pp. 667-687, 1999.
- [52] M. Capelli-Schellpfeffer and A. Golding, "People working on or near marine electrical systems," *IEEE Electric Ship Technologies Symposium*, 2005, pp. 421-424.
- [53] D. Capriglione, C. Liguori, C. Pianese and A. Pietrosanto, "On-line sensor fault detection, isolation, and accommodation in automotive engines," *Instrumentation and Measurement, IEEE Transactions on*, vol. 52, pp. 1182-1189, 2003.
- [54] J. Carroll, K. C. Nagaraj, A. Arapostathis, W. M. Grady and E. J. Powers, "Dynamic reconfiguration preserving stability," *IEEE Electric Ship Technologies Symposium*, 2005, pp. 105-107.
- [55] B. Cassimere, S. Sudhoff, D. Aliprantis and M. D. Swinney, "IGBT and PN junction diode loss modeling for system simulations," *IEEE 0-7803-8987-5/05*, 2005, pp. 941-949.
- [56] B. Cassimere, C. R. Valdez, S. Sudhoff, S. Pekarek, B. Kuhn, D. Delisle and E. Zivi, "System impact of pulsed power loads on a laboratory scale integrated flight through power (IFTP) system," *IEEE Electric Ship Technologies Symposium*, 2005, pp. 176-183.
- [57] Y. T. Chan, A. G. C. Hu and J. B. Plant, "A Kalman Filter Based Tracking Scheme with Input Estimation," *Aerospace and Electronic Systems, IEEE Transactions on*, vol. AES-15, pp. 237-244, 1979.
- [58] D. -. Chang, W. Kang and A. J. Krener, "Normal forms and bifurcations of control systems," *Proceedings of the 39th IEEE Conference on Decision and Control*, 2000, pp. 1602-1607 vol.2.

- [59] J. Chen, R. Patton and G. Liu, "Optimal Residual Design for Fault Diagnosis using Multi-Objective Optimization and Genetic Algorithms," *Int. J. of Sys. Sci.*, vol. 27, pp. 567-576, 1996. 1996.
- [60] J. Chen and R. J. Patton, *Robust Model-Based Fault Diagnosis for Dynamic Systems*. Boston, MA: Kluwer Academic Publishers, 1999.
- [61] C. Chen, *Linear System Theory and Design*. ,3rd ed. New York: Oxford University Press, 1999, pp. 334.
- [62] E. Chow and A. Willsky, "Analytical redundancy and the design of robust failure detection systems," *Automatic Control, IEEE Transactions on*, vol. 29, pp. 603-614, 1984.
- [63] J. G. Ciezki and R. W. Ashton, "Selection and stability issues associated with a navy shipboard DC zonal electric distribution system," *Power Delivery, IEEE Transactions on*, vol. 15, pp. 665-669, 2000.
- [64] J. G. Ciezki and R. W. Ashton, "The design of stabilizing controls for shipboard DC-to-DC buck choppers using feedback linearization techniques," *IEEE 0-7803-4489-8*, 1998, pp. 335-341 vol.1.
- [65] J. G. Ciezki and R. W. Ashton, "The application of a customized DSP board for the control of power electronic converters in a DC zonal electric distribution system," *0-7803-5148-7*, 1998, pp. 1017-1021 vol.2.
- [66] J. G. Ciezki and R. W. Ashton, "The resolution of algebraic loops in the simulation of finite-inertia power systems," *IEEE 0-7803-4455-3*, 1998, pp. 342-345 vol.3.
- [67] J. G. Ciezki and R. W. Ashton, "The application of feedback linearization techniques to the stabilization of DC-to-DC converters with constant power loads," in 1998, pp. 526-529 vol.3.
- [68] R. N. Clark, "The dedicated observer approach to instrument failure detection," in *Proc. of the 18th IEEE Conf. on Decision and Control*, 1979, pp. 237-241.
- [69] R. N. Clark, "Instrument Fault Detection," *IEEE Trans. Aero. & Elctron. Syst.*, vol. AES-14, pp. 456-465, 1978.
- [70] R. N. Clark, "A Simplified Instrument Failure Detection Scheme," *IEEE Trans. Aero. & Electron. Syst.*, vol. AES-14, pp. 558-563, 1978.
- [71] R. N. Clark, D. C. Fosth and V. M. Walton, "Detecting Instrument Malfunctions in Control Systems," *IEEE Trans. Aero. & Electron. Syst.*, vol. AES-11, pp. 465-473, 1975.

- [72] D. H. Clayton, S. D. Sudhoff and G. F. Grater, "Electric ship drive and power system," *IEEE*. 0-7803-5827-9 pp. 85-88, 2000.
- [73] M. Corless and J. Tu, "State and Input Estimation for a Class of Uncertain Systems," *Automatica*, vol. 34, pp. 757-764, 1998.
- [74] R. Cristi, *Modern Digital Signal Processing*. Pacific Grove, CA: Thomson/Brooks/Cole, 2004, pp. 380.
- [75] R. E. Crosbie, "Low-cost, high-speed, real-time simulation for electric ship power systems," *IEEE Electric Ship Technologies Symposium*, 2005, pp. 46-47.
- [76] T. Dade, "Advanced Electric Propulsion, Power Generation, and Power Distribution," *Naval Engineers Journal*, vol. 106, pp. 83-92, March 1994. 1994.
- [77] C. J. Dafis and C. O. Nwankpa, "Investigating singularities of the observability Jacobian for nonlinear power systems," *IEEE Electric Ship Technologies Symposium*, 2005, pp. 75-80.
- [78] M. Dahlez. (2006, 6.241 dynamic systems and control, fall 2003. *MIT OpenCourseWare* [online]. 2007(January), Available: <http://ocw.mit.edu/OcwWeb/Electrical-Engineering-and-Computer-Science/6-241Fall2003/CourseHome/index.htm>
- [79] T. Dalton, P. Klotzek and P. Frank, "Application of Sensitivity Theory to Fuzzy Logic Based FDI," *Int. J. Appl. Math. and Comp. Sci.*, vol. 9, pp. 619-636, 1999.
- [80] M. Darouach, M. Zasadzinski and S. J. Xu, "Full-order observers for linear systems with unknown inputs," *Automatic Control, IEEE Transactions on*, vol. 39, pp. 606-609, 1994.
- [81] A. Davoudi, J. Jatskevich and T. De Rybel, "Numerical state-space average-value modeling of PWM DC-DC converters operating in DCM and CCM," *Power Electronics, IEEE Transactions on*, vol. 21, pp. 1003-1012, 2006.
- [82] R. DeCarlo and P. Lin, *Linear Circuit Analysis*. ,Second ed. New York, NY: Oxford University Press, 2001,
- [83] R. DeCarlo, S. H. Zak and G. P. Matthews, "Variable Structure Control of Nonlinear Multivariable Systems: A Tutorial," *Proceedings of the IEEE*, vol. 76, pp. 212-232, 1988.
- [84] J. C. Deckert, M. N. Desai, J. J. Deyst and A. S. Willsky, "F-8 DFBW Sensor Failure Identification Using Analytic Redundancy," *IEEE Trans. Automat. Contr.*, vol. AC-22, pp. 795-803, 1977.

- [85] T. DeNucci, R. Cox, S. B. Leeb, J. Paris, T. J. McCoy, C. Laughman and W. C. Greene, "Diagnostic indicators for shipboard systems using non-intrusive load monitoring," *IEEE Electric Syip Technologies Symposium*, 2005, pp. 413-420.
- [86] Y. Diao and K. M. Passino, "Intelligent fault tolerant control using adaptive schemes and multiple models," *Proceedings of the American Control Conference*, 2001, pp. 2854-2859 vol.4.
- [87] X. Ding and P. M. Frank, "Frequency domain approach and threshold selector for robust model-based fault detection and isolation," in *IFAC/IMACS Symp. SAFEPROCESS '91*, 1991, pp. 307-312.
- [88] S. X. Ding, P. Zhang, P. M. Frank and E. L. Ding, "Application of probabilistic robustness technique to the fault detection system design," *Proceedings of the 42nd IEEE Conference on Decision and Control*, 2003, pp. 972-977 Vol.1.
- [89] P. M. Djuric, J. H. Kotecha, Jianqui Zhang, Yufei Huang, T. Ghirmai, M. F. Bugallo and J. Miguez, "Particle filtering," *Signal Processing Magazine, IEEE*, vol. 20, pp. 19-38, 2003.
- [90] N. Doerry and J. Davis, "Integrated Power System for Marine Applications," *Naval Engineers Journal*, vol. 106, pp. 77-90, May 1994. 1994.
- [91] N. H. Doerry and D. H. Clayton, "Shipboard electrical power quality of service," *IEEE Electric Syip Technologies Symposium*, 2005, pp. 274-279.
- [92] N. H. Doerry, "Advanced numerical methods for simulating nonlinear multirate lumped parameter models," Ph.D. Dissertation, Massachusetts Institute of Technology, May 1991.
- [93] N. H. Doerry, "Computer simulation of shipboard electrical distribution systems," Master's Thesis, Massachusetts Institute of Technology, May 1989.
- [94] R. A. Dougal, "Design tools for electric ship systems," *IEEE Electric Ship Technologies Symposium*, 2005, pp. 8-9,10,11.
- [95] R. A. Dougal, "Design tools for electric ship systems," *IEEE Electric Syip Technologies Symposium*, 2005, pp. 8-11.
- [96] C. Edwards, "A comparison of sliding mode and unknown input observers for fault reconstruction," *43rd IEEE Conference on Decision and Control*, 2004, pp. 5279-5284 Vol.5.
- [97] C. Edwards and Chee Pin Tan, "Fault tolerant control using sliding mode observers," *43rd IEEE Conference on Decision and Control*, 2004, pp. 5254-5259 Vol.5.

- [98] C. Edwards, S. Spurgeon and R. Patton, "Sliding Mode Observers for Fault Detection and Isolation," *Automatica*, vol. 36, pp. 541-553, 2000.
- [99] P. Eide and P. Maybeck, "An MMAE failure detection system for the F-16," *Aerospace and Electronic Systems, IEEE Transactions on*, vol. 32, pp. 1125-1136, 1996.
- [100] P. Eide and P. Maybeck, "Evaluation of a multiple-model failure detection system for the F-16 in a full-scale nonlinear simulation," 1995, pp. 531-536 vol.1.
- [101] P. Eide and P. Maybeck, "Implementation and demonstration of a multiple model adaptive estimation failure detection system for the F-16," *Proceedings of the 34th Conference on Decision & Control*, 1995, pp. 1873-1878 vol.2.
- [102] G. Einicke, "Robust noncausal filtering," *42nd IEEE Conference on Decision and Control*, 2003, pp. 386-390 Vol.1.
- [103] G. Ellis, *Observers in Control Systems; A Practical Guide*. San Diego, CA: Academic Press, 2002,
- [104] A. Emadi, "Modeling of power electronic loads in AC distribution systems using the generalized State-space averaging method," *Industrial Electronics, IEEE Transactions on*, vol. 51, pp. 992-1000, 2004.
- [105] A. Emadi and M. Ehsani, "Negative impedance stabilizing controls for PWM DC-DC converters using feedback linearization techniques," in 2000, pp. 613-620 vol.1.
- [106] A. Emadi, J. P. Johnson and M. Ehsani, "Stability analysis of large DC solid-state power systems for space," *Aerospace and Electronic Systems Magazine, IEEE*, vol. 15, pp. 25-30, 2000.
- [107] A. Emadi, A. Khaligh, C. H. Rivetta and G. A. Williamson, "Constant power loads and negative impedance instability in automotive systems: definition, modeling, stability, and control of power electronic converters and motor drives," *Vehicular Technology, IEEE Transactions on*, vol. 55, pp. 1112-1125, 2006.
- [108] A. Emami-Naeini, M. M. Akhter and S. M. Rock, "Robust detection, isolation and accommodation for sensor failures," NASA, Tech. Rep. Technical Report NASA CR-174825, 1986.
- [109] A. Emami-Naeini, S. M. Rock and M. M. Akhter, "Robust failure detection with varying reference and failure times," *Proceedings of the 27th Conference on Decision and Control*, 1988, pp. 1055-1057 vol.2.

- [110] H. Emara-Shabaik, "Filtering of Linear Systems With Unknown Inputs," *ASME Journal of Dynamic Systems, Measurement, and Control*, vol. 125, pp. 482-485, 2003.
- [111] G. R. England, V. Clark and J. L. Jones, *Naval Power 21 [Electronic Resource] : A Naval Vision*. Washington, D.C.? : Dept. of the Navy: /, 2002, pp. 6.
- [112] E. Eryurek and B. R. Upadhyaya, "Fault-tolerant control and diagnostics for large-scale systems," *Control Systems Magazine, IEEE*, vol. 15, pp. 34-42, 1995.
- [113] M. S. Fadali and H. E. Emara-Shabaik, "Robust fault detection for a class of multirate linear systems," *Proceedings of the American Control Conference*, 2000, pp. 1210-1214 vol.2.
- [114] M. S. Fadali and W. Liu, "Fault detection for systems with multirate sampling," *Proceedings of the American Control Conference*, 1998, pp. 3302-3306 vol.6.
- [115] M. Farooq and S. Bruder, "Comments on 'Tracking a maneuvering target using input estimation'," *Aerospace and Electronic Systems, IEEE Transactions on*, vol. 25, pp. 300-302, 1989.
- [116] K. A. Fisher and P. S. Maybeck, "Multiple model adaptive estimation with filter spawning," *Aerospace and Electronic Systems, IEEE Transactions on*, vol. 38, pp. 755-768, 2002.
- [117] A. J. Forsyth and S. V. Molloy, "Modelling and control of DC-DC converters," *Power Engineering Journal [See also Power Engineer]*, vol. 12, pp. 229-236, 1998.
- [118] P. M. Frank, "Fault diagnosis in dynamic system via state estimation - A survey," in *System Fault Diagnostics, Reliability & Related Knowledge-Based Approaches* , vol. 1, Tzafestas, Singh and Schmidt, Eds. Dordrecht: D. Reidel Press, 1987, pp. 35-98.
- [119] P. M. Frank and L. Keller, "Sensitivity Discriminating Observer Design for Instrument Failure Detection," *IEEE Trans. Aero & Electron. Syst.*, vol. AES-16, pp. 460-467, 1981.
- [120] P. M. Frank and J. Wunnenberg, "Robust fault diagnosis using unknown input schemes," in *Fault Diagnosis in Dynamic Systems: Theory and Application* R. J. Patton, P. M. Frank and R. N. Clark, Eds. Prentice Hall, 1989, pp. 47-98.
- [121] P. M. Frank and J. Wunnenberg, "Sensor fault detection via robust observers," in *System Fault Diagnostics, Reliability, & Related Knowledge-Based Approaches* , vol. 1, S. G. Tzafestas, M. G. Singh and G. Schmidt, Eds. Dordrecht: D. Reidel Press, 1987, pp. 147-160.

- [122] P. M. Frank, "Fault Diagnosis in Dynamic Systems Using Analytical and Knowledge-based Redundancy - A Survey and Some New Results," *Automatica*, vol. 26, pp. 459-474, 1990. 1990.
- [123] G. F. Franklin, J. D. Powell and A. Emami-Naeini, *Feedback Control of Dynamic Systems*, 4th ed. Upper Saddle River, NJ: Prentice Hall, 2002, pp. 910.
- [124] E. Frisk, "Residual Generation for Fault Diagnosis," *Linkopings Universitet*, vol. Dissertation No. 716, pp. 1-184, 2001. 2001.
- [125] E. Frisk and L. Nielsen, "Robust residual generation for diagnosis including a reference model for residual behavior," *Automatica*, vol. 42, pp. 437-445, 2006. 2006.
- [126] E. Frisk and M. Nyberg, "Using minimal polynomial bases for model-based fault diagnosis," in *Proceedings of the 5th European Control Conference ECC'99*, 1999,
- [127] E. Frisk and J. Aslund, "Lowering orders of derivatives in non-linear residual generation using realization theory," *Automatica*, vol. 41, pp. 1799-1807, 2005/10.
- [128] E. Frisk and L. Nielsen, "Robust residual generation for diagnosis including a reference model for residual behavior," *Automatica*, vol. 42, pp. 437-445, 2006/3.
- [129] E. Garcia and P. Frank, "Deterministic Nonlinear Observer-based Approaches to Fault Diagnosis: A Survey," *Control Engineering Practice*, vol. 5, pp. 663-670, 1997. 1997.
- [130] E. A. Garcia and P. M. Frank, "Multiplicative fault isolation in linear systems," *Proceedings of the 38th Conference on Decision and Control*, 1999, pp. 3114-3115 vol.3.
- [131] J. P. Gauthier, H. Hammouri and S. Othman, "A simple observer for nonlinear systems applications to bioreactors," *Automatic Control, IEEE Transactions on*, vol. 37, pp. 875-880, 1992.
- [132] A. Gelb, *Applied Optimal Estimation*. Cambridge, Mass., M.I.T: Press, 1974, pp. 374.
- [133] J. Gertler, "Fault Detection and Isolation Using Parity Relations," *Control Engineering Practice*, vol. 5, pp. 653-661, 1997. 1997.
- [134] J. Gertler, "All Linear Methods are Equal - and Extendible to (some) Nonlinearities," *International Journal of Robust and Nonlinear Control*, vol. 12, pp. 629-648, 2002.

- [135] J. Gertler, "Residual generation from principal component models for fault diagnosis in linear systems - part I: Review of static systems," in 2005, pp. 628-633.
- [136] J. Gertler, "Residual generation from principal component models for fault diagnosis in linear systems - part II: Extension to optimal residuals and dynamic systems," in 2005, pp. 634-639.
- [137] J. Gertler, M. Staroswiecki and Mengbing Shen, "Direct design of structured residuals for fault diagnosis in linear systems," in 2002, pp. 4519-4524 vol.6.
- [138] J. J. Gertler, "Survey of model-based failure detection and isolation in complex plants," *Control Systems Magazine, IEEE*, vol. 8, pp. 3-11, 1988.
- [139] G. H. Golub and C. F. Van Loan, *Matrix Computations*. ,3rd ed. Baltimore: Johns Hopkins University Press, 1996, pp. 694.
- [140] L. Gomes, J. P. Barros and R. Lino, "Addition of fault detection capabilities in automation applications using petri nets," in 2004, pp. 645-650 vol. 1.
- [141] J. J. Gorman, K. W. Jablokow and D. J. Cannon, "Dynamical robust backstepping using a combined sliding modes and high-gain observer approach," in 2003, pp. 275-281 Vol.1.
- [142] C. Hadjicostis, *Coding Approaches to Fault Tolerance in Combinational and Dynamic Systems*. Boston, MA: Kluwer Academic Publishers, 2002, pp. 189.
- [143] C. Hadjicostis and G. C. Verghese, "Fault-tolerant dynamic systems," *ISIT*, 2000, pp. 444.
- [144] C. N. Hadjicostis, "Finite-state machine embeddings for nonconcurrent error detection and identification," *Automatic Control, IEEE Transactions on*, vol. 50, pp. 142-153, 2005.
- [145] C. N. Hadjicostis, "Nonconcurrent error detection and correction in fault-tolerant linear finite-state machines," *Automatic Control, IEEE Transactions on*, vol. 48, pp. 2133-2140, 2003.
- [146] C. N. Hadjicostis, "Nonconcurrent error detection and correction in fault-tolerant discrete-time LTI dynamic systems," *Circuits and Systems I: Fundamental Theory and Applications, IEEE Transactions on [See also Circuits and Systems I: Regular Papers, IEEE Transactions on]*, vol. 50, pp. 45-55, 2003.
- [147] C. N. Hadjicostis, "Finite-state machine embeddings for non-concurrent error detection and identification," *Proceedings fo the 42nd IEEE Conference on Decision and Control*, 2003, pp. 3215-3220 vol.4.

- [148] C. N. Hadjicostis, "Encoded finite-state machines for non-concurrent error detection and identification," *IEEE 0-7803-7761-3*, 2003, pp. III-858; III-861 vol.3.
- [149] C. N. Hadjicostis, "Probabilistic fault detection in finite-state machines based on state occupancy measurements," *Proceedings of the 41st IEEE Conference on Decision and Control*, 2002, pp. 3994-3999 vol.4.
- [150] C. N. Hadjicostis, "Stochastic testing of finite state machines," *Proceedings of the American Control Conference*, 2001, pp. 4568-4573 vol.6.
- [151] C. N. Hadjicostis, "Non-concurrent error detection and correction in discrete-time LTI dynamic systems," *Proceedings of the 40th IEEE Conference on Decision and Control*, 2001, pp. 1899-1904 vol.2.
- [152] C. N. Hadjicostis, "Fault-tolerant discrete-time linear time-invariant filters," *IEEE 0-7803-6293-4*, 2000, pp. 3311-3314 vol.6.
- [153] C. N. Hadjicostis and G. C. Verghese, "Coding approaches to fault tolerance in linear dynamic systems," *Information Theory, IEEE Transactions on*, vol. 51, pp. 210-228, 2005.
- [154] C. N. Hadjicostis and G. C. Verghese, "Encoded dynamics for fault tolerance in linear finite-state machines," *Automatic Control, IEEE Transactions on*, vol. 47, pp. 189-192, 2002.
- [155] C. N. Hadjicostis and G. C. Verghese, "Power system monitoring based on relay and circuit breaker information," *IEEE 0-7803-6685-9*, 2001, pp. 197-200 vol. 2.
- [156] C. N. Hadjicostis and G. C. Verghese, "Power system monitoring using Petri net embeddings," *Generation, Transmission and Distribution, IEE Proceedings-*, vol. 147, pp. 299-303, 2000.
- [157] C. N. Hadjicostis and G. C. Verghese, "Fault-tolerant linear finite state machines," *IEEE 0-7803-5682-9*, 1999, pp. 1085-1088 vol.2.
- [158] M. Hagan, H. Demuth and M. Beale, *Neural Network Design*, 1st ed. Boston: PWS Publishing Co, 1996,
- [159] H. Hammouri, M. Kinnaert and E. H. El Yaagoubi, "Observer-based approach to fault detection and isolation for nonlinear systems," *Automatic Control, IEEE Transactions on*, vol. 44, pp. 1879-1884, 1999.
- [160] B. Hamzi, Wei Kang and A. J. Krener, "Control of center manifolds," *Proceedings of the 42nd IEEE Conference on Decision and Control*, 2003, pp. 2065-2070 Vol.3.

- [161] P. D. Hanlon and P. S. Maybeck, "Characterization of Kalman filter residuals in the presence of mismodeling," *Aerospace and Electronic Systems, IEEE Transactions on*, vol. 36, pp. 114-131, 2000.
- [162] P. D. Hanlon and P. S. Maybeck, "Multiple-model adaptive estimation using a residual correlation Kalman filter bank," *Aerospace and Electronic Systems, IEEE Transactions on*, vol. 36, pp. 393-406, 2000.
- [163] Hao Ma, Dehong Xu and Yim-Shu Lee, "Fault diagnosis of power electronic circuits based on neural network and waveform analysis," *IEEE International Conference on Power Electronics and Drive Systems*, 1999, pp. 234-237 vol.1.
- [164] P. P. Harihara, Kyusung Kim and A. G. Parlos, "Signal-based versus model-based fault diagnosis-a trade-off in complexity and performance," *Symposium on Diagnostics for Electric Machines, Power Electronics and Drives*, 2003, pp. 277-282.
- [165] R. E. Hebner, "Electric ship power system - research at the University of Texas at Austin," *IEEE Electric Ship Technologies Symposium*, 2005, pp. 34-38.
- [166] H. Hegner and B. Desai, "Integrated fight through power," *IEEE 0-7803-7519-X*, 2002, pp. 336-339 vol.1.
- [167] R. Hermann and A. Krener, "Nonlinear controllability and observability," *Automatic Control, IEEE Transactions on*, vol. 22, pp. 728-740, 1977.
- [168] G. Hostetter and J. Meditch, "Observing systems with unmeasurable inputs," *Automatic Control, IEEE Transactions on*, vol. 18, pp. 307-308, 1973.
- [169] M. Hou and R. J. Patton, "Input Observability and Input Reconstruction," *Automatica*, vol. 34, pp. 789-794, 1998.
- [170] M. Hou and P. C. Muller, "Design of observers for linear systems with unknown inputs," *Automatic Control, IEEE Transactions on*, vol. 37, pp. 871-875, 1992.
- [171] M. Hou, "Comments on 'Tracking a maneuvering target using input estimation'," *Aerospace and Electronic Systems, IEEE Transactions on*, vol. 25, pp. 280, 1989.
- [172] Hsinyung Chin and K. Danai, "Residual generation for fault diagnosis through recurrent nets," *Proceedings of the American Control Conference*, 1994, pp. 1984-1988 vol.2.
- [173] H. Hsu, *Applied Fourier Analysis*. First ed. San Diego: Harcourt Brace, 1984, pp. 223.
- [174] Hu Shousong and Hu Weili, "Decentralized output feedback fault-tolerant control for uncertain large-scale systems," 1994, pp. 20-23.

- [175] S. Hui and S. Zak, "Observer Design for Systems with Unknown Inputs," *International Journal of Applied Mathematics and Computer Science*, vol. 15, pp. 431-446, 2005. 2005.
- [176] N. Hutchison, "An Investigation of the Effect of Current-Sensor Configuration on the Performance of a Three-Phase Current-Controlled Inverter Module Under Fault Conditions," Master's Thesis, Purdue University, pp. 1-133, 2006.
- [177] R. Irawan, M. Ooi, G. Yeung, E. Weyer, D. Nesic and I. Mareels, "A virtual laboratory experience based on a double tank apparatus," *Proceedings of the 40th IEEE Conference on Decision and Control*, 2001, pp. 2815-2820 vol.3.
- [178] R. Isermann and P. Balle, "Trends in the Application of Model-Based Fault Detection and Diagnosis of Technical Processes," *Control Engineering Practice*, vol. 5, pp. 709-719, 1997.
- [179] R. Isermann, "Supervision, Fault-Detection and Fault-Diagnosis Methods, An Introduction," *Control Engineering Practice*, vol. 5, pp. 639-652, 1997. 1997.
- [180] R. Isermann, "Fault Diagnosis of Machines via parameter Estimation and Knowledge Processing - Tutorial Paper," *Automatica*, vol. 29, pp. 815-835, 1993. 1993.
- [181] R. Isermann, "Process Fault Detection Based on Modeling and Estimation Methods - A Survey," *Automatica*, vol. 20, pp. 387-404, 1984. 1984.
- [182] A. Janczak, "Parameter Estimation Based Fault Detection and Isolation in Wiener and Hammerstein Systems," *Int. J. Appl. Math. and Comp. Sci.*, vol. 9, pp. 711-735, 1999. 1999.
- [183] J. Jatskevich, S. D. Pekarek and A. Davoudi, "Fast procedure for constructing an accurate dynamic average-value model of synchronous machine-rectifier systems," *Energy Conversion, IEEE Transactions on*, vol. 21, pp. 435-441, 2006.
- [184] J. Jatskevich, S. D. Pekarek and A. Davoudi, "Parametric average-value model of synchronous machine-rectifier systems," *Energy Conversion, IEEE Transactions on*, vol. 21, pp. 9-18, 2006.
- [185] J. Jatskevich, O. Wasynczuk, E. A. Walters and C. E. Lucas, "A globally continuous state-space representation of switched networks," *IEEE 0-7803-5957-7*, 2000, pp. 559-563 vol.1.
- [186] R. Jayabalan and B. Fahimi, "Fault diagnostics in naval shipboard power system for contingency management and survivability," *IEEE Electric Ship Technologies Symposium*, 2005, pp. 108-111.

- [187] R. Jayabalan, B. Fahimi, A. Koenig and S. Pekarek, "Applications of power electronics-based systems in vehicular technology: State-of-the-art and future trends," *35th Annual IEEE Power Electronics Specialists Conference*, 2004, pp. 1887-1894 Vol.3.
- [188] Jian Wu, Yong Cheng, N. N. Schulz and H. L. Ginn, "The impact of standardized models, programming interfaces, and protocols on shipboard power system," *2005 IEEE Electric Ship Technologies Symposium*, 2005, pp. 48-54.
- [189] Jie Zhang, E. Martin and A. J. Morris, "Fault detection and classification through multivariate statistical techniques," *Proceedings of the American Control Conference*, 1995, pp. 751-755 vol.1.
- [190] Jin Cao and J. Gertler, "Partial PCA-based optimal structured residual design for fault isolation," *Proceedings of the 2004 American Control Conference*, 2004, pp. 4420-4425 vol.5.
- [191] Jing Sun, Shi-Yin Qin and Yong-Hua Song, "Fault diagnosis of electric power systems based on fuzzy Petri nets," *Power Systems, IEEE Transactions on*, vol. 19, pp. 2053-2059, 2004.
- [192] N. H. Jo, Juwha Jin, Sungjun Joo and J. W. Seo, "Generalized luenberger-like observer for nonlinear systems," *Proceedings of the American Control Conference*, 1997, pp. 2180-2183 vol.3.
- [193] D. John and P. Mackay, "Condition and casualty assessment: Proposals for the application of system fault prognosis and healing to plant and systems on future naval platforms," in *Proceedings of the Thirteenth International Ship Control Systems Symposium (SCSS)*, 2003, pp. 1-6.
- [194] H. L. Jones, "Failure Detection in Linear Systems," *PhD Thesis*, 1973.
- [195] S. J. Julier and J. K. Uhlmann, "Unscented filtering and nonlinear estimation," *Proceedings of the IEEE*, vol. 92, pp. 401-422, 2004.
- [196] S. J. Julier, J. K. Uhlmann and H. F. Durrant-Whyte, "A new approach for filtering nonlinear systems," *Proceedings of the American Control Conference*, 1995, pp. 1628-1632 vol.3.
- [197] Jun-ichi Imura, "Well-posedness analysis of switch-driven piecewise affine systems," *Automatic Control, IEEE Transactions on*, vol. 48, pp. 1926-1935, 2003.
- [198] Jusong Yang, M. Montakhab, T. S. Davies, A. G. Pipe and B. Carse, "Fault diagnosis of power distribution systems using a multi-agent approach," 2004, pp. 448-452 Vol. 1.

- [199] P. Kabisatpathy, A. Barua and S. Sinha, "Artificial neural-network model-based observers," *Circuits and Devices Magazine, IEEE*, vol. 21, pp. 18-26, 2005.
- [200] T. Kailath, *Linear Systems*. Englewood Cliffs, N.J: Prentice-Hall, 1980, pp. 682.
- [201] S. S. Kalsi, N. Henderson, D. Gritter, O. Nayak and C. Gallagher, "Benefits of HTS technology to ship systems," *IEEE Electric Ship Technologies Symposium*, 2005, pp. 437-443.
- [202] S. S. Kalsi and O. Nayak, "Ship electrical system simulation," *IEEE Electric Ship Technologies Symposium*, 2005, pp. 63-69.
- [203] W. Kang, "Numerical observers of control systems using computational optimization methods," in *Proceedings of the Eighth IASTED International Conference on Intelligent Systems and Control*, 2005, pp. 120-125.
- [204] W. Kang and J. Barbot, "Discussions on observability and invertibility," 2007.
- [205] M. Kao and J. J. Moskwa, "Model-based engine fault detection using cylinder pressure estimates from nonlinear observers," *Proceedings of the 33rd Conference on Decision and Control*, 1994, pp. 2742-2747 vol.3.
- [206] J. Y. Keller and M. Darouach, "Two-stage Kalman Estimator with Unknown Exogenous Inputs," *Automatica*, vol. 35, pp. 339-342, 1999.
- [207] W. S. Kerwin and J. L. Prince, "On the Optimality of Recursive Unbiased State Estimation with Unknown Inputs," *Automatica*, vol. 36, pp. 1381-1383, 2000.
- [208] A. Khaligh, S. S. Williamson and A. Emadi, "Control and stabilization of DC/DC buck-boost converters loaded by constant power loads in vehicular systems using a novel digital scheme," *EPE-PEMC*, 2006, pp. 1769-1775.
- [209] H. K. Khalil, *Nonlinear Systems*. New York; Toronto; New York: Macmillan Pub. Co; Maxwell Macmillan Canada; Maxwell Macmillan International, 1992, pp. 564.
- [210] M. J. Khosrowjerdi and R. Nikoukhah, "A Mixed H_2/H_{∞} Approach to Simultaneous Fault Detection and Control," *Automatica*, vol. 40, pp. 261-267, 2004.
- [211] D. E. Kirk, *Optimal Control Theory; an Introduction*. Englewood Cliffs, N.J: Prentice-Hall, 1970, pp. 452.
- [212] M. Kitamura, "Detection of Sensor Failures in Nuclear Plant Using Analytical Redundancy," *Trans. Am. Nucl. Soc.*, vol. 34, pp. 581-583, 1980.
- [213] N. Kiupel, B. Koppen-Seliger, H. S. Kellinghaus and P. M. Frank, "Fuzzy residual evaluation concept (FREC)," *IEEE 0-7803-2559-1*, 1995, pp. 13-18 vol.1.

- [214] I. Kolmanovsky, I. Sivergina and J. Sun, "Combined input and parameter estimation with input observers and set-membership parameter bounding," *43rd IEEE Conference on Decision and Control*, 2004, pp. 5192-5197 Vol.5.
- [215] B. Koppen-Seliger, P. M. Frank and A. Wolff, "Residual evaluation for fault detection and isolation with RCE neural networks," *Proceedings of the American Control Conference*, 1995, pp. 3264-3268 vol.5.
- [216] J. Korbicz, K. Patan and A. Obuchowicz, "Dynamic Neural Networks for Process Modelling in Fault Detection and Isolation Systems," *Int. J. Appl. Math. and Comp. Sci.*, vol. 9, pp. 519-546, 1999. 1999.
- [217] J. Koscielny, S. Dariusz and K. Zakroczymski, "Fuzzy-logic Fault Isolation in Large-Scale Systems," *Int. J. Appl. Math. and Comp. Sci.*, vol. 9, pp. 637-652, 1999. 1999.
- [218] J. Koscielny, M. Syfert and M. Bartys, "Fuzzy-Logic Fault Diagnosis of Industrial Process Actuators," *Int. J. Appl. Math. and Comp. Sci.*, vol. 9, pp. 653-666, 1999. 1999.
- [219] Z. Kowalczyk, P. Suchomski and T. Bialaszewski, "Evolutionary Multi-Objective Pareto Optimisation of Diagnostic State Observers," *Int. J. Appl. Math. and Comp. Sci.*, vol. 9, pp. 689-709, 1999. 1999.
- [220] P. C. Krause, O. Wasynczuk, S. D. Sudhoff and Krause, Paul C. *Analysis of Electric Machinery and Drive Systems*. ,2nd ed. New York: IEEE Press, 2002, pp. 613.
- [221] A. Krener and W. Kang, "Locally Convergent Nonlinear Observers," *SIAM J. Control Optim.*, vol. 42, pp. 155-177, 2003. 2003.
- [222] A. J. Krener and MingQing Xiao, "Observer design of linearly unobservable systems," *Proceedings of the American Control Conference*, 2002, pp. 110-115 vol.1.
- [223] A. J. Krener and MingQing Xiao, "A necessary and sufficient condition for the existence of a nonlinear observer with linearizable error dynamics," *Proceedings of the 40th IEEE Conference on Decision and Control*, 2001, pp. 2936-2941 vol.3.
- [224] A. J. Krener, Wei Kang and Dong Eui Chang, "Control bifurcations," *Automatic Control, IEEE Transactions on*, vol. 49, pp. 1231-1246, 2004.
- [225] E. Kreyszig, *Advanced Engineering Mathematics*. ,5th ed. New York: Wiley, 1983, pp. 988, 92.

- [226] R. A. Krishnan and N. Pappa, "Real time fault diagnosis for a heat exchanger — A model based approach," *IEEE Indicon Conference*, 2005, pp. 78-82.
- [227] V. Krishnaswami, C. Siviero, F. Carbognani, G. Rizzoni and V. Utkin, "Application of sliding mode observers to automobile powertrain diagnostics," *Proceedings of the 1996 IEEE International Conference on Control Applications*, 1996, pp. 355-360.
- [228] D. L. Krueger, J. B. Burl and R. Cristi, "Parametric uncertainty reduction in robust multivariable control," pp. 94, Sept. 1993. 1993.
- [229] V. Kucera, *Discrete Linear Control: The Polynomial Equation Approach*. Chichester, England: John Wiley and Sons, 1979,
- [230] P. Kudva, N. Viswanadham and A. Ramakrishna, "Observers for linear systems with unknown inputs," *Automatic Control, IEEE Transactions on*, vol. 25, pp. 113-115, 1980.
- [231] C. Kwan and R. Xu, "A note on simultaneous isolation of sensor and actuator faults," *Control Systems Technology, IEEE Transactions on*, vol. 12, pp. 183-192, 2004.
- [232] H. G. Kwatny, E. Mensah, D. Niebur and C. Teolis, "Optimal shipboard power system management via mixed integer dynamic programming," *IEEE Electric Ship Technologies Symposium*, 2005, pp. 55-62.
- [233] C. Kwon, S. Sudhoff and S. Zak, "Rotor flux and speed observers for induction motors," in *International Conference on Power Electronics and Intelligent Control for Energy Conservation*, 2005, pp. 1-2,3,4.
- [234] M. Labarrere and R. J. Patton, "Detection of sensor failures," in *Concise Encyclopedia of Aeronautics & Space Systems* M. Pelegri and W. M. Hollister, Eds. Pergamon Press, 1993, pp. 101-110.
- [235] Le Xu, S. M. Hsiang and Mo-Yuen Chow, "The development of fault diagnosis methodologies using hierarchical clustering and small world network stratification," *IEEE I-4244-0166-6*, 2006, pp. 149-153.
- [236] Y. Lee, R. Chan, S. Sudhoff and E. Zivi, "Optimization of the Ship Service Converter Module and System Capacitances in the Naval Combat Survivability DC Distribution System," 2006.
- [237] H. Lee and Min-Jea Tahk, "Generalized input-estimation technique for tracking maneuvering targets," *Aerospace and Electronic Systems, IEEE Transactions on*, vol. 35, pp. 1388-1402, 1999.

- [238] G. G. Leininger, "Model degradation effects on sensor failure detection," in *Proc. of the 1981 Joint Amer. Control Conf.* 1981, pp. FP-3A.
- [239] S. Leonhardt and M. Ayoubi, "Methods of Fault Diagnosis," *Control Engineering Practice*, vol. 5, pp. 683-692, 1997.
- [240] Li Liu, K. P. Logan and D. A. Cartes, "Fault detection, diagnostics, and prognostics: Software agent solutions," *IEEE Electric Ship Technologies Symposium*, 2005, pp. 425-431.
- [241] Lingxi Li, C. N. Hadjicostis and R. S. Sreenivas, "Fault detection and identification in petri net controllers," *43rd IEEE Conference on Decision and Control*, 2004, pp. 5248-5253 Vol.5.
- [242] N. Linh-Trung, A. Aissa-El-Bey, K. Abel-Meraim and A. Belouchrani, "Underdetermined blind source separation of non-disjoint nonstationary sources in the time-frequency domain," *IEEE 0-7803-9243-4*, 2005, pp. 46-49.
- [243] S. Liying and C. Zhaolin, "Observer design for discrete-time descriptor systems with unknown inputs and inputs estimation," *5th Asian Control Conference*, 2004, pp. 804-808 Vol.2.
- [244] K. P. Logan, "Operational experience with intelligent software agents for shipboard diesel and gas turbine engine health monitoring," *IEEE Electric Ship Technologies Symposium*, 2005, pp. 184-194.
- [245] B. Loop, "Estimating Regions of Asymptotic Stability of Nonlinear Systems with Applications to Power Electronics Systems," *Purdue University*, vol. 2005, pp. 1-191, May 2005.
- [246] B. P. Loop, S. D. Sudhoff, S. H. Zak and E. L. Zivi, "An optimization approach to estimating stability regions using genetic algorithms," *American Control Conference*, 2005, pp. 231-236 vol. 1.
- [247] Ma Hao and Ying Fengwei, "Investigation on compatible remote fault diagnosis system for power electronic equipments," 2003, pp. 630-635 Vol.1.
- [248] J. -. Magni and P. Mouyon, "On residual generation by observer and parity space approaches," *Automatic Control, IEEE Transactions on*, vol. 39, pp. 441-447, 1994.
- [249] M. Mahmoud, Jin Jiang and Youmin Zhang, "Stochastic stability analysis of fault-tolerant control systems in the presence of noise," *Automatic Control, IEEE Transactions on*, vol. 46, pp. 1810-1815, 2001.

- [250] D. Maksimovic, A. M. Stankovic, V. J. Thottuvelil and G. C. Verghese, "Modeling and simulation of power electronic converters," *Proceedings of the IEEE*, vol. 89, pp. 898-912, 2001.
- [251] J. Malmborg and J. Eker, "Hybrid control of a double tank system," *Proceedings of the 1997 IEEE International Conference on Control Applications*, 1997, pp. 133-138.
- [252] D. Maquin, B. Gaddouna and J. Ragot, "Estimation of unknown inputs in linear systems," *Proceedings of the American Control Conference*, 1994, pp. 1195-1197 vol.1.
- [253] T. Marcu, L. Mirea and P. Frank, "Development of Dynamic Neural Networks with Application to Observer-Based Fault Detection and Isolation," *Int. J. Appl. Math. and Comp. Sci.*, vol. 9, pp. 547-570, 1999. 1999.
- [254] T. Marcu, L. Mirea and P. M. Frank, "Neural observer schemes for robust detection and isolation of process faults," *UKACC International Conference on Control*, 1998, pp. 958-963 vol.2.
- [255] M. -. Massoumnia, G. C. Verghese and A. S. Willsky, "Failure detection and identification," *Automatic Control, IEEE Transactions on*, vol. 34, pp. 316-321, 1989.
- [256] J. V. Meer, A. Bendre, S. Krstic and D. Divan, "Improved ship power system - generation, distribution, and fault control for electric propulsion and ship service," *IEEE Electric Ship Technologies Symposium*, 2005, pp. 284-291.
- [257] A. Megretski. (2006, 6.245 multivariable control systems, spring 2004. MIT OpenCourseWare [online]. 2007(January), Available: <http://ocw.mit.edu/OcwWeb/Electrical-Engineering-and-Computer-Science/6-245Spring2004/CourseHome/index.htm>
- [258] R. K. Mehra and J. Peschon, "An Innovations Approach to Fault Detection and Diagnosis in Dynamic Systems," *Automatica*, vol. 7, pp. 637-640, 1971.
- [259] T. E. Menke and P. S. Maybeck, "Sensor/actuator failure detection in the Vista F-16 by multiple model adaptive estimation," *Aerospace and Electronic Systems, IEEE Transactions on*, vol. 31, pp. 1218-1229, 1995.
- [260] T. E. Menke and P. S. Maybeck, "Multiple model adaptive estimation applied to the VISTA F-16 flight control system with actuator and sensor failures," 1992, pp. 441-448 vol.2.
- [261] H. E. Merritt, *Hydraulic Control Systems*. New York: Wiley, 1967, pp. 358.

- [262] G. Millerioux and J. Daafouz, "Unknown input observers for switched linear discrete time systems," in *Proceeding of the 2004 American Control Conference*, 2004, pp. 5802-5805.
- [263] N. Mohan, T. Undeland and W. P. Robbins, *Power Electronics : Converters, Applications, and Design*. ,3rd ed. ed. Hoboken, NJ: John Wiley & Sons, 2003,
- [264] A. Monti, D. Boroyevich, D. Cartes, R. Dougal, H. Ginn, G. Monnat, S. Pekarek, F. Ponci, E. Santi, S. Sudhoff, N. Schulz, W. Shutt and F. Wang, "Ship power system control: A technology assessment," *IEEE Electric Ship Technologies Symposium*, 2005, pp. 292-297.
- [265] A. Monti, D. Boroyevich, D. Cartes, R. Dougal, H. Ginn, G. Monnat, S. Pekarek, F. Ponci, E. Santi, S. Sudhoff, N. Schulz, W. Shutt and F. Wang, "Ship power system control: A technology assessment," *IEEE Electric Ship Technologies Symposium*, 2005, pp. 292-297.
- [266] A. Monticelli, "Electric power system state estimation," *Proceedings of the IEEE*, vol. 88, pp. 262-282, 2000.
- [267] E. Moulines, P. Duhamel, J. -. Cardoso and S. Mayrargue, "Subspace methods for the blind identification of multichannel FIR filters," *Signal Processing, IEEE Transactions on [See also Acoustics, Speech, and Signal Processing, IEEE Transactions on]*, vol. 43, pp. 516-525, 1995.
- [268] P. Moylan, "Stable inversion of linear systems," *Automatic Control, IEEE Transactions on*, vol. 22, pp. 74-78, 1977.
- [269] H. Niemann, "Fault tolerant control based on active fault diagnosis," *American Control Conference*, 2005, pp. 2224-2229 vol. 3.
- [270] N. S. Nise, *Control Systems Engineering*. ,4th ed.Hoboken, NJ: Wiley, 2004, pp. 983.
- [271] NRAC, "Naval Research Advisory Committee (NRAC) Report: Roadmap to an Electric Naval Force," pp. 1-90, July 2002.
- [272] NRAC, "Naval Research Advisory Committee (NRAC) Report: Optimized Surface Ship Manning," pp. 1-110, April 2000.
- [273] NRAC, "Naval Research Advisory Committee (NRAC) Report: Modelling and Simulation," 1994. 1994.
- [274] K. Ogata, *Modern Control Engineering*. ,4th ed.Upper Saddle River, NJ: Prentice Hall, 2002, pp. 964.
- [275] K. Ogata, *System Dynamics*. Englewood Cliffs, N.J: Prentice-Hall, 1978, pp. 596.

- [276] C. M. Ozveren and A. S. Willsky, "Output stabilizability of discrete-event dynamic systems," *Automatic Control, IEEE Transactions on*, vol. 36, pp. 925-935, 1991.
- [277] C. M. Ozveren and A. S. Willsky, "Observability of discrete event dynamic systems," *Automatic Control, IEEE Transactions on*, vol. 35, pp. 797-806, 1990.
- [278] D. P. Palomar and S. Verdu, "Representation of Mutual Information Via Input Estimates," *Information Theory, IEEE Transactions on*, vol. 53, pp. 453-470, 2007.
- [279] S. H. Park, P. S. Kim, O. Kwon and W. H. Kwon, "Estimation and detection of Unknown Inputs Using Optimal FIR Filter," *Automatica*, vol. 36, pp. 1481-1488, 2000.
- [280] Y. Park and J. L. Stein, "Closed-loop, state and inputs observer for systems with unknown inputs," *International Journal of Control*, vol. 48, pp. 1121-1136, 1988.
- [281] R. J. Patton and J. Chen, "Robust fault detection using eigenstructure assignment: A tutorial consideration and some new results," *Proceedings of the 30th Conference on Decision and Control*, 1991, pp. 2242-2247.
- [282] R. J. Patton, P. M. Frank and R. N. Clark, *Fault Diagnosis in Dynamic Systems, Theory and Application*. New York: Prentice Hall, 1989,
- [283] R. Patton and J. Chen, "Observer-Based Fault Detection and Isolation: Robustness and Applications," *Control Engineering Practice*, vol. 5, pp. 671-682, 1997. 1997.
- [284] R. Patton, C. Lopez-Toribio and F. Uppal, "Artificial Intelligence Approaches to Fault Diagnosis for Dynamic Systems," *Int. J. Appl. Math. and Comp. Sci.*, vol. 9, pp. 471-518, 1999. 1999.
- [285] S. D. Pekarek, J. Tichenor, S. D. Sudhoff, J. D. Sauer, D. E. Delisle and E. J. Zivi, "Overview of a naval combat survivability program," in *Thirteenth International Ship Control Systems Symposium*, 2003, pp. 1-10.
- [286] S. Pekarek, K. Uthaichana, S. Benghea, R. DeCarlo and M. Zefran, "Modeling of an electric drive for a HEV supervisory level power flow control problem," *IEEE 0-7803-9280-5*, 2005, pp. 6.
- [287] S. D. Pekarek, O. Wasynczuk, E. A. Walters, J. V. Jatskevich, C. E. Lucas, Ning Wu and P. T. Lamm, "An efficient multirate Simulation technique for power-electronic-based systems," *Power Systems, IEEE Transactions on*, vol. 19, pp. 399-409, 2004.

- [288] D. Perreault. (2006, 6.334 power electronics, spring 2003. *MIT OpenCourseWare* [online]. 2007(January), Available: <http://ocw.mit.edu/OcwWeb/Electrical-Engineering-and-Computer-Science/6-334Spring2003/CourseHome/index.htm>
- [289] C. Petry and J. Rumburg, "Zonal Electrical Distribution Systems: An Affordable Architecture for the Future," *Naval Engineers Journal*, vol. 105, pp. 45-51, May, 1993. 1993.
- [290] T. Pfeufer, "Application of Model-Based Fault Detection and Diagnosis to the Quality Assurance of an Automotive Actuator," *Control Engineering Practice*, vol. 5, pp. 703-708, 1997. 1997.
- [291] S. Poroseva, S. Woodruff and M. Y. Hussaini, "Topology of the generator bus in a warship integrated power system," *IEEE Electric Ship Technologies Symposium*, 2005, pp. 141-148.
- [292] L. Qi and S. Woodruff, "Stability analysis and assessment of integrated power systems using RTDS," *IEEE Electric Ship Technologies Symposium*, 2005, pp. 325-332.
- [293] S. J. Qin and W. Li, "Detection and identification of faulty sensors with maximized sensitivity," *Proceedings of the American Control Conference*, 1999, pp. 613-617 vol.1.
- [294] A. Rantzer and C. Byrnes, *Directions in Mathematical Systems Theory and Optimization*. New York: Springer, 2002, pp. 173-182.
- [295] C. Rivetta, G. A. Williamson and A. Emadi, "Constant power loads and negative impedance instability in sea and undersea vehicles: Statement of the problem and comprehensive large-signal solution," *IEEE Electric Ship Technologies Symposium*, 2005, pp. 313-320.
- [296] C. H. Rivetta, A. Emadi, G. A. Williamson, R. Jayabalan and B. Fahimi, "Analysis and control of a buck DC-DC converter operating with constant power load in sea and undersea vehicles," *Industry Applications, IEEE Transactions on*, vol. 42, pp. 559-572, 2006.
- [297] M. Rodrigues, D. Theilliol and D. Sauter, "Design of a robust polytopic unknown input observer for FDI: Application for systems described by a multi-model representation," *Proceedings of the 44th IEEE Conference on Decision and Control, and the European Control Conference*, 2005, pp. 6268-6273.
- [298] H. Rodriguez, C. Hadjicostis and A. Stankovic, "Dynamical Models in Fault-Tolerant Operation of Energy Processing Systems," pp. 1-17, 20 May 2003.

- [299] H. Rodriguez-Cortes, C. N. Hadjicostis and A. M. Stankovic, "Model-based broken rotor bar detection on an IFOC driven squirrel cage induction motor," *Proceedings of the 2004 American Control Conference*, 2004, pp. 3094-3099 vol.4.
- [300] H. Rodriguez-Cortes, C. N. Hadjicostis and A. M. Stankovic, "Detuning detection in induction motors," *43rd IEEE Conference on Decision and Control*, 2004, pp. 4330-4335 Vol.4.
- [301] E. R. Ronan Jr, S. D. Sudhoff, S. F. Glover and D. L. Galloway, "Application of power electronics to the distribution transformer," *IEEE 0-7803-5864-3*, 2000, pp. 861-867 vol.2.
- [302] S. Rosado, A. Prasai, F. Wang and D. Boroyevich, "Study of the energy flow characteristics in power electronic conversion systems," *IEEE Electric Ship Technologies Symposium*, 2005, pp. 333-339.
- [303] J. A. Ruiz Vargas and E. M. Hemerly, "Adaptive observers for unknown general nonlinear systems," *Systems, Man and Cybernetics, Part B, IEEE Transactions on*, vol. 31, pp. 683-690, 2001.
- [304] P. S.D and W. E.A , "An accurate method of neglecting dynamic saliency of synchronous machines in power electronic based systems," *Energy Conversion, IEEE Transaction on*, vol. 14, pp. 1177-1183, 1999.
- [305] P. S.D , W. O and H. H.J , "An efficient and accurate model for the simulation and analysis of synchronous machine/converter systems," *Energy Conversion, IEEE Transaction on*, vol. 13, pp. 42-48, 1998.
- [306] A. Saberi, A. A. Stoorvogel and P. Sannuti, "Connections between H_2 /optimal filters and unknown input observers performance limitations of H_2 /optimal filtering," *Proceedings of the 2004 American Control Conference*, 2004, pp. 3460-3465 vol.4.
- [307] A. Saberi, A. A. Stoorvogel and P. Sannuti, "Connections between H_2 /optimal filters and unknown input observers performance limitations of H_2 /optimal filtering," *Proceedings of the 2004 American Control Conference*, 2004, pp. 3460-3465 vol.4.
- [308] A. Sainana, "A novel sliding mode observer applied to the three-phase voltage source inverter," *EPE-2005, ISBN: 90-75815-08-5*, 2005, pp. 12.
- [309] S. R. Sanders, J. M. Noworolski, X. Z. Liu and G. C. Verghese, "Generalized averaging method for power conversion circuits," *Power Electronics, IEEE Transactions on*, vol. 6, pp. 251-259, 1991.

- [310] S. R. Sanders and G. C. Verghese, "Synthesis of averaged circuit models for switched power converters," *IEEE CH2868-8/90/0000*, 1990, pp. 679-683 vol.1.
- [311] N. N. Schulz, H. L. Ginn and S. M. Halpin, "Electric ship research activities and capabilities at Mississippi State University and its partners," *IEEE Electric Ship Technologies Symposium*, 2005, pp. 20-27.
- [312] A. S. Sedra and K. C. Smith, *Microelectronic Circuits*. ,4th ed. New York: Oxford University Press, 1998,
- [313] B. Sfaihi and O. Boubaker, "Full order observer design for linear systems with unknown inputs," *IEEE International Conference on Industrial Technology (ICIT)* 2004, pp. 1233-1238 Vol. 3.
- [314] Shao-Kung Chang, Wen-Tong You and Pau-Lo Hsu, "General-structured unknown input observers," *Proceedings of the American Control Conference*, 1994, pp. 666-670 vol.1.
- [315] S. N. Sheldon and P. S. Maybeck, "An optimizing design strategy for multiple model adaptive estimation and control," *Automatic Control, IEEE Transactions on*, vol. 38, pp. 651-654, 1993.
- [316] J. -. E. Slotine and W. Li, *Applied Nonlinear Control*. Englewood Cliffs, N.J: Prentice Hall, 1991, pp. 461.
- [317] E. N. Skoundrianos and S. G. Tzafestas, "Finding fault - fault diagnosis on the wheels of a mobile robot using local model neural networks," *Robotics & Automation Magazine, IEEE*, vol. 11, pp. 83-90, 2004.
- [318] H. Sneider and P. M. Frank, "Observer-based supervision and fault detection in robots using nonlinear and fuzzy logic residual evaluation," *Control Systems Technology, IEEE Transactions on*, vol. 4, pp. 274-282, 1996.
- [319] S. K. Srivastava and K. L. Butler-Purry, "A pre-hit probabilistic reconfiguration methodology for shipboard power systems," *IEEE Electric Ship Technologies Symposium*, 2005, pp. 99-104.
- [320] M. Staroswiecki and P. Declerck, "Analytical redundancy in nonlinear interconnected systems by means of structural analysis," in *IFAC Advanced Information Processing in Automatic Control (AIPAC)*, 1989, pp. 23-27.
- [321] M. Staroswiecki, V. Cocquempot and J. P. Cassar, "Optimal design of FDI systems via parity space and observer based approaches," *IECON-'91, IEEE CH2976-9*, 1991, pp. 143-148 vol.1.

- [322] R. B. Statnikov and J. B. Matusov, *Multicriteria Analysis in Engineering : Using the PSI Method with MOVI 1.0*. Dordrecht; Boston: Kluwer Academic Publishers, 2002, pp. 262.
- [323] W. D. Stevenson, *Elements of Power System Analysis*. ,3d ed. New York: McGraw-Hill, 1975, pp. 423.
- [324] G. Strang. (2006, 18.06 linear algebra, spring 2005. *MIT OpenCourseWare* [online]. 2007(January), Available: <http://ocw.mit.edu/OcwWeb/Mathematics/18-06Spring-2005/CourseHome/index.htm>
- [325] G. Strang, *Linear Algebra and its Applications*. ,3rd ed. San Diego: Harcourt, Brace, Jovanovich, Publishers, 1988, pp. 505.
- [326] S. H. Strogatz, *Nonlinear Dynamics and Chaos : With Applications to Physics, Biology, Chemistry, and Engineering*. Cambridge, Mass: Perseus Pub., 1994, pp. 498.
- [327] S. D. Sudhoff, S. H. Glover, S. H. Zak, S. D. Pekarek, E. J. Zivi, D. E. Delisle and D. Clayton, "Stability analysis methodologies for DC power distribution systems," in *Thirteenth International Ship Control Systems Symposium*, 2003, pp. 1-10.
- [328] S. Sudhoff, S. Zak, E. Zivi and T. McCoy, "Survivability Performance Formulation, Metrics and Modeling for an Integrated Engineering Plant Modeling (Draft Document)," pp. 1-53, 25 March 2005. 2005.
- [329] S. D. Sudhoff, "Waveform reconstruction from the average-value model of line-commutated converter-synchronous machine systems," *Energy Conversion, IEEE Transactions on*, vol. 8, pp. 404-410, 1993.
- [330] S. D. Sudhoff, K. A. Corzine, S. F. Glover, H. J. Hegner and H. N. Robey Jr, "DC link stabilized field oriented control of electric propulsion systems," *Energy Conversion, IEEE Transaction on*, vol. 13, pp. 27-33, 1998.
- [331] S. D. Sudhoff and S. F. Glover, "Three-dimensional stability analysis of DC power electronics based systems," *IEEE 0-7803-5692-6*, 2000, pp. 101-106 vol.1.
- [332] S. D. Sudhoff, S. F. Glover, P. T. Lamm, D. H. Schmucker and D. E. Delisle, "Admittance space stability analysis of power electronic systems," *Aerospace and Electronic Systems, IEEE Transactions on*, vol. 36, pp. 965-973, 2000.
- [333] S. D. Sudhoff, I. G. Hansen and B. H. Kenny, "Improving power quality in a 20-kHz distribution system," *IEEE CH3306-8*, 1993, pp. 420-427 vol.1.

- [334] S. D. Sudhoff and P. C. Krause, "Average-value model of the brushless D 120° inverter system," *Energy Conversion, IEEE Transactions on*, vol. 5, pp. 553-557, 1990.
- [335] S. D. Sudhoff, S. Pekarek, B. Kuhn, S. Glover, J. Sauer and D. Delisle, "Naval combat survivability testbeds for investigation of issues in shipboard power electronics based power and propulsion systems," *IEEE 0-7803-7519-X*, 2002, pp. 347-350 vol.1.
- [336] S. D. Sudhoff and O. Wasynczuk, "Analysis and average-value modeling of line-commutated converter-synchronous machine systems," *Energy Conversion, IEEE Transactions on*, vol. 8, pp. 92-99, 1993.
- [337] Sun Jitao and Liu Yongqing, "Observer-based robust fault-tolerant control of uncertain systems," *Proceedings of the 3rd World Congress on Intelligent Control and Automation*, 2000, pp. 737-739 vol.1.
- [338] L. Sun, "State and input estimation for singular discrete-time systems with unknown inputs," 2004, pp. 993-996 Vol.2.
- [339] L. Sun and Z. Cheng, "Observer design for descriptor systems with unknown inputs and inputs estimation," *Proceedings of the 5th World Congress on Intelligent Control and Automation*, 2004, pp. 997-1001 Vol.2.
- [340] S. Sundaram and C. N. Hadjicostis, "On delayed observers for linear systems with unknown inputs," *Proceedings of the 44th IEEE Conference on Decision and Control, and the European Control Conference 2005*, pp. 7210-7215.
- [341] S. Sundaram and C. N. Hadjicostis, "Delayed Observers for Linear Systems With Unknown Inputs," *Automatic Control, IEEE Transactions on*, vol. 52, pp. 334-339, 2007.
- [342] T. K. Sung and Jang Gyu Lee, "A decoupled adaptive tracking filter for real applications," *Aerospace and Electronic Systems, IEEE Transactions on*, vol. 33, pp. 1025-1030, 1997.
- [343] Survivability Handbook (2000), *US Navy Survivability Design Handbook for Surface Ships*. The Pentagon: Chief of Naval Operations Ship Safety and Survivability Office N86DC, 2000,
- [344] T. Szabo and G. Horvath, "CMAC and Its Extensions for Efficient System Modelling," *Int. J. Appl. Math. and Comp. Sci.*, vol. 9, pp. 571-598, 1999.
- [345] G. Takos and C. N. Hadjicostis, "Hierarchical decentralized fusion from correlated sensor measurements," *IEEE 0-7803-8812-7*, 2005, pp. 508-513.

- [346] A. Tellili, M. N. Abdelkrim and M. Benrejeb, "Model-based fault diagnosis of two-time scales singularly perturbed systems," *IEEE 0-7803-8379-6*, 2004, pp. 819-822.
- [347] C. W. Therrien, *Discrete Random Signals and Statistical Signal Processing*. Englewood Cliffs, NJ: Prentice Hall, 1992, pp. 727.
- [348] C. W. Therrien and M. Tummala, *Probability for Electrical and Computer Engineers*. Boca Raton, Fla: CRC Press, 2004, pp. 312.
- [349] S. Thomas, B. C. Chang and H. G. Kwatny, "Controller reconfiguration for nonlinear systems using composite observer," *IEEE 0-7803-7896-2*, 2003, pp. 4779-4784 vol.6.
- [350] H. Trentelman, A. Stoorvogel and M. Hautus, *Control Theory for Linear Systems*. ,1st ed. London: Springer-Verlag, 2001, pp. 389.
- [351] G. J. Vachtsevanos, *Intelligent Fault Diagnosis & Prognosis for Engineering Systems*. Hoboken, NJ: Wiley, 2006, pp. 434.
- [352] M. E. Valcher, "State observers for discrete-time linear systems with unknown inputs," *Automatic Control, IEEE Transactions on*, vol. 44, pp. 397-401, 1999.
- [353] M. E. Valcher and J. C. Willems, "Dead beat observer synthesis," *Systems and Control Letters*, vol. 37, pp. 285-292, 1999.
- [354] Z. W. Vilar and R. A. Dougal, "Effectiveness of generator control strategies on meeting pulsed load requirements in ship electric systems," *IEEE Electric Ship Technologies Symposium*, 2005, pp. 459-462.
- [355] N. Viswanadham and R. Srichander, "Fault Detection using Unknown Input Observers," *Control - Theory and Advanced Technology*, vol. 3, pp. 91-101, 1987.
- [356] D. Vos and B. Motazed, "Fault tolerant control design for parameter dependent systems," *Proceedings of the American Control Conference*, 1998, pp. 679-680 vol.2.
- [357] P. G. Voulgaris and C. N. Hadjicostis, "Optimal preprocessing strategies for perfect reconstruction of binary signals under power-constrained transmission," *43rd Conference on Decision and Control*, 2004, pp. 4040-4045 Vol.4.
- [358] B. L. Walcott and S. H. Zak, "Combined Observer-Controller Synthesis for Uncertain Dynamical Systems with Applications," *IEEE Transactions on Systems, Man, and Cybernetics*, vol. 18, pp. 88-104, 1988.

- [359] B. L. Walcott and S. H. Zak, "State Observation of Nonlinear Uncertain Dynamical Systems," *IEEE Transactions on Automatic Control*, vol. AC-32, pp. 166-170, 1987.
- [360] F. Wang, C. J. Cass, D. Boroyevich and F. C. Lee, "Overview of research activities at center for power electronics systems," *IEEE Electric Ship Technologies Symposium*, 2005, pp. 28-33.
- [361] H. Wang, S. Pekarek and B. Fahimi, "Elimination of position and current sensors in high performance adjustable speed AC drives," *IEEE 0-7803-8987-5*, 2005, pp. 1902-1911.
- [362] H. Wang, S. Pekarek, B. Fahimi, E. Zivi and J. Ciezki, "Improvement of fault tolerance in AC motor drives using a digital delta-hysteresis modulation scheme," *35th Annual IEEE Power Electronics Specialists Conference*, 2004, pp. 944-949 Vol.2.
- [363] O. Wasynczuk and S. D. Sudhoff, "Automated state model generation algorithm for power circuits and systems," *Power Systems, IEEE Transactions on*, vol. 11, pp. 1951-1956, 1996.
- [364] O. Wasynczuk, S. D. Sudhoff, T. D. Tran, D. H. Clayton and H. J. Hegner, "A voltage control strategy for current-regulated PWM inverters," *Power Electronics, IEEE Transactions on*, vol. 11, pp. 7-15, 1996.
- [365] O. Wasynczuk, E. A. Walters and H. J. Hegner, "Simulation of a zonal electric distribution system for shipboard applications," 1997, pp. 268-273 vol.1.
- [366] Weidong Zhu, S. Pekarek, J. Jatskevich, O. Wasynczuk and D. Delisle, "A model-in-the-loop interface to emulate source dynamics in a zonal DC distribution system," *Power Electronics, IEEE Transactions on*, vol. 20, pp. 438-445, 2005.
- [367] I. H. Whang, Jang Gyu Lee and Tae Kyung Sung, "Modified input estimation technique using pseudoresiduals," *Aerospace and Electronic Systems, IEEE Transactions on*, vol. 30, pp. 220-228, 1994.
- [368] I. H. Whang, Jang Gyu Lee and Tae Kyung Sung, "A modified input estimation technique using pseudoresiduals," *Aerospace and Electronic Systems, IEEE Transactions on*, vol. 30, pp. 591-598, 1994.
- [369] A. Willsky and H. Jones, "A generalized likelihood ratio approach to the detection and estimation of jumps in linear systems," *Automatic Control, IEEE Transactions on*, vol. 21, pp. 108-112, 1976.
- [370] A. S. Willsky, "Relationships between digital signal processing and control and estimation theory," *Proceedings of the IEEE*, vol. 66, pp. 996-1017, 1978.

- [371] N. E. Wu, "Reliability of fault tolerant control systems: Part I," in 2001, pp. 1460-1465 vol.2.
- [372] N. E. Wu, "Reliability of fault tolerant control systems: Part II," in 2001, pp. 1466-1471 vol.2.
- [373] Xiaobing Huang, Jizhen Liu and Yuguang Niu, "Whole course fault diagnosis based on fuzzy dynamical model," *Proceedings of IEEE TENCON '02*, 2002, pp. 1371-1376 vol.3.
- [374] Xiaowen Fang, J. Gertler, M. Kunwer, J. Heron and T. Barkana, "A double-threshold-testing robust method for fault detection and isolation in dynamic systems," *Proceedings of the American Control Conference*, 1994, pp. 1979-1983 vol.2.
- [375] Y. Xiong and M. Saif, "Unknown Disturbance Inputs Estimation Based on a State Functional Observer Design," *Automatica*, vol. 39, pp. 1389-1398, 2003.
- [376] Y. Xiong and M. Saif, "Unknown Disturbance Inputs Estimation Based on a State Functional Observer Design," *Automatica*, vol. 39, pp. 1389-1398, 2003.
- [377] L. Xu and Mo-Yuen Chow, "A classification approach for power distribution systems fault cause identification," *Power Systems, IEEE Transactions on*, vol. 21, pp. 53-60, 2006.
- [378] I. Yaesh and U. Shaked, "Multi-objective robust H_2/H_∞ deconvolution via evolutionary algorithms," *IEEE 0-7803-8427-X*, 2004, pp. 56-59.
- [379] F. Yang and R. W. Wilde, "Observers for linear systems with unknown inputs," *Automatic Control, IEEE Transactions on*, vol. 33, pp. 677-681, 1988.
- [380] Yann-Chang Huang, Hong-Tzer Yang and Ching-Lien Huang, "A new intelligent hierarchical fault diagnosis system [for power networks]," *Power Systems, IEEE Transactions on*, vol. 12, pp. 349-356, 1997.
- [381] Yeong Jia Cheng and E. K. K. Sng, "Transient analysis and fault compensation during module failure in paralleled power modules," *Industry Applications, IEEE Transactions on*, vol. 42, pp. 591-601, 2006.
- [382] Yingbo Hua, K. Abed-Meraim and M. Wax, "Blind system identification using minimum noise subspace," *Signal Processing, IEEE Transactions on [See also Acoustics, Speech, and Signal Processing, IEEE Transactions on]*, vol. 45, pp. 770-773, 1997.

- [383] Yingquan Wu and C. N. Hadjicostis, "Non-concurrent fault identification in discrete event systems using encoded petri net states," *Proceedings of the 41st IEEE Conference on Decision and Control*, 2002, pp. 4018-4023 vol.4.
- [384] Yong Hwan Park, J. H. Seo and J. G. Lee, "Tracking using the variable-dimension filter with input estimation," *Aerospace and Electronic Systems, IEEE Transactions on*, vol. 31, pp. 399-408, 1995.
- [385] Yu-quan Cui, Li-jie Ma and J. Wang, "A new method of estimating inputs," *Proceedings of the 6th International Conference on Intelligent Systems and Applications*, 2006, pp. 718-723.
- [386] S. H. Zak, *Systems and Control*. ,1st ed. New York: Oxford University Press, 2003,
- [387] B. Zhang and S. D. Pekarek, "Analysis and average value model of a source-commutated 5-phase rectifier," *35th Annual IEEE Power Electronics Specialists Conference*, 2004, pp. 362-368 Vol.1.
- [388] D. H. Zhou and P. M. Frank, "Fault diagnostics and fault tolerant control," *Aerospace and Electronic Systems, IEEE Transactions on*, vol. 34, pp. 420-427, 1998.
- [389] P. Zitek, R. Mankova and J. Hlava, "Neural Network evaluation of Model-Based Residuals in Fault Detection of Time Delay Systems," *Int. J. Appl. Math. and Comp. Sci.*, vol. 9, pp. 599-617, 1999. 1999.
- [390] E. Zivi, "Design of Robust Shipboard Power Automation Systems," *Annual Reviews in Control*, vol. 29, pp. 261-272, 2005.
- [391] E. Zivi and T. McCoy, "Control of a shipboard integrated power system," in *Proceedings of the Thirty-Third Annual Conference on Information Sciences and Systems*, 1999, pp. 1-2,3,4,5,6.
- [392] E. L. Zivi, "Integrated shipboard power and automation control challenge problem," 2002, pp. 325-330 vol.1.
- [393] Ziyang Qiu and J. Gertler, "Robust FDI systems and H_{∞} -optimization-disturbances and tall fault case," *Proceedings of the 32nd Conference on Decision and Control*, 1993, pp. 1710-1715 vol.2.
- [394] R. B. Zubaly, *Applied Naval Architecture*. ,1st ed. Centreville, MD: Cornell Maritime Press, 1996, pp. 349.

- [395] D. Clayton, “Generation Integrated Power Systems Opportunities for Collaboration,” Presented to Electric Ship Research and Development Consortium, Washington, D.C., May 24, 2007.

THIS PAGE INTENTIONALLY LEFT BLANK

INITIAL DISTRIBUTION LIST

1. Defense Technical Information Center
Ft. Belvoir, VA
2. Dudley Knox Library
Naval Postgraduate School
Monterey, CA
3. John D. Stevens, LCDR, USN
Naval Sea Systems Command 05Z3B
Washington Navy Yard
Washington, DC
4. Ed Zivi
U.S. Naval Academy
Annapolis, MD
5. John Ciezki
U.S. Naval Academy
Annapolis, MD
6. Roberto Cristi
Naval Postgraduate School
Monterey, CA
7. John D. Stevens, LCDR, USN
Crofton, MD
8. Robert E. Stevens
The Villages, FL
9. Eric W. Stevens
California, MD
10. John D. Stevens, LCDR, USN
Crofton, MD
11. William B. Stevens, CDR, USN
Crofton, MD
12. Robert W. Schaeffer
Emmaus, PA

13. John D. Stevens, LCDR, USN
Naval Sea Systems Command 05Z3B
Washington Navy Yard
Washington, DC
14. Robert E. Stevens II, CDR, USN
Beaver Creek, OH